UNIVERSITEIT VAN PRETORIA
UNIVERSITY OF PRETORIA
YUNIBESITHI YA PRETORIA
Denkleiers • Leading Minds • Dikgopolo tša Dihlalefi

CHEMICAL SPECIATION THROUGH SEQUENTIAL INJECTION ANALYSIS

by

Vusi Ludwig Mulaudzi

(98230434)

Thesis submitted in fulfilment of the requirements for the degree of

Doctor of Philosophy (Chemistry)

In the Faculty of Natural and Agricultural Sciences

University of Pretoria

2019

Supervisor: **Professor K.I. Ozoemena**

UNIVERSITEIT VAN PRETORIA
UNIVERSITY OF PRETORIA
YUNIBESITHI YA PRETORIA
Denkleiers • Leading Minds • Dikgopolo tša Dihlalefi

Declaration

I, Vusi Ludwig Mulaudzi, hereby declare that this Ph.D. thesis entitled "CHEMICAL SPECIATION THROUGH SEQUENTIAL INJECTION ANALYSIS was entirely through my own research. This work was carried out under the guidance and supervision of Prof. J.F. van Staden and co-supervised by Prof. R.I. Stefan. It was concluded in 2003 but there was a delay in submission as they both left the employ of the university and moved to a different country. Prof. K.I. Ozoemena intervened at a very late stage as the writing supervisor for the final submission. I am aware of the University of Pretoria's policy in regard to plagiarism and I fully understand it. The interpretations put forth are based on my reading and understanding of related material. The other books, articles and websites, which I have made use of are acknowledged at the respective place in the text. I have not previously submitted any part or in its entirety this thesis at any university for a degree.

Name of student: Vusi Ludwig Mulaudzi

Student number: 98230434

Signature of student:

Date:

Dedication

To my dear departed mother, may her soul rest in peace. You are always part of me

And

To my God given blessings my children Hulisani and Khathutshelo and my wife Masingita who stood by me as always throughout any journey.

Psalm 23:1-3 (KJV) **"***The Lord is my shepherd; I shall not want. He maketh me to lie down in green pastures; He leadeth me beside the still waters. He restoreth my soul; He leadeth me in the paths of righteousness for His name's sake."*

(Galatians 6:9) (ESV) "And let us not grow weary of doing good, for in due season we will reap, if we do not give up."

Acknowledgements

The Lord is my shepherd, he guided me though out this journey and he is the author and perfecter of my life.

This work was concluded in 2003 and without the combined efforts and valuable contribution of the following people it would not have seen the light of day.

- ✓ Prof. J.F. van Staden, for his valuable mentorship and the scientific input into this work
- ✓ Prof. R.I. Stefan for her encouragement and fruitful contribution.
- ✓ Prof K.I. Ozoemena for his professionalism, and countless engagement in taking up extra work, care and dedication to see to it that this work is finalised, this is indeed another notch in your belt you are such a blessing. Your scientific knowledge and selflessness is invaluable to the scientific community. You have earned your keep amongst the world's top 1% chemists.
- ✓ Prof. E. Rohwer for the encouragement and taking it upon himself that all ends well.
- ✓ All my family members who gave me unwavering support in one way or the other.

ABSTRACT

This work gives a thorough insight into the objectivity of adapting the sequential injection analysis (SIA) technique as a tool for chemical speciation. The use of ultraviolet visible spectrophotometry as a single detector greatly simplified the analysis process. This work further ascertained the versatility of the SIA system and broadened its scope of application. This was exemplified through Chapters 3, 4, and 5 which focused on chemical speciation of heavy metals. In Chapter 6 a non-metallic speciation was done with special reference to bromine/bromide. The application spectrum of SIA was furthermore displayed in the chemical speciation of α-amylase and β-amylase as examples of biological substances in Chapters 7. Chapter 8 concludes this research by extending this procedure into organic chemical species through speciation of (R and S)-penindopril. Chapter 9 gives an overall conclusion of the chemical speciation project. Table 3.4 shows the recovery of the developed method and for Fe(III) the % recovery was 100 % and for total Fe it was ± 98 %. From Table 3.5 the % relative standard deviation (RSD) was 0.58 and 0.73 for Fe(II) and Fe(III) respectively by the proposed method whereas in comparison Atomic Absorbtion Spectroscopy (AAS) method had 1.67 % and the titration 2.35 %. At the 95 % confidence level $t_{calculated} \leq t_{tababulated}$ showing that the standard method and the proposed method yielded similar results.

Mn(II)/ Mn(VII) speciation gave similar results as shown in Table 4.3 by statistical evaluation of the results of the proposed method and the standard method. Table 4.4 shows the results of the recovery upon spiking with 0.2 mg Mn (VII) and the average % recovery was 98. Table 4.5 shows simultaneous determination of Mn(II) and Mn(VII) from synthetic samples by SIA method and the % recovery was ± 99 %. The % RSD was 0.27 and 0.34 for Mn(II) and Mn(VII) respectively which shows great precision. Table 5.3 displays simultaneous determination of Cr(III) and Cr(VI) from samples by the proposed SIA method in comparison with the titrimetric and AAS methods and there was no significant difference for all three methods. Table 5.4 shows the results of the recovery upon spiking with 0.4 mg Cr(III) and there was a 98 % recovery. Table 6.4 shows recovery results and in all cases the average % recovery was 98 %. The % RSD values were 0.8 and 0.7 % for bromine and total bromine, respectively (Table 6.3). Using the proposed system, one can monitor both bromine and total bromine at 30 samples per hour with a very low sample carry-over (~ 1.1%). Table 7.4 displays % Recovery after addition of 0.02 fungal amylase unit (FAU) of both α and β amylase and in both cases it was 98 %. The proposed SIA method and the iodine diastatic method gave similar results as shown in Table 7.5. The calculated % RSD was lower than 0.80 showing excellent precision. The detection limit for α- amylase determination was calculated to be 0.0046 FAU within a working range of (0.015 – 0.04) FAU and the corresponding values for β-amylase were calculated out to be 0.0043 FAU with the same working range. Table 8.3 shows the results obtained for the assay of S-perendopril (S-pdp) in the presence of R-perendopril (R-pdp), and the recovery was above 98 %. Table 8.4 shows results obtained for the assay of R-pdp in the presence of S-pdp and with 98 % recovery. This work highlighted the broad spectrum of SIA adapted to chemical speciation.

TABLE OF CONTENTS

TABLE OF FIGURES.

CHAPTER 1

CHAPTER 2

CHAPTER 3

CHAPTER 4

CHAPTER 5

CHAPTER 6

CHAPTER 7

CHAPTER 8

LIST OF TABLES

Chapter 3

Chapter 4

Chapter 5

Chapter 6

Chapter 7

Chapter 8

List of abbreviation

AAOD	Amino acid oxidase
AAS	Atomic absorbtion spectroscopy
ACE	Angiotensin converting enzyme
ASV	Anodic stripping voltammetry
ATI	Angiotensinogen
BCR	Community bureau of reference
BET	Brunauer-Emmet-Teller
CCFAC	Codex Committee on food additives
CE-ICPS	Capillary electrophoresis inductively coupled plasma sector field mass spectrometry
CEN	Centre of Excellence for Nutrition's standard
CFA	Continuous Flow Analyser system
CFA	Continuous flow analysis
CID-MS/MS	Collision induced mass-mass spectroscopy
CO	Carbon monoxide
CO_2	Carbon dioxide
CRM	Certified reference material
DCT	Distal convoluted tubule
DNA	3.5 dinitrosalycilic acid
DPC	Diphenyl carbazide

EDS	Energy dispersive X-ray analysis
EPA	Environmental Protection Agency
EPMA	Electron probe micro-analyzer
ESP	Eletro spin resonance
FAO	Food and Agriculture Organization
FAU	Fumgal amylase unit
FIA	Flow injection analysis
FID	Flame ionization detector
FTIR	Fourier transform infra red
FTIR	Fourier transform infrared spectroscopy
GC	Gas chromatograph
GC-ICP-MS	Gas chromatography inductively coupled plasma mass spectrometry
GC-MIP/GC-AAS	Gas chromatography microwave induced plasma/Gas chromatography atomic absorption spectroscopy
H_2	Hydrogen
HC	Holding coil
HPLC	High performance liquid chromatography
HR-ICP-MS	High resolution inductively coupled plasma mass spectrometry
HRTEM	High-resolution transmission electron microscopy
i.d	Internal diameter
IBT	Ion beam technniques
ICP-AES	Inductively coupled plasma atomic emission spectroscopy
ICP-MS	Inductively coupled plasma- mass spectrometry
IR	Infrared spectroscopy

ISE	Ion selective electrode
ISO	International Organization for Standardization
IUPAC	International Union of Pure and Applied Chemistry
JESS	Chemical, Joint Expert Speciation System
JETDEM	Joint European Thermodynamic Database for Environmental Modeling
LC-ICP-MS	Liquid chromatography inductively coupled plasma mass spectrometry
LMA	Law of Mass action
MICROQL	Multicomponent chemical equilibrium computer program
MINEQL	Chemical equilibrium modeling system for water chemistry
MS-MS	Mass spectrometer- mass spectrometer
NMR	Nuclear magnetic resonance
NRC	National Research Council
O_2	Oxygen
OC	Oxidation coil
p/p_o	Relative pressure of the nitrogen adsorbed per saturated pressure
PAR	4(-2-Pyridylazo) resorcinol
pdp	Perindopril
PEMFC	proton-exchange membrane fuel cell
PROX	Preferential oxidation
PTFE	Polytetraflouroethylene
PVP	Polyvinylpyrolidone
RC	Reaction coil
RELMP	Regional Lagranian Model of Air Pollution
rpm	Revolutions per minute
RSD	Relative standard deviation

SCFA	Segmented continuous flow analysis
SDS-PAGE	Sodium dodecyl sulphate-polyacrylamide gel electrophoresis
SEM	Scanning electron microscopy
SERP	Serpentine
SFA	Segmented flow analysis
SIA	Sequential injection analysis
SV	Selection valve
TAR	4-(2-thialazo)-resorcinol
TEM	Transmission electron microscopy
TGA	Thermo gravimetric analysis
UV/Vis	Ultraviolet visible spectroscopy
WGS	Water gas shift
WHAM	Windermere Humic Thermodynamic Database for Environmental Modeling. Model
WHO	World Health Organization
wt%	Weight percentage
XPS	X-ray photoelectron spectroscopy
XRD	X-ray powder diffraction
XRF	X-ray fluorescence spectroscopy
α amylase	Alpha amylase
β amylase	Beta amylase

CHAPTER 1

Introduction

1.1 Advances of analytical chemistry.

"*Analytical chemistry is the science of applying appropriate techniques for measuring the nature and quantity of chemical composition within a sample art at that instant and denoted space.*" [1].

Analytical chemistry is active and forever changing to adapt to areas of modern chemical research. All scientific fields are in one way or the other dependent on the results of chemical analyses. The study of analytical chemistry provides an avenue for teaching and emphasizing the truly quantitative thinking and quantitative approach to solve problems within the chemistry field [2]**.**

Hyphenated and non-destructive methods have become key fundamental aspects of analytical chemistry. Analytical chemists strive to improve the quality of existing techniques and to innovate better chemical measurements for our ever changing world [3]. They carry out research for new principles of measurement and make important contributions to a wide spectrum of fields keeping abreast with technical and medicinal innovations [3].

Figs. 1.1 and 1.2 show interdependence of all fields to analytical chemistry and its classification as either basic or applied science, respectively. The importance of incooporating quality assurance and quality control into all analytical processes has been schematically represented in Fig. 1.3.

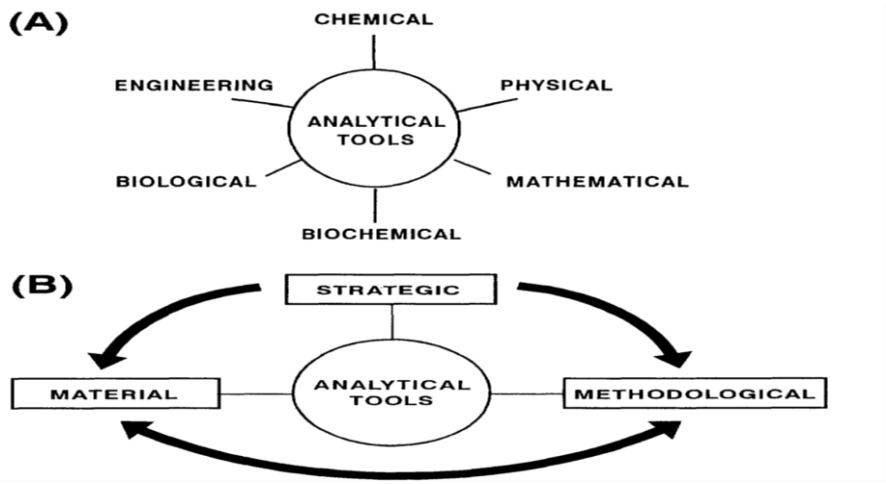

Figure 1. 1. **(A)** An abridged scheme showing how the different scientific disciplines interconnect

(B) Shows how chemical analysis is achieved through a detailed structural approach [2].

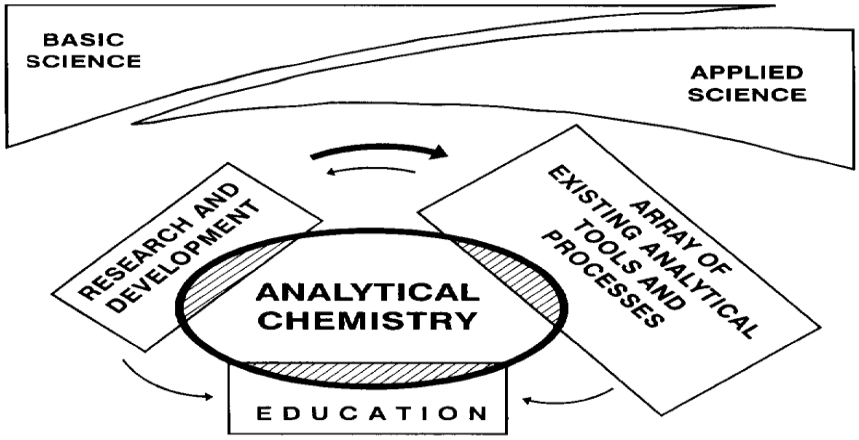

Figure 1. 2. Interaction of analytical chemistry as basic science and applied science [3].

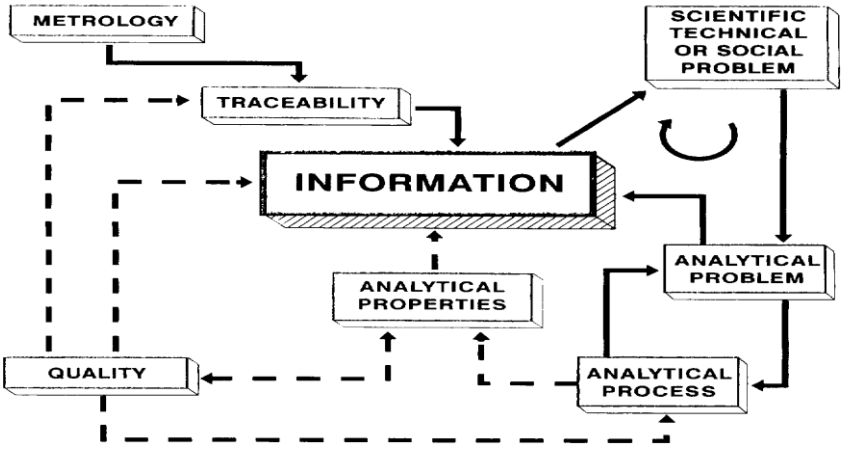

Figure 1. 3. Flow diagram for the analytical process [3].

1.2. Flow systems enhancing chemical analysis.

The advancement of analytical chemistry incooporated flow techniques with an appreciable automation. They are dependent on the pattern of flow dynamics employed such as:

a) Segmented continuous flow analysis which are air segmented and flow injection analysis,
b) Unsegmented continuous flow which is sequential injection analysis.

The automated analyzer was the first recorded automated instrument; it operated through a special flow process named continuous flow analysis (CFA), as shown in Fig. 1.4.

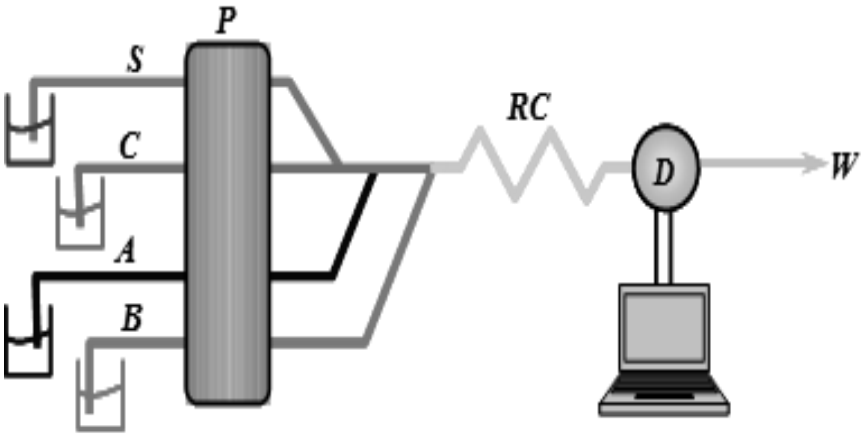

Figure 1. 4. Continuous Flow Analyser system (CFA) [4].

P – pump, RC – reaction coil, D – detector, C – carrier, S – sample, A and B – reagents, and W – waste.

In CFA the concentration of the analyte is measured uninterruptedly in a stream of liquid or gas. In Air-segmented flow analysis (SFA) displayed in Fig. 1.5 a continuous stream of material is divided by air bubbles into discrete segments in which chemical reactions occur.

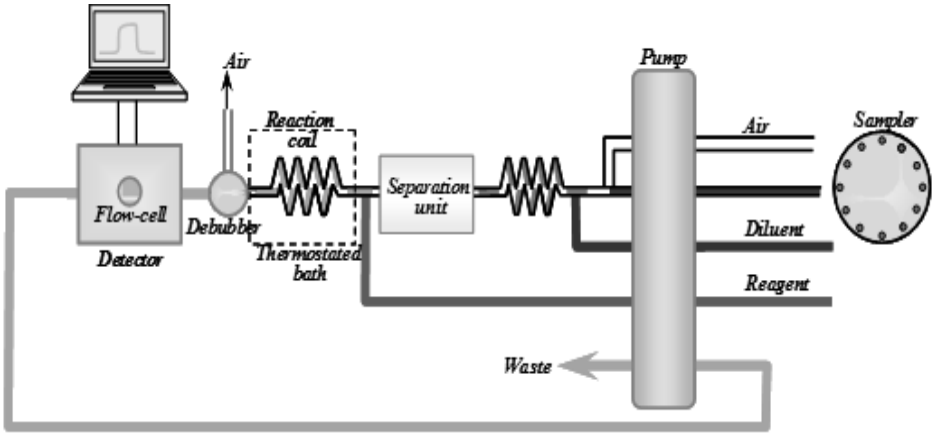

Figure 1. 5. Air-segmented flow analysis (SFA) system [4].

Fig. 1.6 shows flow injection analysi (FIA) characterized by the sequential insertion of discrete sample solution into unsegmented continuously flowing stream with subsequent detection of the analyte [4].

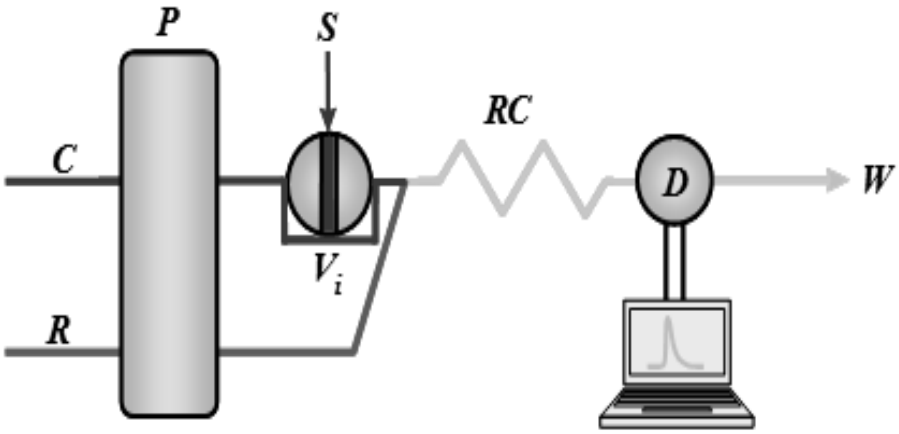

Figure 1. 6. Flow injection analysis system [4].

P - pump, V - injection device, RC - reaction coil, D - detector, C - carrier, S - sample, R - reagent, W - waste, H - peak height, T - residence time.

Fig. 1.7 below is SIA (sequential injection analysis) which is based on microfluidic manipulation of samples and reagents.

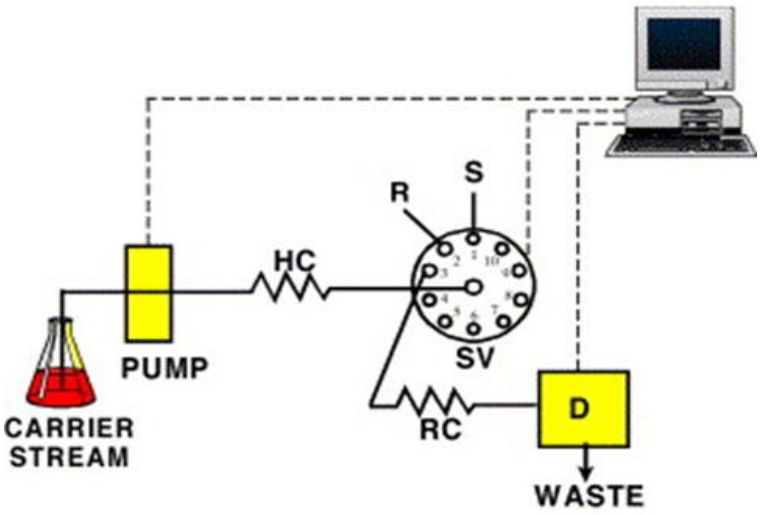

Figure 1. 7. Sequential injection system (SIA) [5].

HC - holding coil, R-reagent solution, S- sample solution, D- detector, RC- reaction coil, SV- selection valve, PC- computer for data readout and control software.

1.3. Chemical speciation.

International Union of Pure and Applied Chemistry (IUPAC) states that "Speciation analysis is the process leading to identification and determination of the different chemical and physical forms of an element existing in a sample" [6]. Each particular species form is controlled by chemical and physical parameters and is time dependent. The importance of speciation hinges on its pathway, background and distribution. Fig. 1.8 is a scheme of different metal coordinates.

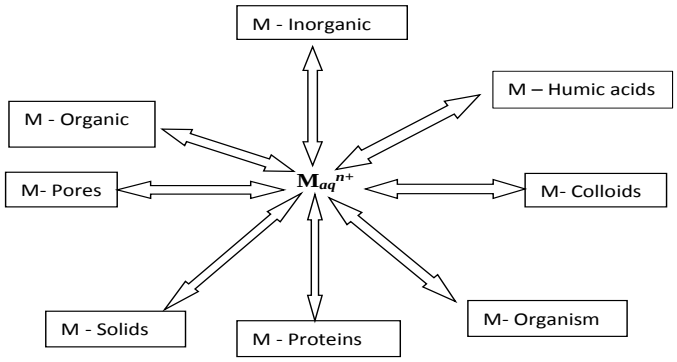

Figure 1. 8. Distribution scheme of various species where M represent metal [6].

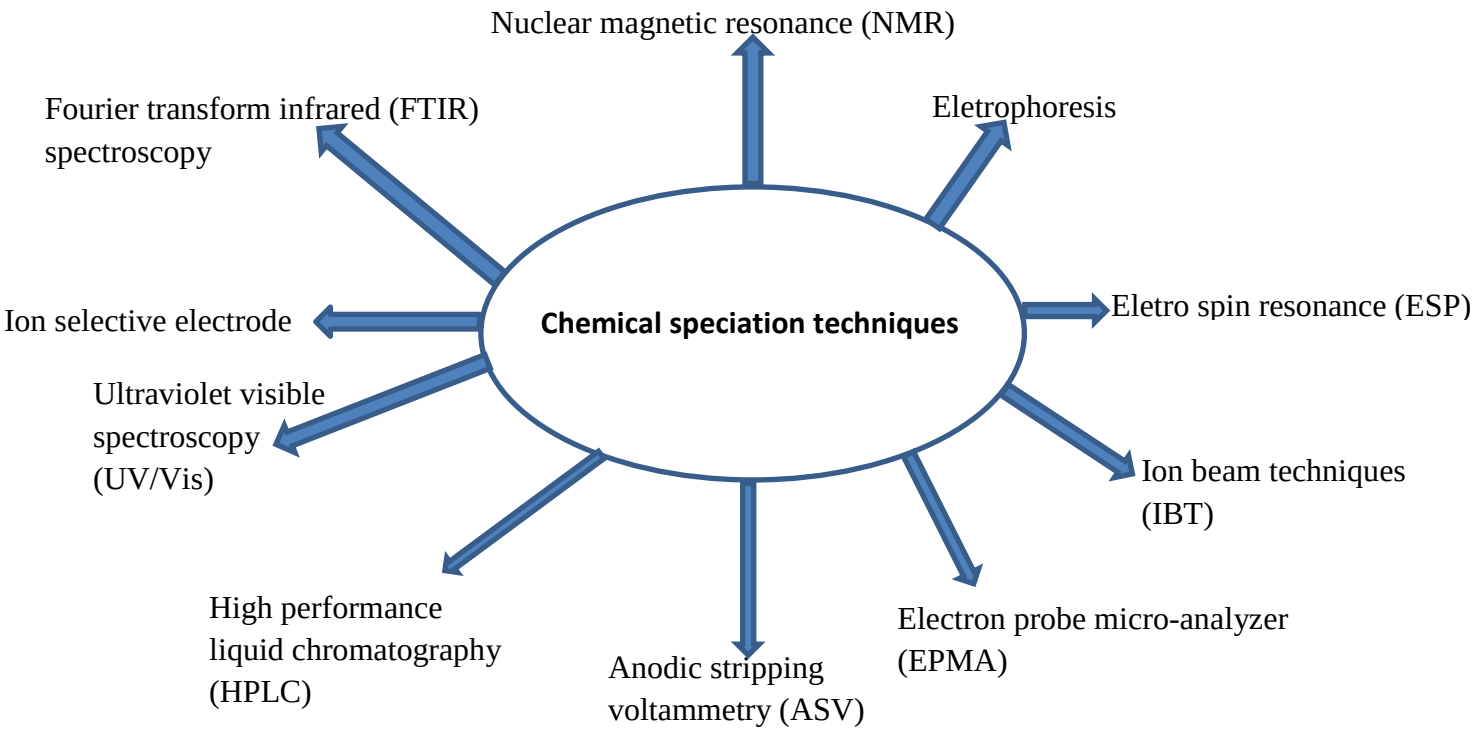

Figure 1. 9. Techniques and methodologies for speciation analysis [6].

Fig. 1.9 shows single instruments independently used for direct chemical speciation analysis Hyphenated techniques are those where two or more instruments are coupled together and will be discussed further in Chapter 2.

1.4. The aim of the study.

Recent developments have shown the need for interdisciplinary approach to solve the myriad challenges that the modern world is facing. This has revealed the role of chemical species in both flora and fauna health. Disease control and nutritional aspects are also dependent on the chemical species [6]. The chemical form of these elements or compounds determines their bioavailability and mobility within the environment. Their toxicological effects tend to correlate more with chemical forms than with the total concentration [6], thus requiring accurate and specific techniques for their analyses such as sequential injection analysis.

The critical significance of monitoring inorganic and organic contaminants in the environment, biota, food, water, air, soil and aquatic systems is of prime importance for both developing and developed countries [7]. A rapid, economical, reliable and sensitive methodology with as low detection limits is thus required.

The SIA technique has the hall marks to satisfy this role, with its inherent simplicity, low need for maintenance and simultaneous multiple chemical analyses [5]. The fact that there is no need to change the flow manifold to perform parallel analysis is best suited for multianalyte determination and for particular chemical speciation.

Reduced consumption of reagents, ease of versatility for varying chemical and instrumental operating parameters, ease of system calibration, single manifold channel, and the reverse/ forward flow processes make SIA ideal for chemical speciation [8].

The aim of this work was exemplified by speciation of the following elements which were all published except for α / β amylase.

1. Speciation of Fe^{2+}/Fe^{3+},
2. Speciation of $Cr_2O_4^{7-}/CrO_3^{4-}$,
3. Speciation of Mn^{2+}/Mn^{7+},
4. Speciation of Br_2/Br^-,
5. Speciation of S / R-perindopril,
6. Speciation of α / β amylase.

SIA gave results with no significant differences to conventional analytical methods, only that it was more accurate which are commonly used with improved detection limits and detection range.

1.5. Outline of the Thesis.

The outlay of the dissertation follows a four prong approach with each chapter smoothly intergrating into the successive one. **Chapter 1** introduces the analytical approach for general chemical analysis. This is then followed by flow systems as automated analytical tools. Chemical speciation is then introduced and briefly discussed and then merged into sequential injection analysis to show the aim of the dissertation. The concluding chapter outlines the success of sequential injection analysis technique to enhance chemical speciation. **Chapter 2** gives an expanded analysis of flow systems and the culmination into sequential injection analysis. Chemical speciation is then comprehensively discussed starting from the definition, types, and techniques to achieve this. Finally, how flow systems can be exploited to enhance chemical speciation. From **Chapter 3** to **Chapter 8** are examples of the experimental chemical speciation through sequential injection analysis as per aim of the research. The divisions of the research output are as follows; **Chapter 3** (Fe_2^+/Fe_3^+), **Chapter 4** (Mn^{2+}/Mn^{4+}), **Chapter 5** (Cr^{3+}/Cr^{7+}), **Chapter 6** (Br^-/ Br_2), **Chapter 7** (α/β)-amylase and **Chapter 8** (S/R)-perindopril. **Chapter 9** gives the conclusion about the research, highlighting the success of achieving the aim through the positive attributes of the objectives as set out in the design of the project. Results from both real and synthesized samples gave conclusive evidence that the research proved the versatility of the SIA technique and its ease of adaptability.

1.6. References.

1. I.M. Kolthoff, P.J. Eling, Treatise in Analytical Chemistry, Part I-III, Volumes, Interscience (1959).
2. H.F. Walton, Principles and Methods of Chemical Analysis, 2nd Ed., Prentice Hall (1966).
3. F.W. Fied, D. Kealey, Principles and Practices of Analytical Chemistry, 3rd Springer. US (1990) pp 1.
4. C.J. Patton, S.R. Crouch, Anal. Chim. Acta**,** Volume 179, (1986), pp 189.
5. J. Ruzicka, G.D. Marshall, Anal.Chem, 237 (1990), pp 335.
6. D.M. Templeton, F. Ariese, R. Corielis, L.G Danielson, H. Muntau, H.P. van Lewen, and R. Lobinski; IUPAC Guidelines for terms related to speciation of Trace Elements, Pure Appl. Chem. 72/8 (2000) pp 1455.
7. R. Cornelis, J. Caruso, H. Crews, K. Heumann, Handbook of Elemental Speciation 11: Species in the environment, food, medicine and occupational health, (2005), Wiley on line Library.
8. R.E. Taljaard, Application of sequential injection analysis as a process analyser, MSc-Dissertation, University of Pretoria, (1996).

LIST OF PEER-REVIEWED PUBLICATIONS ARISING FROM THIS WORK

1. J.F. van Staden, L.V. Mulaudzi, R.I. Stefan, Speciation of Mn (II) and Mn(VII) by on-line spectrophotometric sequential injection analysis, Anal. Chim. Acta, 499 (2003), pp 129.
2. J. F. van Staden, L. V. Mulaudzi and R. I. Stefan, On-line speciation of bromine and bromide using sequential injection analysis with spectrophotometric detection. Anal Bioanal. Chem., 375 (2003), pp1074.
3. L.V. Mulaudzi, J.F. van Staden and R.I. Stefan. On line speciation of Fe (II) and Fe(III) by sequential injection analysis. Anal.Chim. Acta, 467 (2002) pp 35.
4. L.V. Mulaudzi, J.F. van Staden and R.I. Stefan. On line speciation of Cr (III) and Cr(IV) by sequential injection analysis. Anal.Chim. Acta, 467 (2002) pp 51.
5. R.I. Stefan, J.F. van Staden and L.V. Mulaudzi. On line simultaneous determination of S- and R-peridopril using amperometric biosensors as detectors in flow systems, Anal. Chim.Acta. 467 (2002) pp 189.

CHAPTER 2

Literature review

2.1. Introduction

SIA was developed from FIA and has slotted very well to alleviate the demand of the modern analytical needs [1]. Although the principle of SIA is based on a defined pattern of sample and reagent aspiration, it follows the "random walk" model [2]. The effect of stopping and reversing in SIA is well documented [2]. The quality of results obtained from SIA is dependent on controlled dispersion and synchronised reagent sequencing [3]. These two parameters have a great influence on the degree of penetration that influences the type of dispersion.

SIA makes use of a single flow-channel at all times, through a synchronized action of the multi-position selection valve and the bi-directional pump. The sample and reagent zones are sequentially stacked but as they are propelled forward dispersion takes place which results in product formation.

2.2. Design and set-up of the Sequential Injection System.

The design and arrangement of SIA was earlier represented in Fig. 1.7 with the following parts;

2.2.1. Pumps.

Commomnly used pumps are syringe and peristaltic types. A high quality pump should have precision over long periods. The pump that was used through this research project was a Model 321, Gilson (Villiers-le-bel, France) with specifications as per manufacturer and is represented by Fig. 2.1 [4]. It is a single channel pump with bi-directional action. These are

propulsion (forward) and aspiration (reverse) of sample and reagent solutions. It has a remote control switch contacts that enable immediate stop, start, forward, and reverse.

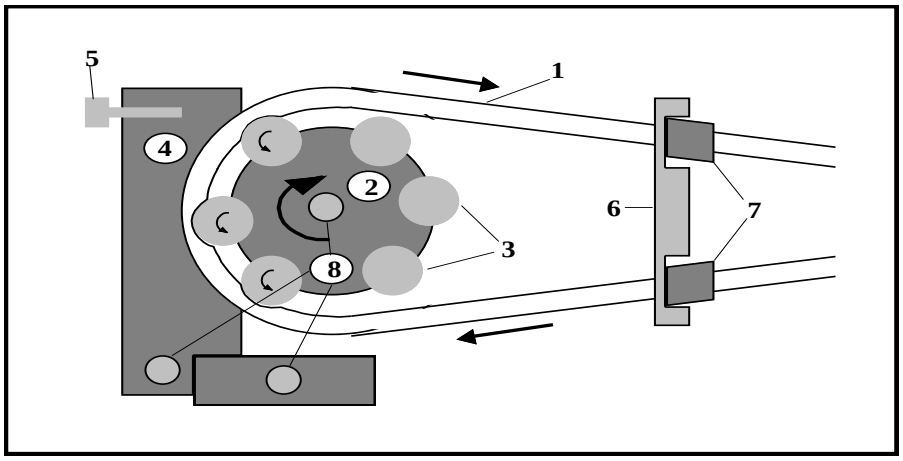

Figure 2. 1. Peristaltic pump [4].

1 - flexible tube, 2 - rotor, 3 - rolls, 4 - semi-cylindrical plate, 5 - screw, 6 - frontal plate, 7 - stoppers, 8 - cylindrical axes.

2.2.2. Pump tubing.

The most common tubing materials that have been so far used are Teflon, stainless steel, and other polymers. The most ideal tubings are those that are pliable and retain their physical characteristic for longer periods. Different tubings are supplied by various companies with clearly indicated specifications. Stainlesss steel would require a different type of pumping system as they are not pliable. The sequential injection manifolds are connected by the transport conduits commonly made up of PTFE (polytetraflouroethylene) tubing, resistant to a variety of solutions.

Below is Fig. 2.2 where (A) shows the effect of tube radius on sensitivity and (τ) displays the inverse response of peak height against tube radius and direct proportionality between peak width and tube radius.

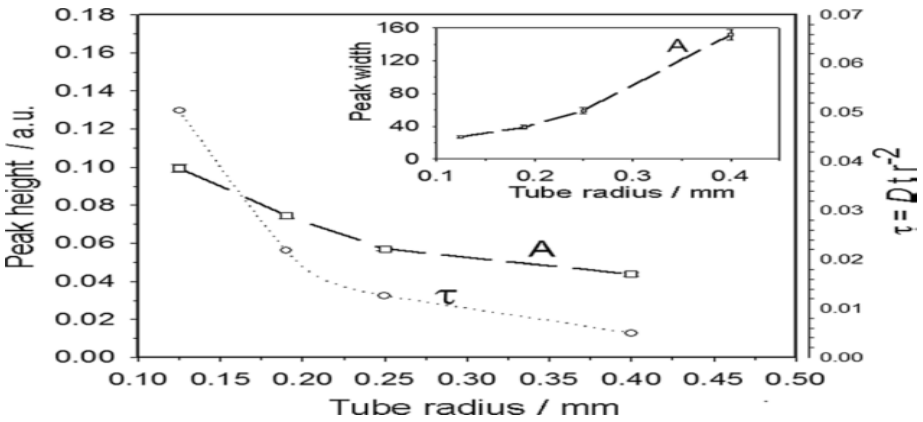

Figure 2. 2. Influence of tube radius on response signal [5].

2.2.3. Selection valve.

The selection valve (Fig. 2.3) is complementary to the bi-directional pump as the core of the SIA. The selection valve has several ports through which specific reagents could be sequentially aspirated.

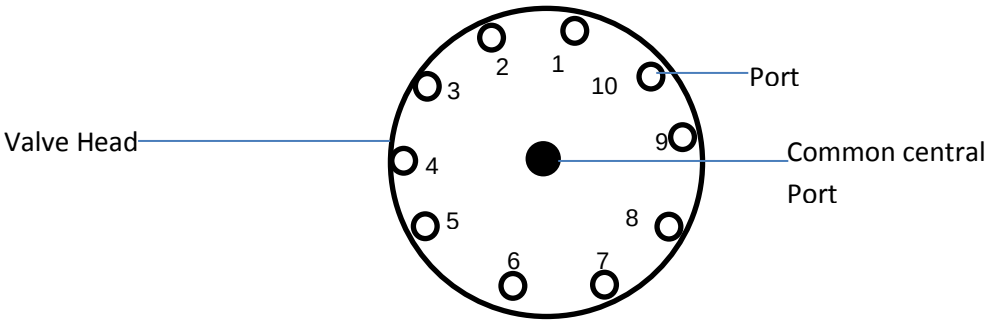

Figure 2. 3. A 10-port selection valve [3].

The selection valve used for this research was a 10-port Valco valve (Model ESCD10P) [3], Valco Instruments, Houston, TX, USA), actuated by a computer signal. The valve is designed to move only in an anti-clockwise direction. It can be directed to move from any port any number as denoted in Fig. 2.4, to the home or central common port in one single step. Its operational technique was thoroughly discussed [5].

2.2.4. Reactor geometries.

Fig. 2. 4 gives the physical patterns of the different coil patterns. The geometry of the reaction coil has a profound influence on dispersion and consequently on the performance of the flow analysis system as displayed in Fig. 2.5. The coil geometry is more sensitive and was used for this project, and is generally preferred to the knotted geometry [6].

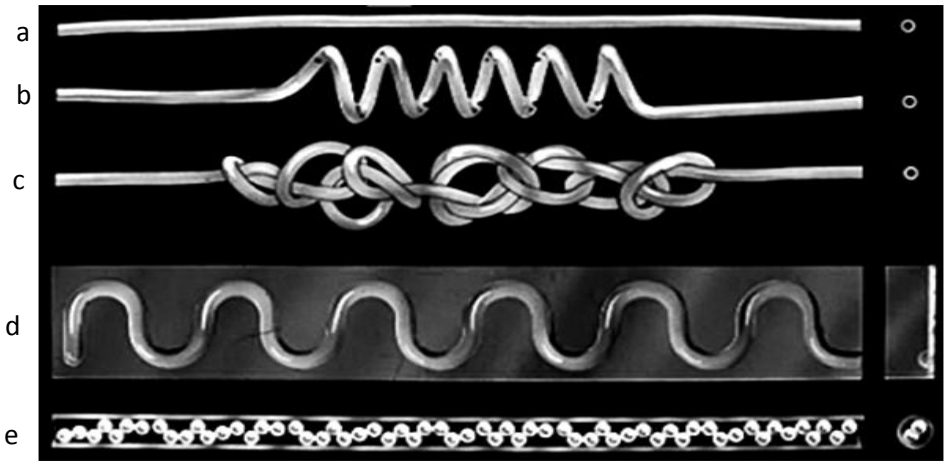

Figure 2. 4. Reactor geometry patterns [6].

(a) straight tube, (b) coiled tube, (c) knotted (knitted) tube, (d) sinusoidal shaped tube,

(e) sinusoidal bead impregnated tubes.

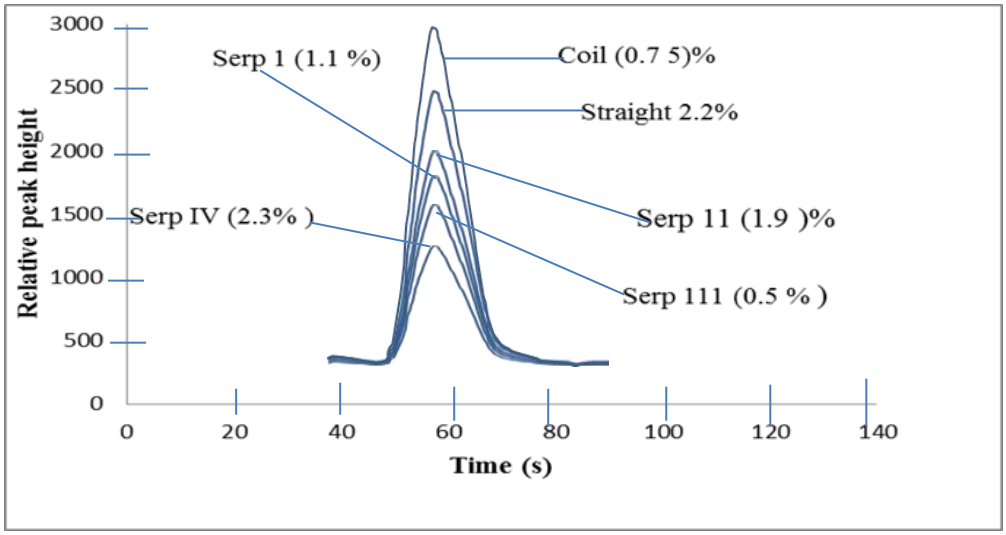

Figure 2. 5. Comparison of signal output in respect of reactor geometry [6].

2.2.5. Detectors.

An ideal SIA detector should be denoted by special attributes that are in line with the aims and objectives of the SIA process [5]. Several detectors can be coupled to SIA [3].

2.3. The operation of the systems is as follows:

2.3.1. Zone Injection profile.

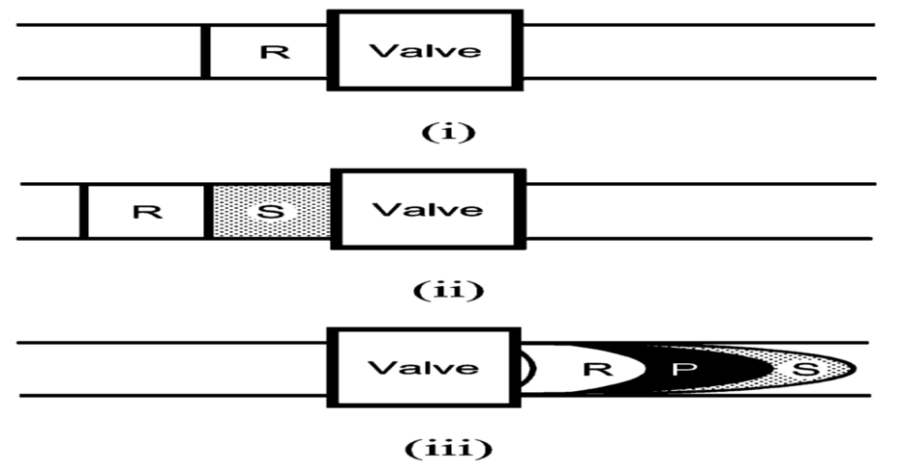

Figure 2. 6 Sequential injection processes. (i) Start position, (ii) sectional zones reagent and sample packing, (iii) forward position product sandwiched between unreacted sample and product zone.the structures of sequenced and injected zones (bottom). S, P, and R are the sample, product, and reagent zones. Note that flow reversal occurs during zone injection [6].

SIA was dicussed fully under Chapter 1 in section 1.4 with all its benefits. Fig. 2.6 shows the sequence of events within the conduits with time. The inter-dispersion is controlled by the sequence of aspiration and forwarding of the zones within the conduits of the SIA system. Fig. 2.7 illustrate the peak height with the passage of time with Fig. 2.7 (2a) no reaction, Figs. 2.7 (2b, 2c, 2d) ascending peak height with time and Fig. 2.7 (e) product decomposition.

Fig. 2.8 is the overall representation of peak height indicating the base line and isodispersion and all related representations. The isodispersion (I_D) is the point which indicates the area where the sample and reagent zones have identical dispersion.

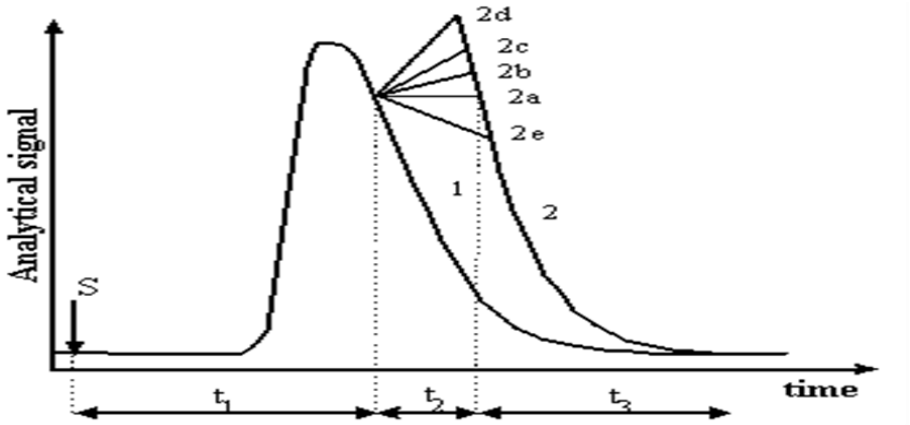

Figure 2. 7. Shape of the signal recorded in the case of the stopped-flow technique by gradients. 1– Signal shape for the case of continuous functioning of the pump; 2a– no chemical reaction takes place, 2b, 2c, 2d– chemical reactions with different rates, 2e– decomposition of the reaction [6].

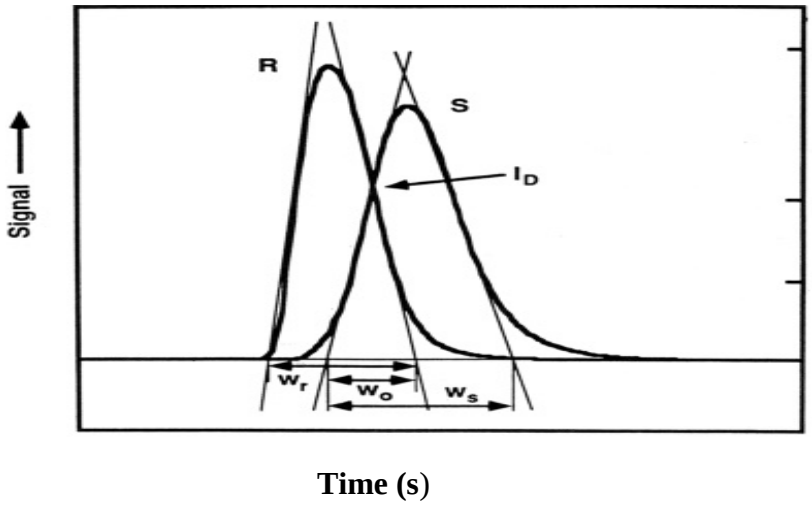

Figure 2. 8. Peak profile of actual zone penetration representation [6].

R-reagent zone, S-sample zone, I_D-dispersion coefficient, W_r-baseline width of reagent zone, W_s-baseline width of sample zonea nd W_o-baseline of overlap.

2.3.2. Reagent: sample ratio and sequence of aspiration.

van Staden et al. [7] evaluated the influence of reagent: sample ratio and the order of aspiration between the sample and any reagent. The results were shown in Fig. 2.9 and are dictated upon by the stoichiometric relationship based on the reaction.

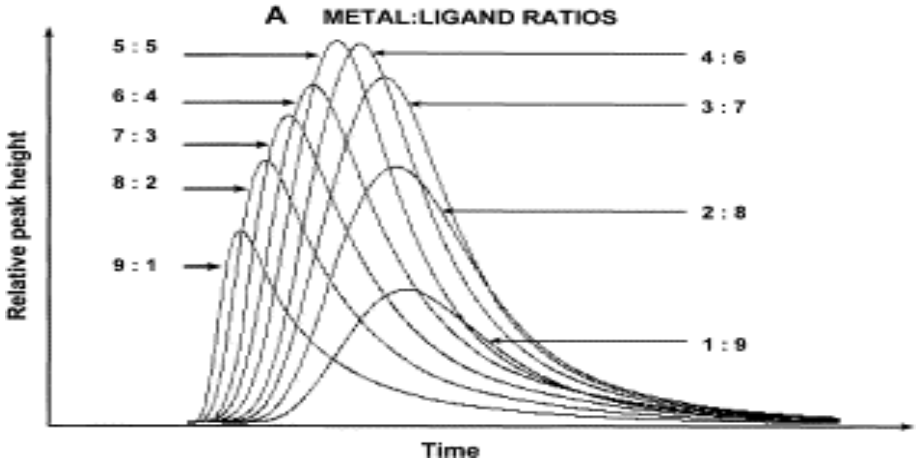

Figure 2. 9 Influence of different sample: reagent ratios in a total constant volume, in the order of metal followed by ligand [7].

2.4. Specific Operational Techniques.

Different operational techniques for single, double and three zones were fully explained [7]. For multizones operation where six zones were used in auto analysers was successfully carried out [8]. Dilution and mixing chambers was carried out automatically through coupling of several devices to the SIA system [9, 10]. Peterson et al. demonstrated extraction and flow reversal using organic and aqueous solutions [11]. Calibration, dialysis, titration and preconcentration have also been used in SIA [12 - 15].

2.4.1. Device control.

Computers control the different parts within SIA. Several researchers have developed their own individual specialised software. For example, Turbo C++ [16], Visual Basic [17], Windows 95 environment [18], LabVIEW [19], DARRAY [20] and FIALab [1].

2.4.2. Data output.

In this research the software package employed was the FlowTEK [16] where the signal

output is displayed as peak height, peak width, peak time or concentration.

2.4.3. Interface board.

For the interface of the software and the hardware (individual physical parts) the (PC-30B, Eagle Electric, Cape Town, South Africa) was used and the manufacturer includes relevant specifications. [5].

2.4.4. Distribution board.

A distribution board (assembled at Mintek, Randburg, South Africa) was inserted between the computer and the instrumental components [5].

2.5. Chemical speciation.

2.5.1. Historical background.

The term “speciation” was first used by O.F. Cook [21] stemming from the the pioneering work of Darwin et al. [22] about species description. Trace element analysis became prominent three decades following World War 2 for ecological sustainability, environmental rehabilitation and economic development [23]**.** In the chemical field there is inconsistency about the meaning of “speciation” [24]. Initially the study was limited to selected species [25]. This was extended for a variety of heavy metals [26]. Fig. 2.10 shows interlink of chemical speciation to other disciplines.

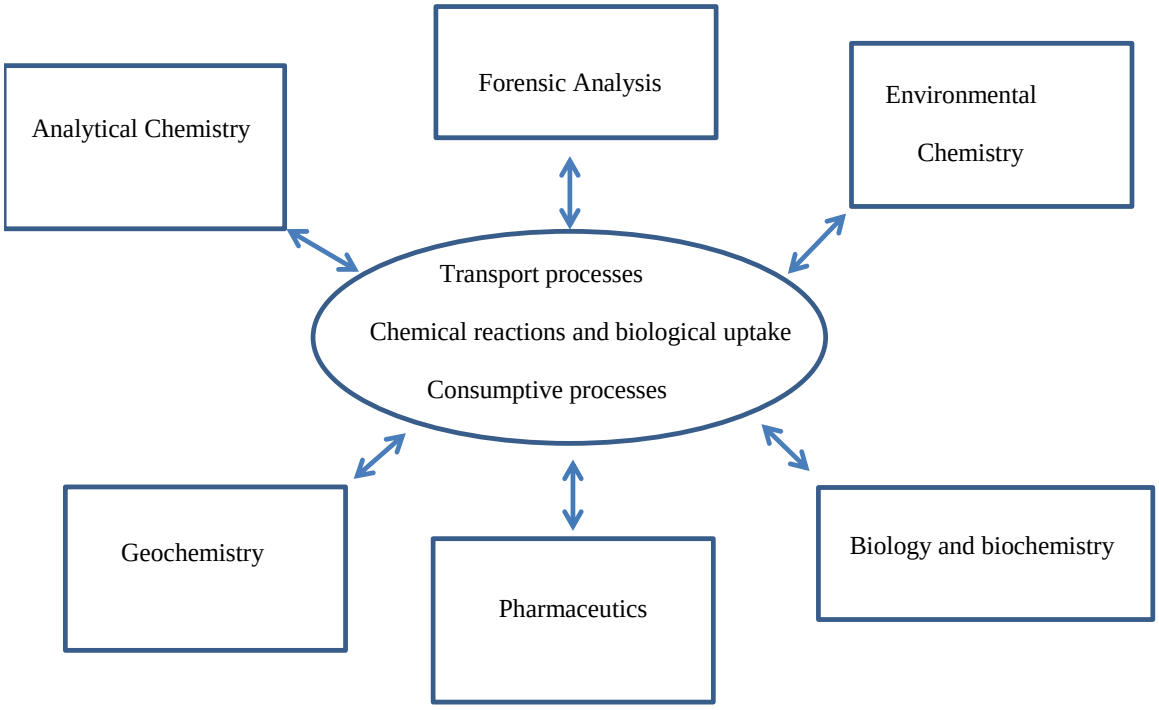

Figure 2. 10. Interdisciplinary flow of speciation analysis [27].

2.5.2. Finding common ground for terms related to Speciation and Fractionation.

(A) Different meaning of Speciation:

- Evolution or development of different genetic traits in an isolated sub-population, leading to a species distinctly different from the original parent population [21].
- Indicates the analytical activity of identifying chemical species and measuring their distribution [25].
- Indicate the distribution of species in a particular sample matrix [23].
- Distribution of an element amongst defined chemical species in a system **[**25].
- Partitioning of trace metals among solids, colloids, surfaces, dissolved free ions, complexed with dissolved inorganic ligands in the dissolved phase, and complexed with organics in the dissolved phase [26].
- Description of the abundance of species of an element [26].
- Reactivity and transformation of a given species into another [24].

(B) **Chemical species**: Specific chemical form of an element defined as to isotopic composition, electronic or oxidation state, and/or complex or molecular structure [25]**.**

(C) Speciation analysis: Analytical Chemistry, the activities of identifying and/ or measuring the quantities of one or more individual chemical species which together make up the total concentration in a sample [26].

(D) Fractionation: Process of classification of an analyte or a group of analytes from a certain sample matrix according to physical or chemical properties [27]**.**

Bernhard et al. suggested the term speciation should either be totally avoided or thoroughly defined when used [28], and the IUPAC definition was given in section 1.3.

2.5.3. Types of chemical species.

This was introduced in section 1.3, below follows some of the common types available within the environment in appreciable concentrations [29].

- Redox systems which are Se^{IV}/Se^{VI}, As^{III}/As^{V}, Sn^{II}/Sn^{IV}, Cr^{III}/Cr^{VI}, Mn^{II}/Mn^{IV}),
- Alkylated forms: Methyl (Hg, Ge, Sn, Pb, As, Sb, Se, Ethyl Pb),
- Bio-molecules: Organo: (As, Se, Cd, Li, chlorides),
- Metalloproteins and metalloenzymes,
- Colloidal,
- Morphological forms.

2.5.4. Importance of Chemical Speciation [28].

Some important aspects were explained in section 1.3. It is an integral part of risk assessment and the toxicity of an element hinges on speciation type and/or on specific organ [27]. This relationship can be represented as a following chain:

Risk → Concentration → speciation → Sensitivity of target organ or bio-fluid

The National Research Council (NRC) 2002 review on bioavailability explained "Bioavailability processes" through the following three key [28],

- **Contaminant interactions between phases.**
  (Association-Dissociation/Bound-Released)
- **Transport of contaminants to organisms.**
- **Passage across physiological membrane.**

Individual chemical species analysis provides comprehensensive toxicoligal effects [28]

2.5.5. The role of speciation in legislation.

This field has shed light on the far reaching impact of element speciation and its role in both fauna and flora. The revelation of the exact mode of action of the different chemical species on the organisms helps in drafting the relevant legislative control mechanisms. This was also important for Food and Agriculture Organization (FAO) and (WHO) World Health Organization to establish the Codex Committee (CCFAC) [30]. Environmental Protection Agency (EPA) aided in as well for export markets [31]. Supported by Europe, North America, Asia and Australia [29, 30].

2.5.6. Important application of speciation.

This is briefly discussed in Chapter 1, and then summarised in Fig. 2.11, which is outlined as a flow of different steps that indicate the chemical environment that influences the form in which the chemical species will exist as and their impact on the organism.

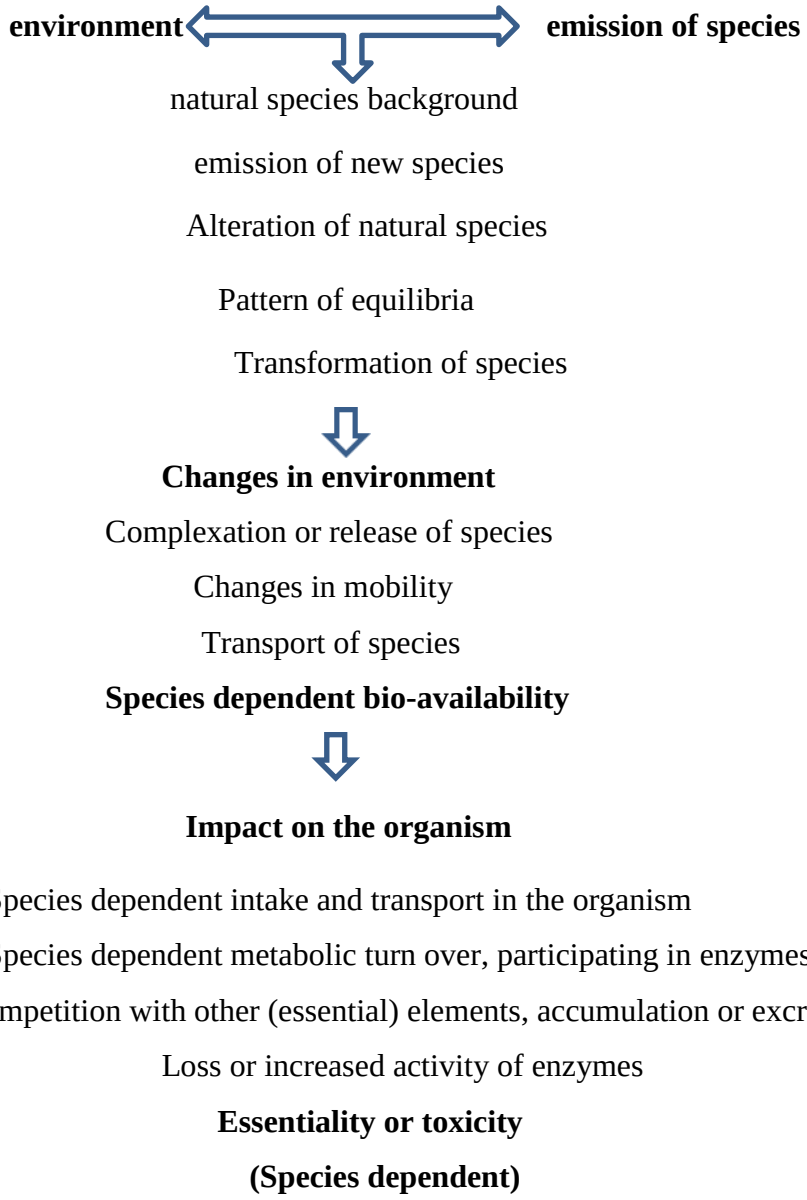

Figure 2. 11. Interrelation between “environmental speciation” and “biomedical speciation” [29].

2.5.7. Techniques and methodologies for speciation analysis.

Chemical speciation can be carried out through one of the following [30];

- Screening speciation this targets only one analyte.
- Group speciation; in this is for compounds or elements existing in different compounds and forms and at the specific oxidation level.
- Distribution speciation only for biological samples.
- Individual speciation which relies on fractionation and separation. Innovative techniques for speciation analysis rely on the isolation part of the targeted species from the other constituents making up the sample and the second being the detector bias the species of interest. The general common methods are [29]:

- direct method of analysis,
- hyphenated techniques,
- separation techniques,
- Modeling techniques.

Significant challenges for effective speciation analysis are as follows [30]:

- difficulties isolating compound(s) of interests from complex matrix,
- generally almost all the available techniques disturb the equilibrium,
- the great uncertainty of almost all known speciation methods,
- the very low concentration of analyte sought,
- The increased possibility of contamination.

2.5.8. Direct methods of chemical speciation.

These are the straight forward strategies which use a single step. These specialised methods for species determination exist as a small fraction. Spectroscopy is the most prevalent with very simple sample preparation that requires only one or two steps. These were discussed in Chapter 1.

2.5.9. Hyphenated techniques.

Integration of two or more methods mainly arranged in sequence where the product from the first technique subsequently becomes the sample for the next technique. These techniques generally involve many analytical steps such as extraction, derivatization, separation and detection which have to be carried out in such a way so that the species is conserved during the analytical process. This is because of the low concentration of the trace element present and the complexity of the matrix [31].

Conventional methods could no longer cope with new analytes that were being introduced into the environment. Advances in medicine and industries revealed more complex array of analytes within equaly complex matrices. It became apparent that to keep in par with this, more advanced methods and instruments needed to be introduced. These hyphenated techniques are computer controlled.

Advantages of these applications are;

- higher degree of automation,
- higher degree of sample throughput,
- better reproducibility,
- shorter time of analysis,
- reduced contamination as it is a closed system, and

- higher degree of information due to enhanced combined selectivity.

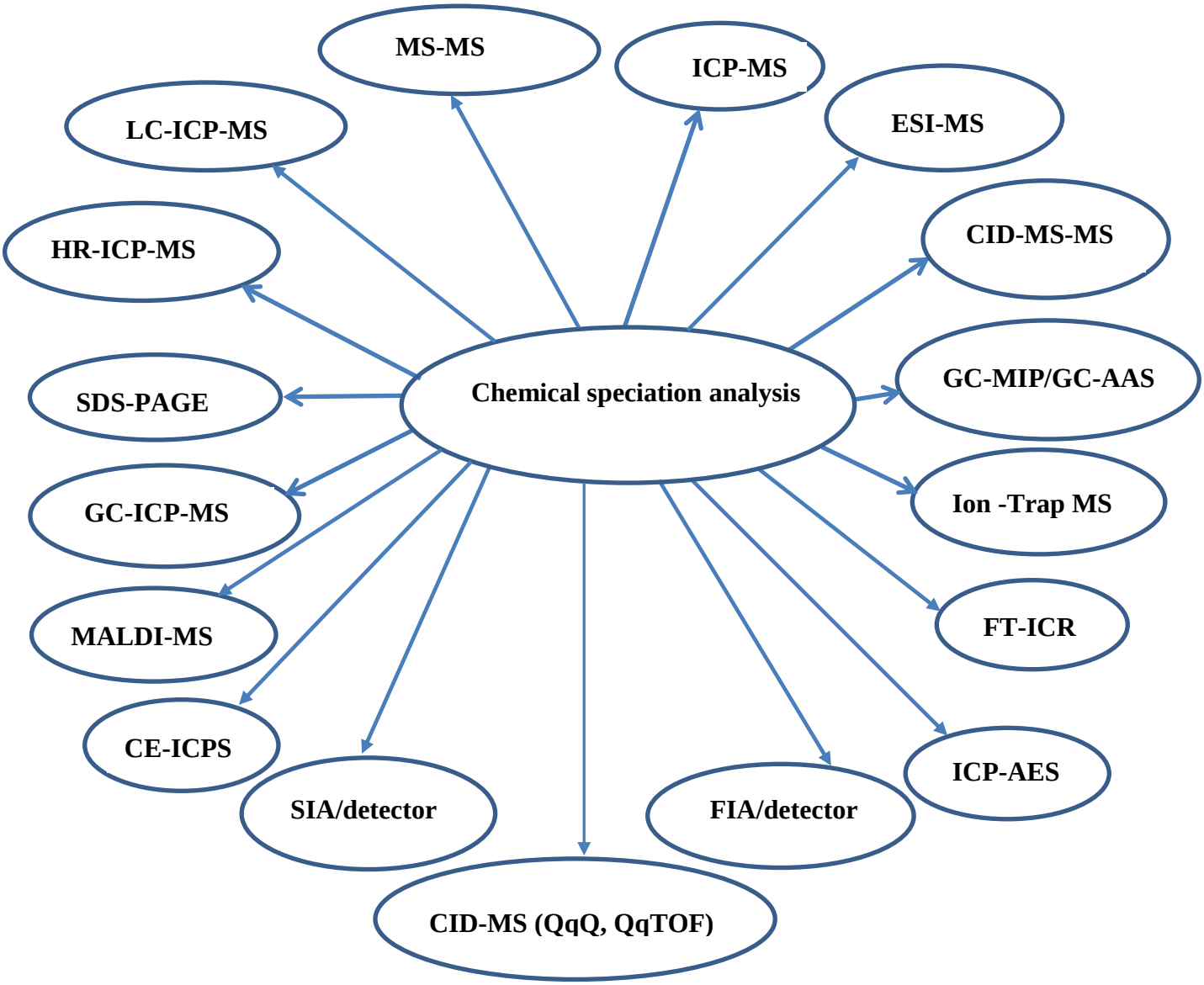

Figure 2. 12. Hyphenated techniques [31].

Fig. 2.12 gives a comprehensive summary of the various hyphenated techniques that are designed to deal with the new scopes of material to be analysed.

Hereunder is a list of some examples given [32-38],

- Mass spectrometer- mass spectrometer (MS-MS),
- Inductively coupled plasma- mass spectrometry (ICP-MS),
- Liquid chromatography inductively coupled plasma mass spectrometry (LC-ICP-MS),

- High resolution inductively coupled plasma mass spectrometry (HR-ICP-MS),
- Gas chromatography inductively coupled plasma mass spectrometry (GC-ICP-MS),
- Capillary electrophoresis inductively coupled plasma sector field mass spectrometry (CE-ICPS),
- Collision induced mass-mass spectroscopy (CID-MS/MS),
- Inductively coupled plasma atomic emission spectroscopy (ICP-AES), and
- Gas chromatography microwave induced plasma/Gas chromatography atomic absorption spectroscopy (GC-MIP/GC-AAS).

2.6. Speciation by (FIA).

FIA has a high versatility that allows discrimination of the various chemical species. FIA can be adapted for use in other related oxidized-reduced pair with either a single or double beam photometric spectroscopy [39], Reversed FIA configurations and open-closed systems are generally applied with great successs. Sometimes reversed asymmetric merging-zones with either potentiometric or photometric detectors have been applied [36].

To extend the range of chemical species detectors may be put in series or in parallel and the different injection valves used as well. Manipulation of the sample either on-line or off-line has also been used [39]. Some case studies for FIA speciation have already been used [40-44].

2.7. Sequential injection analysis (SIA).

SIA has potential to perform multiparametric analyses [45]. Just altering the sequence or type of reagents with the same manifold and use of different detectors will widen the scope of analysis. An additional advantage of SIA is the ease of coupling of separation devices to the

valve. A few examples of chemical speciation by SIA have been reported from literature [46-48].

2.8. Chemical speciation through computation.

The physical separation and determination of the various forms usually disturb the chemical state of the sample even though it is necessary to do so. This limitation is by-passed by the use of chemical models [49]. Thermodynamic data from such models only yield meaningful and reliable results when significant complexes are all encountered for. This leads to computer simulation which uses theoretical chemical concepts to predict the concentration of chemical species [49]. The 21st century has seen a wide array of new technologies being introduced more especially those which are computer based and models.

Modeling is only valid when numerical constants are from equilibrium reactions. The Analytical Chemistry Division Commission provides the equilibrium data [50]. Advantages of computational speciation methods are clearly outlined [51]

The choice of a particular model for speciation is based on prior knowledge for the speciation technique used. The adaptation of using complicated ion equilibria computer program and predetermined data for pH, total ionic concentrations and equilibrium constants, trace element speciation can be calculated [52].

Ball et al. [53] used the WATEQ2 program. PHREEQE was developed for aluminum speciation [54]. A few of the recent speciation models used were [55]:

- Regional Lagranian Model of Air Pollution (RELMP),
- Law of Mass action (LMA),

- Windermere Humic Thermodynamic Database for Environmental Modeling. Model (WHAM),
- Joint European Thermodynamic Database for Environmental Modeling (JETDEM),
- Chemical, Joint Expert Speciation System (JESS),
- Multicomponent chemical equilibrium computer program (MICROQL), and
- Chemical equilibrium modeling system for water chemistry (MINEQL).

2. 9. Quality assurance and quality control in chemical speciation analysis [56].

Quality assurance and quality control were introduced in Section 1.1. Quality control is not strictly practised in chemical speciation as yet. Those used for trace analysis can be adapted for chemical speciation analysis [56, 57]. The community of Bureau of Reference (BCR) deals with accreditation and production of certified reference material (CRM) [58]. International Organization for Standardization (ISO) or Centre of Excellence for Nutrition's standard (CEN) may be sourced [59].

Some of the more specific reference material used for speciation are provided by different companies and specific for particular species analysis, for example CRM 544 used for lyophilized solution in the speciation analysis for Cr(III)/Cr(VI). CRM 2108 for Cr(III), and CRM 2109 for Cr(VI) [60].

2.10. References.

1. J. Ruzicka, G.D. Marshall, Anal. Chim.Acta, 237 (1990) pp 329.
2. J. Ruzicka, Anal. Chim.Acta, 261 (1992) pp 3.
3. J.F. van Staden, H. du Plesis, S.M. Linsky, R.E. Taljaard and B. Kremer, Anal. Chim. Acta, 354 (1997) pp 143.
4. J. Ruzicka and T. Gubeli, Anal. Chem., 63 (1991) pp 1680.
5. R.E. Taljaard, Application of sequential injection analysis as a process analyser, MSc-Thesis, University of Pretoria, (1996).
6. D.C. Gregory, J.M. Hungerford, and G.D. Christian, Anal. Chem., 61 (9) (1989) pp 973.
7. A. Danet, L. Laherta-Zamora, J. Martinez-Calatayud, J. Flow Injection Anal., 15 (1998) pp 168.
8. J.F. van Staden, H. du Plesis, S.M. Linsky, R.E. Taljaard and B. Kremer, Anal. Chim. Acta, 354 (1997) pp 143.
9. F. E.O. Suliman and S.M. Sultan, Talanta, 43 (1996) pp 559.
10. J.F. van Staden, H. du Plessis and R.E. Taljaard, Instrum. Sci. and Techn., 27 (1999) pp 1.
11. V. Cerdà, A. Cerdà, A. Cladera, M.T. Oms, F. Mas, E. Gómez, F. Bauzá, M. Miró, R. Forteza, J.M Estela, TrAC Trends in Analytical Chemistry, Volume 20, Iss. 8, pp 407.
12. C. Zang, Y. Naruzawa and S. Kitahama, Chem. Lett., 5 (1993) pp 877.
13. J. Ruzicka, Analyst, 119 (1994) pp 1925.

14. M. Guzman and B.J. Compton, Talanta, 40 (1993) pp 1943.

15. J.F. van Staden and R.E. Taljaard, Fresenius' J. Anal. Chem., 357 (1997) pp 577.

16. G.D. Marshall, PhD Thesis, Universitry of Pretoria (1994).

17. W. Schuhmann, H. Wohlschlager, H.L. Schimdt and H. Stadler, Anal. Chim. Acta, 315 (1995) pp113.

18. E. Becera, A. Cladera and V. Cerda, Lab. Robot. Autom. 11 (1999) pp 131.

19. C.E. Lenehan, N.W. Barnett and S.W. Lewis, J. Autom. Methods Manag. Chem.24 (4) (2002) pp 99.

20. C. Zang, Y. Naruzawa and S. Kitahama, Chem. Lett., 5 (1993) pp 877.

21. O.F. Cook, "Factors of species formation" Science 23 (587) (1906) pp 506.

22. C. Darwin, "On the origin of species by means of natural selection, or the preservation of favoured Races in the struggle for life, (1859), London, John Murray Albermarle Street

23. W. Lund.W. Fresenius J. Anal. Chem. 337 (1990) pp 557.

24. J.A. Carasu, and M. Montes-Bayon, Ecotoxicology and Environmental Safety 56 (2003) pp 148.

25. H.E. Allen, R.H. Hall, T.D. Briston, Environ. Sci. Technol., 14 (4) (1980) pp 441.

26. J.A. Caruso, K.L. Sutton, K.L. Ackley, (EDS), Elemental Speciation: New approach for Trace Element Analysis, 1ST Ed. Comprehensive Analytical Chemistry, Vol. 33, Elsivier, Amsterdam, (2000) pp 581.

27. R. Lobinski, Fres. J. Anal Chem., 369 (2001) pp 113.

28. M. Bernard, F.E. Brinckman, and P.J. Sadler, (Eds) Importance of Chemical speciation in Environmental Processes, Springer Verlag Berlin Germany, (1986).

29. P.G. Reeves, A. Rufus, L. Chaney, Science of The Total Environment Volume 398, Iss 1–3, 15 July (2008) pp 13.

30. M. A. Champ, The Science of the Total Environment, 258 (2000) pp 21.

31. A.S. Orabi, A.E. Marghany, M.A. Shaker, A.E. Ali, Bulletin of the Chemists and Technologists of Macedonia, Vol.24, No. 1, pp 11.

32. R. Cornelis, J. Caruso, H. Crews, K. Heumann, Handbook of Elemental Speciation 11: Species in the environment, food, medicine & occupational health, (2005), Wiley On Line Library.

33. C.W. Connie Respiratory Function of Haemoglobin. HSIA, M.D.N Engl. J Med., 338 January 22 (1998) pp 239.

34. A. Violante, V. Cozzolino, L. Perelomov, A.G. Caporale, and M. Pigna, J. Soil.Sci. Plant. Nutr. 10 (3) (2010) pp 268.

35. R. Cornelis, Ann.Clin.Lab. Sci.; 26(3), May-June (1996) pp 252.

36. A. Senz-Medel, Spectrochimica Acta Part B Atomic Spectroscopy, Vol: 53, Iss. 2, (1998) pp 197.

37. K. Hirose, Anal. Sc. August; Vol: 22 (2006) pp1055.

38. A. Senz-Medel, Spectrochimica Acta Part B Atomic Spectroscopy Vol. 53, Iss. 2 (1998), pp 197.

39. A. Florence and Dietrich Busselberg, Bio-Metals, 19 (2006) pp 419.

40. I. Omae, Appl.Organomel.Chem. 17 (2003) pp 8.

41. M.A. Champ, The Science of the Total Environment 258 (2000) pp 21.

42. R.C. Santore, D.M. Di Toro, P.R. Paquin, H.E. Allien, and J. S. Meyer, Environmental Toxicology and Chemistry, Vol. 20, No. 10 (2001) pp 2397.

43. A. Davis. J.W. Drexter, M.V. Ruby and A. Nicholson, Micromineralogy of mine wastes in relation to lead bioavailability, Butte, Montana. Environ. Sci. Technol.27 (1993) pp 1415.

44. V. Michael, R.P. Bergstrom, A. Davis, Environ. Sci. Technol., Vol. 26, No. 3 (1992).

45. J.W. Drexler, P. Mushak, Health risks from extractive industry wastes: In: R. Prost (ed.), Contaminated Soils, Proc. 3rd Int. Conf. Biogeochemistry Trace Elements, Paris (France), May (1995) pp 15.

46. D.T.E. Hunt, A.L. Wilson, The Chemical Analysis of Water: General Principles and Techniques, 2nd Ed. (1987).

47. M. Trojanowicz, P.J. Worsfold, J.R. Clinch, TrAC Trends in Analytical Chemistry Solid-state photometric detectors for flow injection analysis Volume 7, Iss. 8 September (1988) pp 30.

48. J. Ruzicka, G.D. Marshal, Anal.Chim. Acta, 237 (1990) pp 329.

49. A. Economou, P.D. Tzanavaras, and D.G. Thelmelis, J. Chem. Educ. Vol. 82 No 12 Dec., (2005) pp 1820.

50. R.B.R. Mesquita, A.O.S.S. Rangel, Anal.Chim. Acta. Vol. 648, Iss. 1, 19 August, (2009), pp 7.

51. T.D. Waite, "Mathematical modeling of trace element speciation," In Trace Element

Speciation: Analytical methods and problems, G.E. Batley, editor, CRC Press. Inc. Boca Raton, Florida, (1989) pp 117.

52. E. Lombi, G.M. Hettiarachchi, and K.G. Scheckel, J. Environ. Qual.Vol. 40 (2011) pp 659.

53. J.W. Ball, D.K. Nordstrom, and E.A. Jenne, "Additional and revised thermochemical data and computer code for WATEQ2, A computerized chemical mode for trace and major element speciation and mineral equilibria of natural waters," U.S. Geologoical Survey Water Resources Investigations Report, pp 78.

54. B. Michalke, Ecotoxicology and Environmental Safety Vol. 56 Iss. 1 Sept., (2003) pp 122.

55. L. Enzo, M. G. Hettiarachchi, and K.G. Scheckel, J. Environ. Qual.Vol. 40, (2011) pp 659.

56. M.G. Keizer, W.H. van Riemsdijk, ECOSAT: A computer program for the calculation of speciation and transport. User Manual Version 4.7. Wageningen University. The Netherlands, (1999) pp 76.

57. W. D. Schecher and C.T. Driscoll.: Water Resour. Res., 24(4) (1988) pp 533.

58. R. Cornelius, H. Crews, Caruso, and K. Heumann., Hand Book of Elemental Speciation Techniques and Methodology, John Wiley and Sons, (2003) Chichester.

59. Ph. Quivauviller, E.A. Maier, B. Griepink, Quality consideration of results of speciation in Bioinorganic Chemistry, John Wiley and Sons, Chichester, (1996) pp 195.

60. A. Economou, P.D. Tzanavaras, and D.G. Thelmelis, J. Chem. Educ. Vol. 82 No 12 Dec., (2005) pp 1820.

CHAPTER 3

On-line Speciation of Iron (II) and Iron (III) using a Spectrophotometric Sequential Injection Analaysis System.

3.1. Introduction

3.1.1. Basic information.

Iron (Fe) is a group 8 element discovered around 5000 BC with an average atomic mass of 55.845 ± 0.002 μ and an electron configuration of [Ar] $3d^6 4s^2$ [1]. It is named from *(ferrum)* a Latin word and assigned an atomic number of 26. It has a melting point of 1811 K and boiling point of 3134 K [1]. It is a metal in the first transition series characterized by oxidation states ranging between -2 to +6, with +2 and +3 being the most common ones. Its normal colour is lustrous silver-grey but display a rusty colour upon oxidation. It has a cubic crystal structure with a density of 7.86 g/cm^3 at 293 K [1].

3.1.2. Natural occurrence.

Table 3.1. Isotopes of Fe [1].

Isotope	Atomic mass	Natural abundance	Stable
54 Fe	53.940	5.84 %	Stable
56 Fe	55.940	91.754 %	Stable
57 Fe	56.935	2.119 %,	Stable
58 Fe	57.933	0.282 %.	Stable

Naturally occurring iron consists of four isotopes as given in Table 3.1. The most abundant isotope is ^{56}Fe and makes up 5% of the Earth's crust.

3.1.3. Applications of iron.

Iron contributes to 95 % of worldwide metal production. This is because of its low cost and strength, making it ideal to be used in engineering applications such as construction of machinery, machine tools, automobiles, hulls of ships, and structural components for buildings. Its forms alloys with other elements [2]. It has many other roles in industry [3] and biology [4].

3.1.4. Iron and its speciation.

Several FIA techniques have been exploited to effect chemical speciation [5], such as reversed injector loading technique [6] and sandwich techniques [7]. A combination with atomic absorption spectroscopy (AAS) was also demonstrated [8]. Another method used a redox reagent in one stream and no redox reagent in another [9]. In other cases, a selective indicator for each iron species was used [10]. Also, it should be noted that the use of automatic pre-concentration has been reported for the determination of ammonia, sulphate and Fe ions [11].

Kurodo et al [12] reported the simultaneous determination of Fe(III) and total iron by flow injection analysis. Oliveira et al.[13] were able to determine Fe(II) and Fe(III) using spectrophotometric method. Chemiluminescence was used to determine Fe(II), Fe(III) and total iron [14]. Differential pulse anodic stripping voltammetry in a flow-through configuration was used for iron speciation on a glassy carbon electrode [15].

Bermejo et al. [16], reported the use of techniques such as size exclusion chromatography and electrothermal AAS for the speciation of iron speciation. The theoretical background behind

(SIA) has been thoroughly discussed in Chapter 2 with its benefit clearly outlined. This chapter attempts to explore the possible adaption of SIA system that allows for a reliable, simple, and fast speciation of iron. In this SIA system, Fe(III) is first determined using the tiron, then the total iron, including the Fe(III) obtained via the oxidation of Fe(III) by H_2O_2.

3.2. Experimental.

3.2.1. Reagents solutions.

Every reagent used here was prepared using pure analytical reagent grades unless otherwise stated. Also, every analytical solution was prepared from de-ionised water (Modulab system, Continental water systems, San Antonio, TX).

3.2.1.1. Fe (III) stock solution.

A 500 mg/L Fe(III) stock solution was prepared by dissolving 2.1575g of $FeNH_4(SO_4).12H_2O$ (Merck) in the minimum quantity of 0.01 mol/L $HClO_4$. This was made up to 500 mL with the same acid. Working standard solutions in the range 0.05 to 120 mg/L were prepared from the stock solution by appropriate dilution using a 0.01 mol/L $HClO_4$.

3.2.1.2. Fe (II) stock solution.

A 1.755 g of $Fe(NH_4)_2(SO_4)_2.6H_2O$ were dissolved in a solution containing 10 mL concentrated H_2SO_4 and 25 mL of de-ionised water this was made up to 250 ml with de-ionised water to give a 500 mg/L Fe(II) stock solution. This solution was freshly prepared just before use and the standards were prepared in the range 0.20 to 100 mg/L.

3.2.1.3. Tiron solution (4.5- dihydroxy-1. 3-benzenedisulfonic acid).

A 0.1 mol/L tiron solution was prepared by dissolving 3.142 g of tiron in 100 mL of 0.07 mol/L $HClO_4$. A 2.5 x 10^{-3} mol/L tiron solution was prepared by dilution from the stock tiron

solution of 0.07 mol/L $HClO_4$. The $HClO_4$ was always freshly prepared before it could be used. This was to ensure that the quality of the overall results is guaranteed and should not be compromised by the decomposition of the critical reagents.

3.2.1.4. Hydrogen peroxide oxidising solution (H_2O_2).

A 1 % H_2O_2 was prepared by diluting 3.33 ml of 30 % H_2O_2 to 100 mL total volume by de-ionised water. This was also freshly prepared before it could be used.

3.2.1.5. (Perchlorate) $HClO_4$ carrier solution.

The 0.07 $HClO_4$ mol/L was prepared from 34.23 mL of the 70 % $HClO_4$ were diluted to 5 L with de-ionised water.

3.2.2. Apparatus.

The system for this project was assembled with components as described in Chapter 1 Fig. 1.7. and a Unicam 8625 UV-Vis spectrophotometer (Cambridge, UK) equipped with a 10mm Hellma-type (Hellma GmbH and Co., Mulheim/Baden, Germany) with a flow through cell (volume 80µL**)** [17]. The use of a valve to switch between the streams or the exploitation of the sandwich technique has been used. Fe(III) forms a complex with tiron in a 1:1 ratio that was monitored with a UV-Vis spectrophotometer at 667 nm. The proposed SIA system operated according to Fig. 3.1 for the speciation of iron includes the following procedures:

(i) determination of Fe(III) using valve ports 1-3,

(ii) the oxidation of Fe(II) to Fe(III) involving valve ports 4-6, and then,

(iii) valve ports 7-9 for total iron determination.

sample	Tiron	detector	wash carrier	sample	H_2O_2	← mixing	tiron	detector
←	←	→	←	←	←	→	←	→
3s	3s	25s	4s	3s	3s	7s	3s	119s

Figure 3. 1. Sequence of pump direction and time of operation for the Fe(II) total Fe speciation.

Fig. 3.1 above gives an abridged version of the programmed sequence of the Fe speciation steps, which are also given in an expanded form in Table 3.2. The optimized parameters are expected to meet the requirements for the speciation of Fe. Careful attention was given to this and all the data given (relative peak heights) in the optimisation of both physical and chemical parameters the relative standard deviation (% RSD) computed. Fig.3.2 displays the results in the form of independent and well resolved peaks for Fe^{2+} and total Fe.

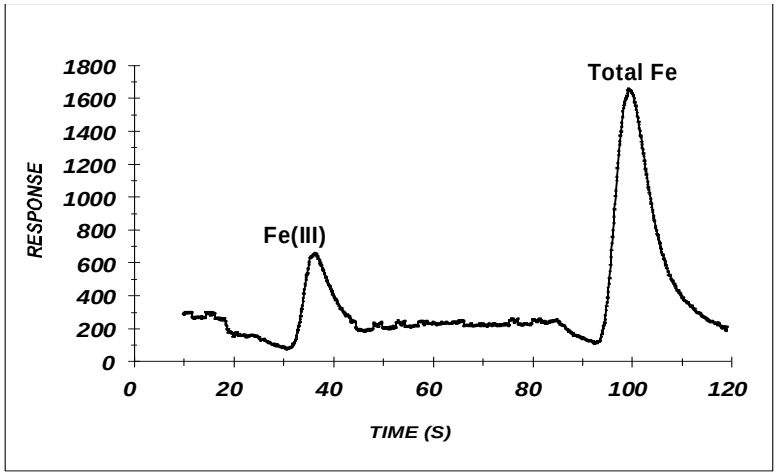

Figure 3.2 Graph depicting the peak profiles for the Fe species.

3.2.3. Procedure.

Table 3.2. Sequence of pump action and direction for iron speciation.

Time (s)	Pump	Valve	Description
0.0	**Off**	**Sample**	**pump stop, select sample stream (valve position 1)**
2.0	**Reverse**		**draw up sample solution**
5.0	**Off**		**pump stops**
6.0		**Tiron**	**select tiron stream (Advance valve to position 2)**
7.0	**Reverse**		**draw up tiron solution**
10.0	**Off**		**pump stops**
11.0			**advance valve to position 3**
12.0	**Forward**		**forward mixture (tiron & sample)**
36.0	**Off**		**pump stops**
37.0	**Carrier**		**advance valve to position 4**
38.0	**Reverse**		**draw up carrier solution**
42.0	**Off**		**pump stops**
43.0	**Sample**		**select sample stream (advance valve to position 5)**
44.0	**Reverse**		**draw up sample stream**
47.0	**Off**		**pump stops**
48.0		**H_2O_2**	**select H_2O_2 stream (advance valve to position 6)**
49.0	**Reverse**		**draw up H_2O_2 solution**
52.0	**Off**		**pump stops**
53.0			**advance valve to position 7**
54.0	**Forward**		**automatic mixing of H_2O_2 and sample**
61.0	**Off**		**pump stops**
62.0	**Reverse**		**automatic mixing of H_2O_2 and sample**
72.0	**Off**		**pump stops**
73.0	**Off**		**pump off, select tiron stream (valve position8)**
74.0	**Reverse**		**draw up tiron solution**
77.0	**Off**		**Stops**
78.0			**advance valve to position 9**
79.0	**Forward**		**forward mixture (tiron & oxidised sample) to detector**
120.0	**Off**		**pump stops**

3.3. Optimization, results and discussion.

The results were obtained by the mean of ten repetitions for each determination. The optimum wavelength was found to be 667 nm after running the complex solution of iron-tiron over the 300-700 nm window to make sure that the two species are catered for. This would help with finding solutions and making the necessary interventions to the negative effect of interferences. Considering that some of the physico-chemical properties are mutually shared between the quantification of Fe(III) and total iron, it is necessary to be cautious in the optimisation step to cater for both.

3.3.1. Physical parameters.

From the physical parameters, it is possible to establish both the degree of dispersion and zone penetration since the zones of the reagent, sample or product are driven to the detector via the system's flow conduits. The system relies on absorbency, which is converted into peak heights, and so any factor that may affect either the nature or the size of the peak should be deemed pivotal to the optimum performance of the system. It is very important that these these parameters are subjected to full optimization with the view to obtaining the most suitable mixing of the zones and obtain the right quantity of the detectable species.

3.3.1.1. Holding coil physical parameters.

The holding coil is the region where different zone stacking occurs. The way in which these zones are stacked determines the mixing as well as the penetration of these zones since they are pushed to the reaction coil, ultimately impacting on the final response of the system [18]. The impact of this parameter is depicted in Figs. 3.3 (a) and 3.3 (b), and the internal diameter chosen was 1.02 mm as it displayed the lowest % RSD with a good relative peak height.

Optimization for internal diameter (i.d) and length (L) holding coil (HC)

Peak height	i.d (mm)	% RSD
2.768	1.65	1.835
2.57	1.6	1.98
2.3019	1.14	0.8614
2.1168	1.02	0.4361
1.836	0.76	0.731

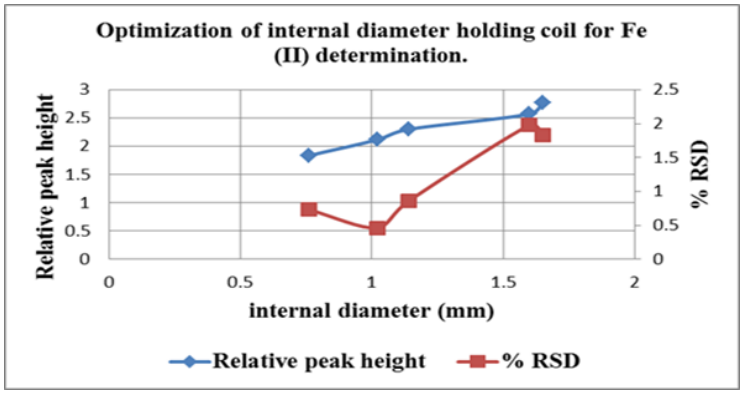

Figure 3.3. (a) i.d optimization for [Fe (II)] determination.

Peak height	i.d (mm)	% RSD
3.4811	1.65	1.032
3.2679	1.6	0.674
2.9885	1.14	0.884
2.886	1.02	0.2318
2.6934	0.76	0.9431

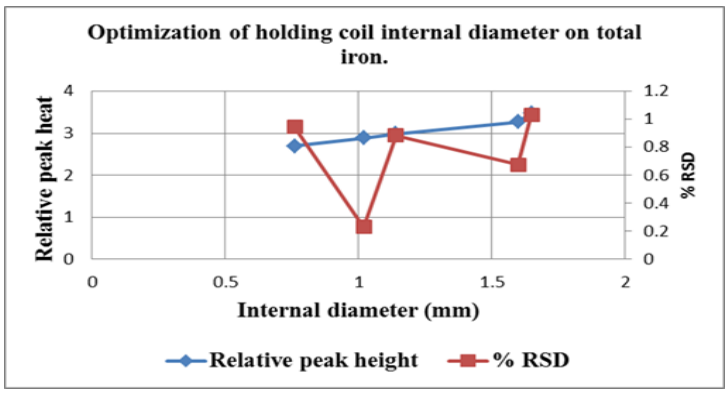

Figure 3.3. (b) (HC) i.d optimization for total (Fe) determination.

Peak height	**Length (m)**	**% RSD**
0.870	1.5	1.010
2.06	2.0	0.880
1.980	2.5	0.880
2.1168	3.0	0.436
2.276	3.5	1.360

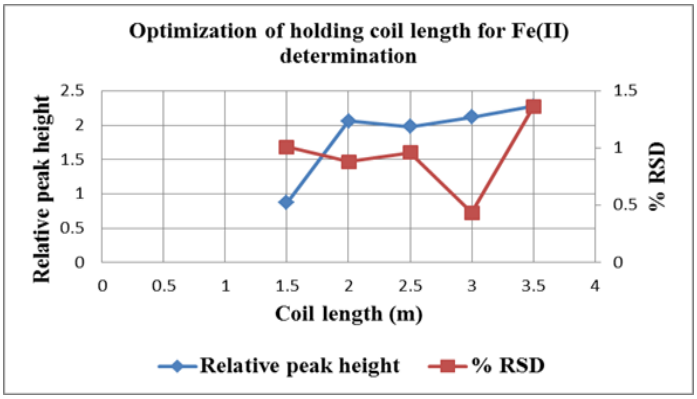

Figure 3.4. (a) (HC) L optimization for Fe(II) determination.

Peak height	**Length (m)**	**% RSD**

1.54	1.50	0.97
3.096	2.00	1.02
2.781	2.50	1.60
2.9885	3.00	0.88
3.163	3.50	0.84

Optimization of holding coil length for Fe(II) determination as displayed in Figs. 3.4. (a) and 3.4. (b) gave the best results for the coil length as 3m.

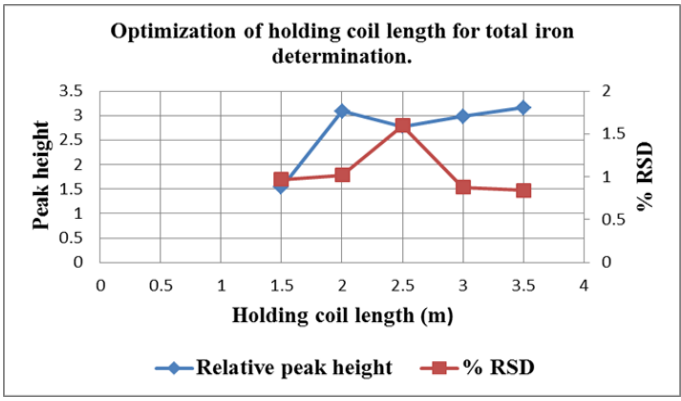

Figure 3.4. (b) (HC) L optimization for total Fe determination.

3.3.1.2. Physical parameters for reaction coil (RC).

The physical parameters should be regarded as a crucial part of the SIA system since it determines the SIA region where chemical reactions occurs and produces the main colour which is utilized in monitoring the target analyte. Indeed, the reaction coil should be sufficiently long to permit the development of the colour and restrict excessive dispersion.

The optimization of reaction coil i.d and length.

Peak height	i.d (mm)	% RSD
2.3019	0.025	0.1614
2.4985	0.03	1.36
2.9811	0.64	2.4
3.014	0.76	1.6

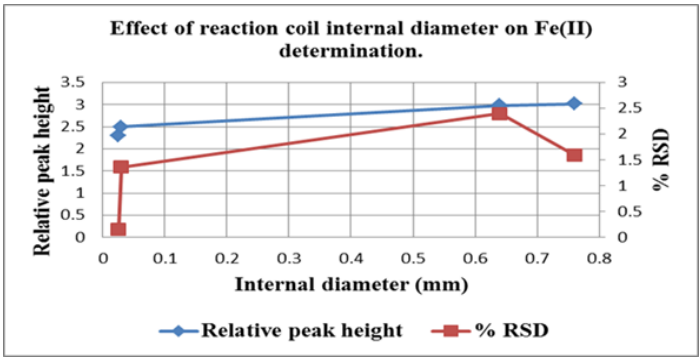

Figure 3.5 (a) Optimization of (RC) i.d on Fe (II) determination.

Figs.3.5 (a) and 3.5 (b) were evaluated for optimum internal diameter for the reaction coil and 0.76 mm was identified as the best internal diameter.

Peak height	i.d (mm)	% RSD

3.4811	1.65	1.032
3.2679	1.6	0.674
2.9885	1.14	0.884
2.886	1.02	0.931
2.7322	0.76	0.458

Figure 3.5. (b) Optimization (RC) i.d on total Fe determination.

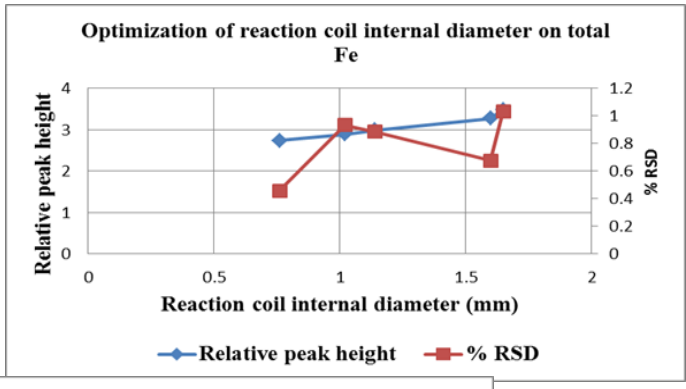

Optimization of reaction coil length.

Peak height	**(RC) length(m)**	**% RSD**
2.3019	0.6	0.161
1.9804	0.8	1.33
1.7658	1	1.36
1.58	1.2	0.8

Figure 3.6. (b) Optimization (RC) L on total determination.

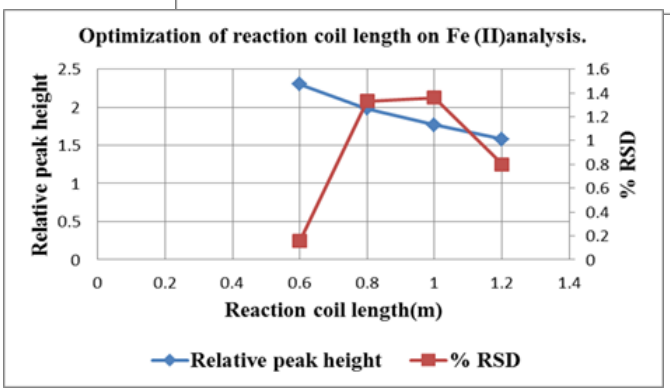

Figure 3.6. (a) Optimization (RC) L on Fe (II) determination.

Results from Figs.3.6. (a) and 3.6 (b) as the optimum length for the reaction

Peak height	**Length (m)**	**% RSD**
2.441	0.6	0.361
1.896	0.8	0.974
1.685	1	1.02
1.553	1.2	0.81

Fe gave 0.6 m coil.

3.3.1.3. Oxidation coil (OC) length and internal diameter optimization.

The oxidation coil is important for total iron (oxidised Fe(II) + original Fe(III). The coil must provide sufficient internal area to permit sufficient oxidation and limit dispersion of the oxidation product to the detector after colour development.

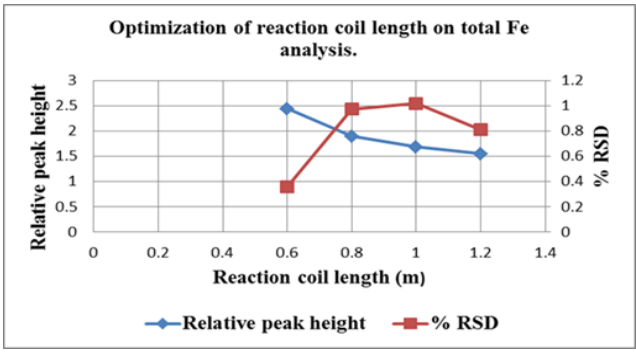

Peak height	i.d (mm)	% RSD

3.4811	1.65	1.232
3.2679	1.6	0.967
2.9885	1.14	1.088
2.886	1.02	0.944
2.856	0.76	0.411

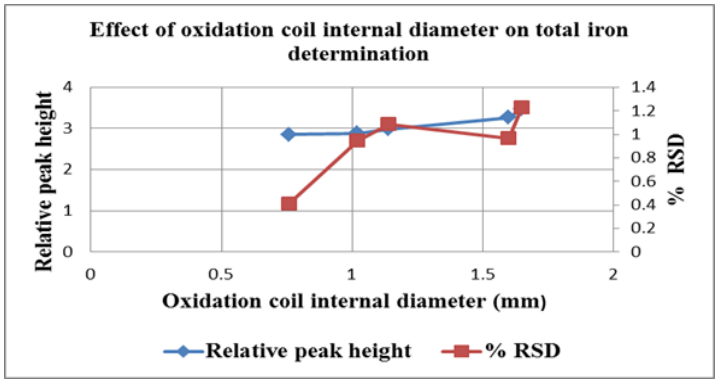

Figure 3.7. Effect of (OC) i.d on total iron determination.

Fig. 3.7 gave 0.76 mm as the best i.d for this analysis.

Peak height	**L (m)**	**% RSD**
2.71	1.20	0.61
2.72	1.10	0.63
3.23	1.00	0.51
3.14	0.90	0.68
2.98	0.80	0.96
3.12	0.70	0.53
3.31	0.60	0.47
2.53	0.50	2.48

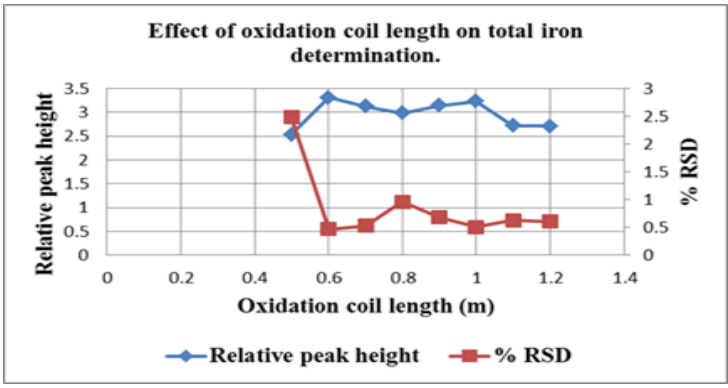

Figure 3.8 Effect of (OC) L on total iron determination.

0.6m was the best length of the oxidation coil for total Fe determination, this was shown in Fig. 3.8.

3.3.1.4. Flow rate.

The flow rate plays the role of controlling the rate of chemical reaction by supplying the reactants at a pre-determined rate. The reaction tiron-Fe(III) reaction occurs very fast resulting in an immediate colour development. At a very high flow rates (> 8 mL/min) the flowing stream of reagents is so rapid that the time required for for complex formation is restricted and consequently the final complex product obtained is insufficient, thus leading to low sensitivity of the system. This is why a slow flow rate was chosen.

The oxidation of Fe(II) is the rate-limiting step for this system and needs enough time for all the available Fe(II) or at least a higher percentage to be oxidized. It was then decided to use flow rate ranging from 1 to 7 mL/min to establish an optimum flow rate for this system. The flow rate of between 4 and 6 mL/min competed for the optimum flow rate. These two flow rates did not differ very much in terms of performance. It was decided to use 4 mL/min as this would also save the reagents as per Figs. 3.9 (a) and 3.9 (b).

Effect of flow rate on Fe(II) determination.

Peak Height	**Flow rate (mL/min)**	**% RSD**
2.2409	1	1.1
2.5897	2	1.3
2.8585	3	1.42
3.1337	4	0.613
3.377	5	1.02
3.7011	6	0.59
4.098	7	0.78

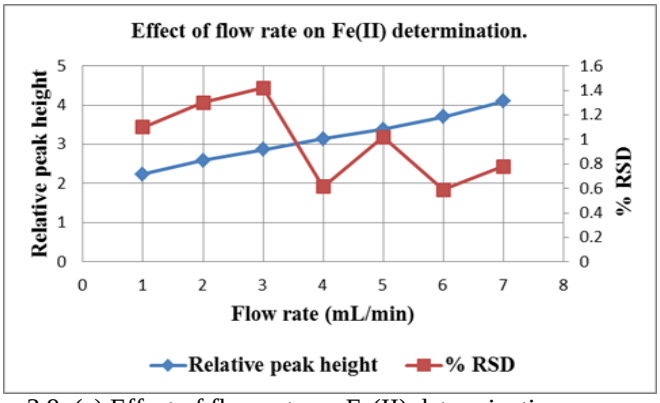

Figure 3.9. (a) Effect of flow rate on Fe(II) determination.

Figs. 3.9. (a) and 3.9 (b) show that 4 mL/min is the optimized flow rate.

Influence of flow rate on total iron determination

Peak Height	**Flow rate (mL/min)**	**% RSD**
2.8787	1	1.3
3.1986	2	0.97
3.3642	3	0.88
3.6985	4	0.387

3.9014	5	0.945
4.3886	6	0.988
4.6849	7	1.01

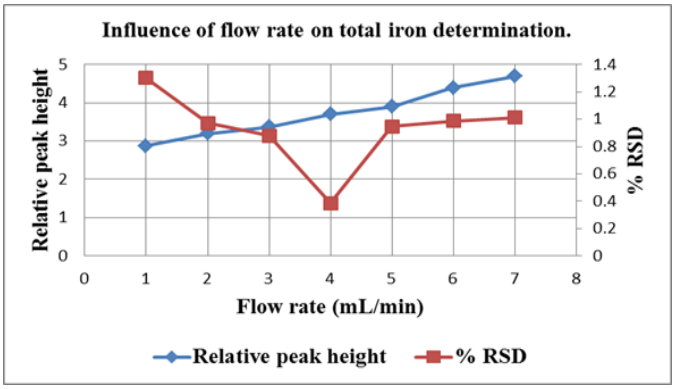

Figure 3.9. (b) Influence of flow rate on total iron determination.

3.3.1.5. Reagent and sample volumes.

The sample and reagent volumes are very important for the successive exploitation of the method. The objective was simply to determine the least consumption of the reagents without compromising on the best sensitivity and the widest possible linear range. The best setup is achieved when the colour reagent is in excess to ensure full reaction of all the available analytes.

Effect of sample volume, Figs. 3.10 (a) and 3.10 (b) gave 250 µL as optimum.

Peak Height	Sample (V)lume (µL)	% RSD
1.5117	180	0.209
1.8559	240	0.583
2.2133	300	0.870
2.7064	360	1.800
3.2022	420	2.800

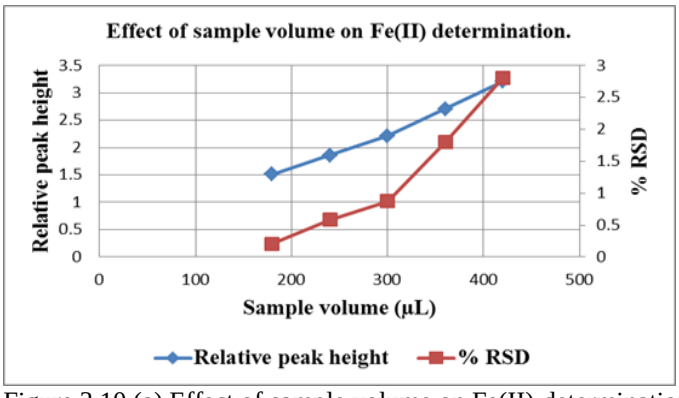

Figure 3.10 (a) Effect of sample volume on Fe(II) determination

Peak Height	Sample	% RSD

	volume (µL)	
1.7223	180	0.234
2.4785	240	0.518
2.6436	300	0.921
2.8751	360	1.031
3.5118	420	1.705

Influence of sample volume on total iron concentrations determination

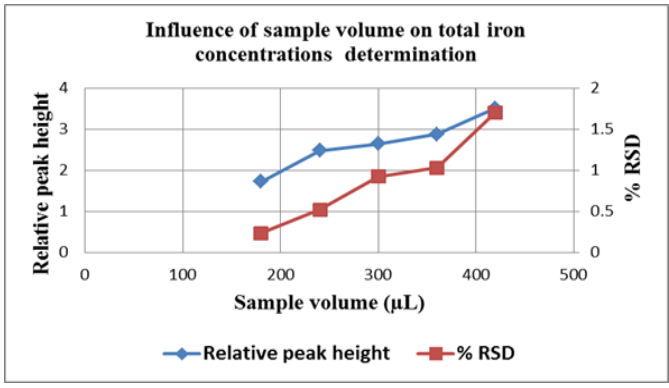

Figure 3.10 (b) Sample volume total Fe determination

Peak Height	Tiron volume (µL)	% RSD
1.51	150	0.22
1.65	200	0.38
2.28	250	0.31
2.81	300	0.87
3.28	350	1.38
3.53	400	0.79

Figure 3.11. (a) Tiron volume on Fe(II) determination.

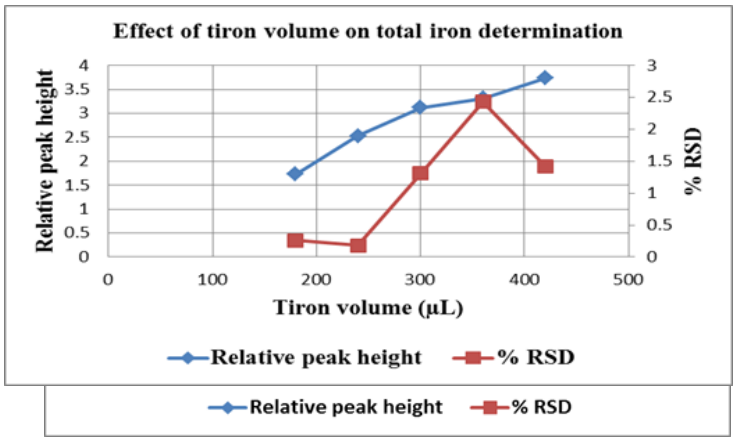

Figure 3.11. (b) Tiron volume on total (Fe) determination

Peak Height	Tiron volume (µL)	% RSD
1.73	180	0.26
2.53	240	0.18
3.12	300	1.31
3.31	360	2.43
3.73	420	1.42

Effect of tiron volume, from Figs. 3.11 (a) and 3.11(b) 250 µL was the optimized volume

3.3.2. Chemical parameters.

3.3.2.1. Colour reagent (tiron).

In general, when the concentration of the reagent increases, peak height (sensitivity) increases. However, at a very high concentration, the linear range and sensitivity of Fe(III) are reduced.

The concentration chosen should improve sensitivity, so that just the minimal change in the volume or concentration should result in a response that could be of analytical significance.

Effect of tiron concentration.

Peak height	Tiron (mg/L)	% RSD
1.3024	1.0 x 10 $^{-3}$	0.613
1.6311	1.5 x 10 $^{-3}$	0.581
2.2011	2.0 x 10 $^{-3}$	0.431
2.3117	2.5 x 10 $^{-3}$	0.588
2.2425	3.0 x 10 $^{-3}$	0.611

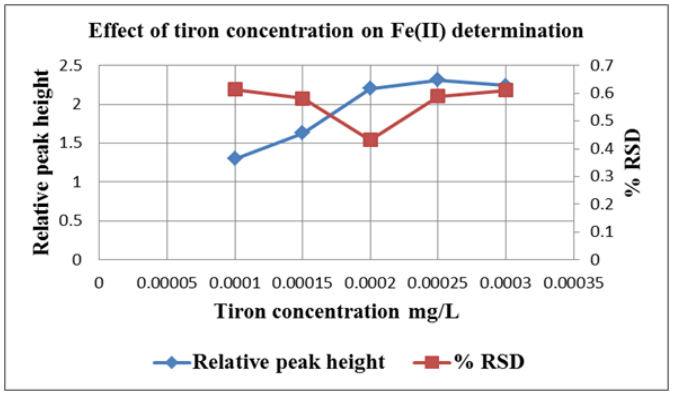

Figure 3.12 (a) Tiron concentration on Fe(II) determination.

Peak height	Tiron (mg/L)	% RSD
1.4833	1.0 x 10 $^{-3}$	0.722
1.7481	1.5 x 10 $^{-3}$	0.691
2.4028	2.0 x 10 $^{-3}$	0.564
2.7296	2.5 x 10 $^{-3}$	0.759
3.0977	3.0 x 10 $^{-3}$	0.821

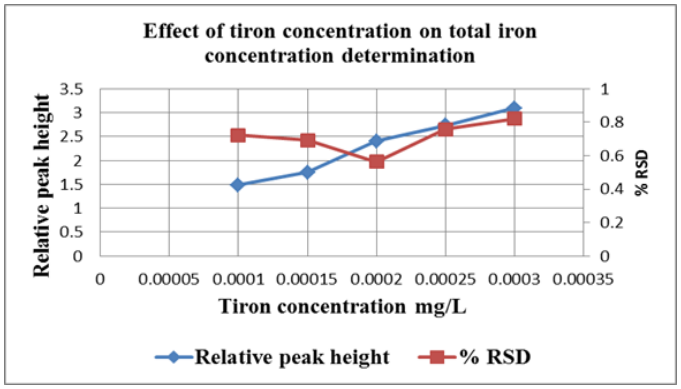

Figure 3.12 (b) Tiron concentration on total Fe determinations.

Figs. 3.12 (a) and 3.12(b) gave 2 x10^{-3} mg/L tiron concentration as ideal to be used.

3.3.2.2. Carrier type and concentration.

The ability to form a complex with a metal ion and conventional spectrophotometric reagents mostly depends on the pH of the reaction medium and the nature and concentration of the ligand, and this is prevalent with protonated ligands. The complexation of Tiron depends on

the type and concentration of the acid employed in the reaction. For this system, the effects of the acids at different concentrations were thoroughly investigated. It was found that H_2SO_4 and HNO_3 at 1mol/L and 2mol/L gave low sensitivity compared to $HClO_4$ at similar concentrations. Thus, in this work, $HClO_4$ (0.07 mol/L) was used.

3.3.2.3. Hydrogen peroxide.

Hydrogen peroxide is the oxidant or reagent that is responsible for the Fe(II) oxidation to the Fe(III) species which is then detected. Thus, it is very critical that every Fe(II) species present is completely oxidised by using an excess oxidant. As shown in Fig. 3.13, the oxidant was optimized with 1 % adopted as the optimum concentration for optimum performance and lowest % RSD.

Effect of H_2O_2 concentration on total iron determination

Peak height	H_2O_2 (mol/L)	% RSD
1.4258	0.5	0.861
1.9347	1.0	0.662
1.9441	1.5	1.92
1.9533	2.0	3.64

Figure 3. 13. H_2O_2 concentration on total iron determination.

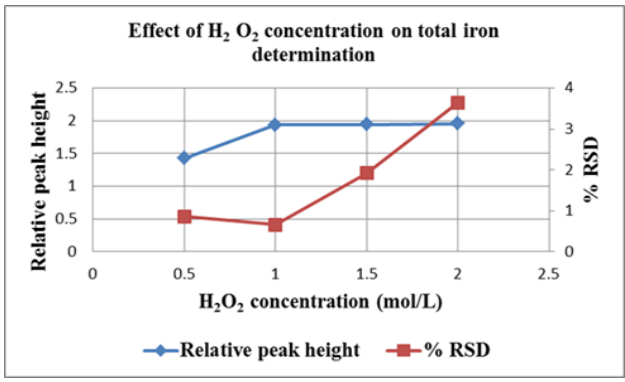

A 1 % H_2O_2 concentration as derived by Fig. 3.13 was chosen.

3.4. Evaluation of the SIA method.

The list of the different validation processes are as follows: linearity, sample frequency, accuracy, precision, detection limit and major interferences.

3.4.1. Linearity.

The linearity studies for the system for both Fe(II) and Fe(III) were carried out. The solutions were prepared by keeping the concentration of one species constant while varying the concentration of the other species. The equations of the calibration for Fe(II) and Fe(III) are follows: (a) Fe(III): $H_{Fe(III)} = 0.0487c + 0.3616$; r = 0.9993, n = 10.

Where H = peak height and c = Fe(III) concentration in mg/L

(b) Total iron: $H_{Total\ iron} = 0.0505\ c + 0.514$; r = 0.9996

Fig. 3.14 gives the calibration curve for the proposed system which is linear within 10.00 to 50.00 mg/L. However, this range could be greatly improved by appropriate manipulation of the system. For the samples that were analysed this range was quite sufficient. The Fe(III) concentration has to be slightly more since the oxidation step introduces some form of dilution.

Concentration (mg/L)	Peak Height Total Fe	Peak Height Fe^{3+}
10	1.71	1.23
20	2.223	1.61
30	2.81	1.96
40	3.38	2.37
50	3.96	2.74

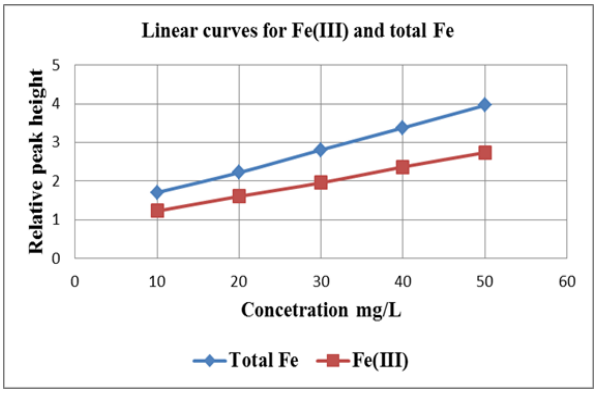

Figure 3. 14. Linear curves for Fe(III) and total Fe.

Table 3.3. Regression outputs for Fe^{2+} and total Fe.

Regression Output	Fe^{2+}	Total Fe
Constant	0.9586	1.235
Std Err of Y Est	0.0230	0.047
R Squared	0.9993	0.998
No. of Observations	5	5

Degrees of Freedom	3	3
X Coefficient(s)	0.049	0.052
Std Err of Coef.	0.001	0.001

3.4.2. Accuracy and precision.

Results from proposed SIA method were compared with thosed from standard methods. The results for this step are given in Tables 3.4 , 3.5 and 3.6 with % RSD included.

Table 3.4. Recovery studies for Fe (III) and Fe (II) from synthetic mixtures.

Added mg/L			Recovered mg/L		
Fe (III)	Fe (II)	Total (Fe)	Fe (III)	Fe (II)	Total (Fe)
0.00	50.00	50.00	0.00	49.96	49.96
10.00	40.00	50.00	10.00	39.88	49.88
20.00	30.00	50.00	20.00	29.95	49.95
30.00	20.00	50.00	30.00	19.98	49.98
40.00	10.00	50.00	40.00	9.97	49.97
50.00	0.00	50.00	50.00	0.00	50.0

Table 3.5. Results from effluent water samples.

Effluent	Concentration in mg/L					
	Proposed method			Standard method		
				Titration		AAS[1]
Water samples		Fe(11)	Total (Fe)	Fe(111)	Fe(11)	Total(Fe)

		Fe(111)					
Sample A		30.00	2.00	32.00	29.58	1.85	31.88
	% RSD	0.58	-	0.73	1.64	2.16	1.34
Sample B		35.00	3.00	38.00	34.60	3.00	38.20
	% RSD	0.84	-	0.64	1.81	2.35	1.67
Sample C		19.00	0.85	19.85	19.00	0.90	20.00
	% RSD	0.56	-	0.48	2.53	2.01	1.36

Sample A (First processing site Iscor plant), Sample A (Second processing site Iscor plant) Sample C (last refinery Iscor plant) and AAS[1] atomic absorbtion spectroscopy.

Samples		Concentration in mg /L					
		Proposed method			Standard method		
		Fe(III)	Fe(II)	Total Fe	Fe(III) [19]	Fe(II) [20]	Total Fe by AAS [21]
Weetol		13.00	50.00	63.00	13.40	49.65	64.00

iron extract	% RSD	0.81	-	0.63	1.34	1.66	1.14
Vital for women		2.00	4.50	6.50	1.60	4.00	6.00
	% RSD	1.24	-	0.76	1.84	0.98	1.13
Vital for pregnant women		2.00	7.30	9.30	1.95	7.00	8.98
	% RSD	0.66	-	0.56	2.33	2.18	1.10
Bettaway iron extract		12.00	40.00	52.00	11.87	39.79	52.00
	% RSD	0.91	-	0.75	2.18	3.11	2.14
Bettaway sports man		12.30	30.00	42.30	12.18	30.05	42.8
	% RSD	0.38	-	0.84	2.33	1.35	1.22
Sample A		30.00	2.00	32.00	29.58	1.85	31.88
	% RSD	0.58	-	0.73	1.64	2.16	1.34
Sample B		35.00	3.00	38.00	34.60	3.00	38.20
	% RSD	0.84	-	0.64	1.81	2.35	1.67
		19.00	0.85	19.85	19.00	0.90	20.00
	% RSD	0.56	-	0.48	2.53	2.01	1.36

Table 3.6. Results from real samples.

Sample (A) and Sample (B) obtained from Pharmaceutical chemistry honors preparation project.

3.4.3. Detection limit.

The detection limit for this system would mean the lowest concentration of each iron species that the proposed method can distinguish from the base-line with a 97 % certainty. The detection limit can be calculated from the following equation :

$$\text{Detection limit} = \frac{(3\sigma + K)(K - c)}{m}$$

where σ represents the RSD of the baseline, K is the average signal value of the baseline, c is the intercept while m is the slope of the calibration curve. The obtained limits of detection were 0.10 mg/L for Fe(II) and 0.20 mg/L for Total Fe.

3.4.4. Sample interaction and frequency.

SIA is a highly automated system, and the incorporation of the wash solution is aimed at reducing the carry-over effect. The was solution greatly increases the rate of analysis since rinsing can be automatically performed between the consecutive analysis. The SIA system proposed in this work can simultaneously monitor both Fe(III) and Fe(II) species at a rate of 30 samples per hour.

3.4.5. Major interferences.

The effects of the various ions (both cations and anions) which are commonly associated with the Fe were studied. Various synthetic samples were spiked with known amounts of the ions and then their tolerance for these interfering or foreign ions investigated (Table 3.7 gives the results obtained). The level at which these foreign ions is tolerated (tolerance level) is determined as its concentration o that causes a shift in the response of not greater than 2 %. For this system, none of the foreign species showed any detectable inteference except Cu ion that showed intereference when its concentration was more than half of the concentration of the total iron. Ti and Pb showed strong interference but it should be noted that neither Ti nor Pd is known to co-exist with Fe. However, should the sample matrix contain these two ions, they can easily be eliminated by appropriately masking them or pre-separating iron from mixtures by the use of mesityl oxide [13].

Table 3. 7. Effect of interferences [20].

Ion	Interferent (mg L^{-1}) [a]	% Recovery
Cu (11)	100	104
Mg (11)	100	99.0
Zn (11)	100	103
Na	100	97.1
Cl^-	100	102
SO_4^{2-}	100	98.7
CO_3^{2-}	100	86.1
OH^-	100	95.3

3.5. Statistical comparison between the two methods.

The comparison was done between the proposed SIA method and the Titration method to see whether the two methods gave the same results at the 95% confidence level. The t-test with multiple samples (paired differences) was applied to examine whether the two methods for total iron determination differ significantly at the 95% confidence level. The results are summarised in Table 3.4 for the first five pharmaceutical samples. The mean of the tabulated differences was : $\overline{x}D = 0.554$ and the sample standard deviation was $S_d = 1.4711$. For the Null hypothesis [22] we can conclude that the two methods agree only when the population mean difference is : H_0: $\mu_1 = \mu_2$. The alternative hypothesis, H_1 $\mu_1 \neq \mu_2$, implies the two-tailed test. There are five determinations (N-5), therefore $\nu = 4$. At the 95% confidence level $t_{0.025,4}$ is 2.78. The critical t-values are therefore ±2.78. Finally $t_{calculated}$ was computed to be 1.68 and

$t_{tabulated} = 2.78$. From observation $t_{calculated} < t_{tabulated}$ we therefore accept the Null hypothesis and reject the alternative confirming that the two methods give results with no significant difference.

3.6. Conclusions.

This thesis work has successfully opened up a whole new direction in speciation and proves the versatility of the SIA technique. The key objective of the proposed method has been achieved as SIA system has been successfully integrated into metal speciation. This approach has the advantage of using a single detector, thus limiting the need for numerous calibrations. The analysis time is highly reduced and the quantities of both the sample and the reagents are economically used.

SIA is a simple and low-cost system for the speciation of metals. The simplicity of the SIA's manifold makes it ideal for application in process streams, effluent solutions and in production lines. The proposed SIA method exhibited satisfactory accuracy, speed, precision, with very low sample interaction.

The application of sequential injection analysis for metal speciation is presented. The proposed method was used for the quantitative discrimination of the two iron species, Fe(II) and Fe(III). Tiron was used as the chromogenic reagent for Fe(III) and total iron after Fe(II) was oxidised to Fe(III) by H_2O_2 .The linear range, % RSD and detection limit show that the analytical performance is good. The method is fully computerized and able to run 30 samples per hour. The method is rapid and has a very high precision. The average % RSD for the analysis results was 0.55 for Fe(III) and 0.75 for total Fe.

3.7. References.

1. R. J. Forbes, Studies in Ancient Technology, IX, (1965) pp 247.
2. J. R. de Laeter; J. K. Böhlke; P. De Bièvre; H. Hidaka; H. S. Peiser; K. J. R. Rosman; P. D. P. Taylor (2003). Pure and Applied Chemistry. 75 (6) (2003) pp 683.

3. J.D. Verhoeven, Fundamentals of Physical Metallurgy, Wiley, New York, (1975) pp 326.
4. S.J. Lippard, J.M. Berg, Principles of Bioinorganic Chemistry, (1994) Mill Valley: University Science Books.
5. L. Campanella, K. Pyrzyńska, M. Trojanowicz., Talanta, Vol. 43, Iss. 6 June (1996) pp 825.
6. J.W. Dieker, W.E van der Linden, Anal. Chim. Acta.114 (1980) pp 267.
7. B.P. Bubnis, M.R. Straka, G.E. Pacey, Talanta 30 (1983) pp 841.
8. A.T. Senior, J.D. Glennon, Anal. Chim. Acta. 196 (1987) pp 333.
9. K. Rokuro, N. Tadashi, K. Oguma, Analyst 113 (1988) pp 1557.
10. A.T. Faizula, A. Townshend, Anal. Chim. Acta. 167 (1985) pp 225.
11. J.S. Cosano, M.D. Luque de Castro, M. Valcarcel, J. Automatic. Chem. Vol 15: No 4 (1993) pp 141.
12. R. Kurodo, T.T. Nara, K. Oguma, Analyst 113 (1988) pp 1557.
13. F.A. Oliveira, A.J. Nobrega, O. Fatibello-Fihlo, Talanta 49 (1998) pp 505.
14. E.G. Sarantonis, A. Townshend, Anal. Chim. Acta. 184 (1986) pp 311.
15. M.D Luque de Castro, Talanta 33 (1986) pp 45.
16. P. Bermejo, E. Pena, A. Dominguez, A. Bermejo, J.M. Fraga , J.A. Cocho, Talanta 50 (2000) pp 1211.
17. J.F. van Staden, H.Du Plessis, S.M. Linksy, R.E. Taljaard, B. Kremer, Anal. Chim. Acta. 354 (1997) pp 59.
18. J. Ruzicka, G.D. Marshall, G.D. Christian, Anal. Chem. 62 (1990) pp 1861.
19. A.I. Busev, G.P. Radrik, I.A. Tsurika, Zh. Anal. Khim. 25 (1979) pp 2151.
20. J. Martatti, F.J. Krug, L.C.R. Pessena, E.A.G. Zagatto, S.S. Jorgensen, Analyst 107 (1982) pp 659.

21. S. Blain, P. Treguer, Anal.Chim. Acta. 308 (1995) pp 425.
22. J.C. Miller, J.N. Miller., Statistics for analytical chemistry, New York : Ellis Horwood PTR Prentice Hall, (1993).

CHAPTER 4

Speciation of Mn (II) and Mn (VII) by spectrophotometric Sequential Injection Analysis.

4.1. Introduction.

Manganese stems from the Greek term (*magnes*) meaning magnet was isolated by Johann Gottlieb Gahn in 1774 and has an atomic number of 25 with its symbol as Mn [1]. It is a

silvery-grey metal and is the 12 th most abundant element on the earth's crust. It has a melting point of 1519 K and a corresponding boiling point of 2334 K with an electron configuration of [Ar] $3d^5 4s^2$ [2]. It has 25 isotopes ranging from Mn 44 to Mn 69 with the most abundant being Mn 55 followed by Mn 53 [2]. The average atomic mass from all these isotopes is 54.938 ± 0.000005 μ. The most prevalent oxidation states are Mn(II) and Mn(VII).

4.1.1. Application.

It is used in cosmetic products, manufacture of colourless glass, and as a black-brown pigment in paint as filler in. It is used in steel production and a variety of alloys as in aluminium for most beverage cans. Organo-manganese is used as an additive in gasoline to increase the octane content and prevent engine knock [3]. It also has important biological roles [4-6].

4.1.2. Manganese and its speciation.

It is of great importance to determine manganese in natural waters, domestic waters, industrial effluents, food, beverages and medicine. Ground and natural water bodies contain manganese as the results of the chemical erosion of the earth's crust and it occurs in various oxidation states [7, 8].

The undesirable effect of managenese even at low concentrations causes decolourisation of products, stains laundry, clogs pipelines and lead to black deposits [8]. Permanganate has several important industrial applications, for example as an oxidant in the organic chemical industry and in the cleaning preparation for the metallurgical industry. It forms the basis for classical qualitative and quantitative determination of manganese [6].

Several researchers have developed a variety of methods for the determination of manganese that include titrimetry, spectrophotometry, anodic stripping, differential pulse polarography,

and chemiluminescence [9-11]. Oxidation of manganese to permanganate serves as the basis for classical spectrophotometric manganese determination [12]. Although it is selective its disadvantage is low sensitivity. Analytical methods for manganese are mostly redox with photometric detection being the most common [13-16]. van Staden et al. used a lead (IV) oxide reactor in FIA [17] for the determination of manganese in natural waters and effluent streams. 4-(2-Pyridylazo)-resorcinol (PAR) and 4-(2-thialazo)-resorcinol (TAR) are phenol dyes frequently used for quantitative manganese analysis [18].

The aim of this chapter was to develop a simple, easy, stable, reliable and cost effective SIA system for the speciation of Mn(II) and Mn(VII) with PAR as the colour regent. The following sequence is followed in the procedure of this proposed SIA system. First Mn(II) is directly determined followed by the determination of the total manganese concentration after the reduction of Mn(VII) to Mn(II) by ascorbic acid.

4.2. Experimental.

4.2.1. Reagents and standard solutions.

All reagents were prepared analytically similarly to those as in Chapter 3.

4.2.1.1. [4(-2-Pyridylazo) resorcinol] (PAR) solution].

A 10^{-4} mol/L solution was prepared by dissolving 0.0022 g PAR in 100 mL phosphate buffer (pH 11.2) and 0.4199 g NaF (0.1 mol/L) was added to the PAR solution as a masking agent for Fe and Al.

4.2.1.2. Mn(II) solution.

A 100 mg/L Mn(II) solution was prepared by dissolving 0.0457 g $Mn(NO_3)_2 \cdot 4H_2O$ (Merck) in 100 mL of de-ionised water. This solution was standardised complexiметrically with EDTA (Ethylene diamine tetra acetic acid).

4.2.1.3. Mn(VII) solution.

A 100 mg/L Mn(VII) solution was prepared by dissolving 0.0288 g $KMnO_4$ in 80 mL of de-ionised water boiled for an hour, filtered through glass wool (a quarter of the filtering funnel) and quantitatively diluted to 100 mL with de-ionised water after it has cooled to room temperature.

4.2.1.4. Buffer solution.

Disodium phosphate (0.1 mol/L) solution and (0.1 mol/L) NaOH were appropriately mixed to in relevant volume ratios to prepare a buffer solution of pH 11.20.

4.2.1.5. Ascorbic acid solution.

The ascorbic acid solution was prepared by dissolving 0.1 g ascorbic acid in 100 mL of de-ionised water with a solution of pH 3.62.

4.2.2. Instrumentation.

The SIA system used was adapted from the one in Fig. 1.7 with appropriate adjustment and its exact operation and set up will be further discussed in section 4.3. All the data given (mean peak height values) are the average of 10 replications. Fig. 4.1 displays an abridged version of all the steps and timing for the speciation of manganese.

Sample	PAR	Detector	Wash carrier	Sample	Ascorbic acid	Mixing	PAR	Detector
3s	2s	25s	4s	3s	3s	15s	2s	119s

Figure 4.1.Summary of pump direction and period of operation.

4.3. Operation of the system.

The detailed device sequence of the proposed system is displayed in Table 4.1. The procedure is carried out by using the phosphate buffer with a pH of 11.20 as carrier. The sample is drawn up into the holding coil via port 1 followed by the PAR reagent via port 2 and the product forwarded via port 3 to the reaction coil 2, then finally to the UV-Vis spectrophotometric detector for monitoring the Mn^{2+} as the Mn^{2+}-PAR complex at 500 nm.

The carrier stream is then drawn through port 4, followed by the sample via port 5, and ascorbic acid as reducing agent via port 6 into the holding coil and then forwarding into a reduction coil 1 via port 7. The mixture from the reduction coil was then drawn via port 7 into the holding coil, followed by the PAR reagent through port 8 and forwarded to the detector via port 9 where it was monitored as the total Mn concentration which is Mn(II) and the Mn(VII) reduced to Mn(II)).

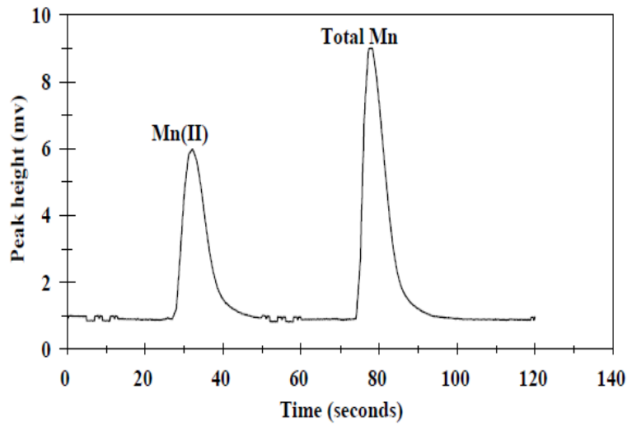

Figure 4.2. Peak profile for both Mn(II) and total (Mn).

Fig. 4.2 above clearly shows completely resolved peaks, with about 36 minutes as the first peak representing Mn(II) and the second peak which emerges at around 85 minutes for the total manganese.

Table 4.1. Shows direction and time operation of the pump.

0	**Off**	**Sample**	**Pump stops, select sample stream (valve position 1)**
2	**Reverse**		**Draw up sample solution**
5	**Off**		**Pump stops**
6		**Advance**	**Select 4-(2 pyridylazo-resorcinol) (valve port 2)**
7	**Reverse**		**Draws up 4-(2 pyridylazo-resorcinol)**
9	**Off**		**Pump stops**
10		**Advance**	**Valve advances to new position (valve port 3)**

11	**Forward**		**Pumps stacks of zone to detector**
35	**Off**		**Pump stops**
36		**Advance**	**Valve advances to new position (valve port 4)**
37	**Reverse**		**Draws up carrier stream**
41	**Off**		**Pump stops**
42		**Advance**	**Valve advances to new position (valve port 5)**
43	**Reverse**		**Draws up sample**
46	**Off**		**Pump stops**
47		**Advance**	**Valve advances to new position (valve port 6)**
48	**Reverse**		**Draws up ascorbic acid**
51	**Off**		**Pump stops**
52		**Advance**	**Valve advances to new position (valve port 7)**
53	**Forward**		**Forward mixture (ascorbic acid and sample) through port 7**
60	**Off**		**Pump stops**
61	**Reverse**		**Draws up (reduction product) into holding coil**
71	**Off**		**Pump stops**
72		**Advance**	**Valve advances to new position (valve port 8)**
73	**Reverse**		**Draws up 4-(2 pyridylazo-resorcinol)**
75	**Off**		**Pump stops**
76		**Advance**	**Valve advances to new position (valve port 9)**
77	**Forward**		**Forward mixture (reduction product and 4-(2 pyridylazo-resorcinol)**
119	**Off**		**Pump stops**
120		**Home**	**Valve moves to home position**

4.4. Optimisation, results and discussion.

Mn^{2+} complexes with PAR to form a red product under alkaline conditions and this is the basis for the proposed spectrophotometric SIA system.

Preliminary studies showed no considerable effect when different Mn(II): Mn(VII) ratios were used and a 1:1 ratio gave the best results. All the optimization steps outlined here were performed by mixing equal amounts of 0.4 mg/L solutions of Mn(II) and Mn(VII).

The optimisation steps involve those parameters that affect both parts of the system. All the data given (relative peak heights) and % RSD in the optimization steps are the mean values from 10 successive determinations.

4.4.1. Physical parameters.

The performance of the system reaches its peak when the all the physical parameters of both parts are optimised.

4.4.1.1. Holding coil (HC) optimum physical parameters.

Effect of holding coil length on Mn speciation determination

Peak Height	HC length (cm)	% RSD
0.791	150	0.986
1.985	200	0.797
1.877	250	0.801
2.085	300	0.424
2.199	350	1.348

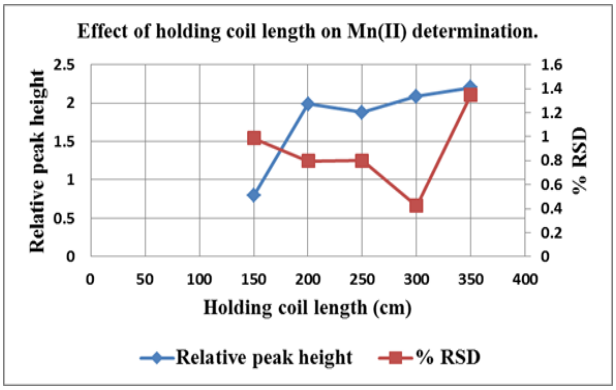

Figure 4.3 (a) HC length on Mn(II) determination.

From Figs. 4.3 (a) and 4.3 (b) showed that 300 cm (HC) length was best for this analysis.

Effect of holding coil length on total manganese determination

Peak Height	HC length (cm)	% RSD
1.486	150	0.975
2.985	200	0.987
2.674	250	1.583
2.668	300	0.816
2.968	350	0.933

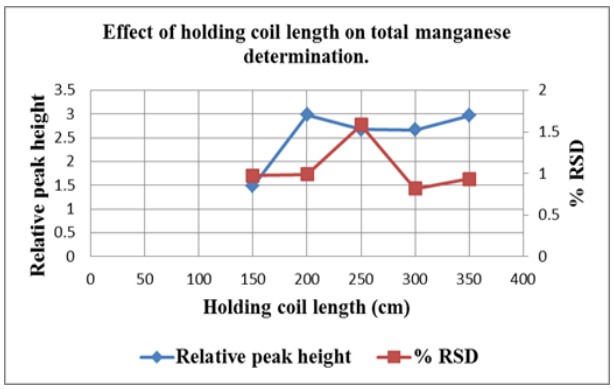

Figure 4.3 (b) HC length on total Mn determination.

Effect of holding coil internal diameter (I_D) on Mn(II) and total Mn determination.

Peak Height	HC (i.d) (mm)	% RSD
2.635	1.65	1.796
2.481	1.60	1.855
2.297	1.14	0.848
2.098	1.02	0.422
1.822	0.76	0.728

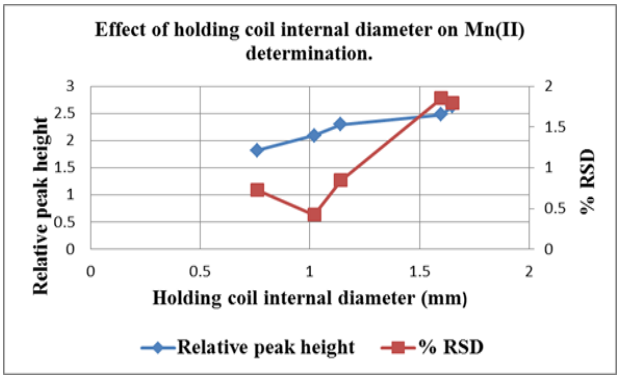

Figure 4.4. (a) HC (i.d) on Mn(II) determination.

From Figs. 4.4 (a) and 4.4 (b) the internal diameter for the holding coil chosen was 1.02 mm.

Peak height	HC (i.d) (mm)	% RSD
3.4334	1.65	1.019
3.2745	1.60	0.698
2.7757	1.14	0.848
2.5284	1.02	0.342
2.4465	0.76	0.857

Figure 4.4. (b) HC (i.d) on total Mn determination.

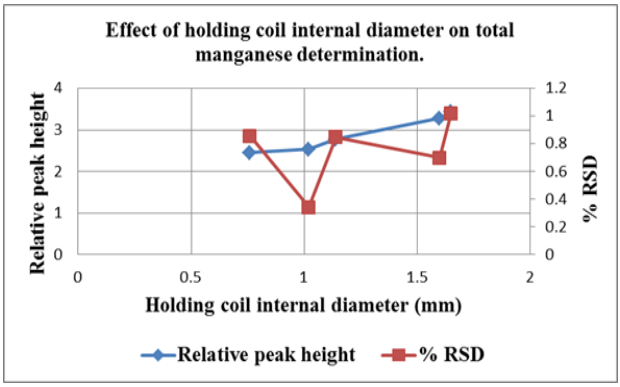

4.4.1.2. Reaction coil optimum physical parameters.

Effect of reaction coil length (L) on Mn(II) and total Mn determination.

Peak height	RC L (cm)	% RSD

0.7314	20	0.9788
1.6895	40	1.2364
2.2317	60	0.5976
2.0239	80	1.1097
1.9877	100	1.1988

Figure 4.5 (a) RC L on Mn(II) determination.

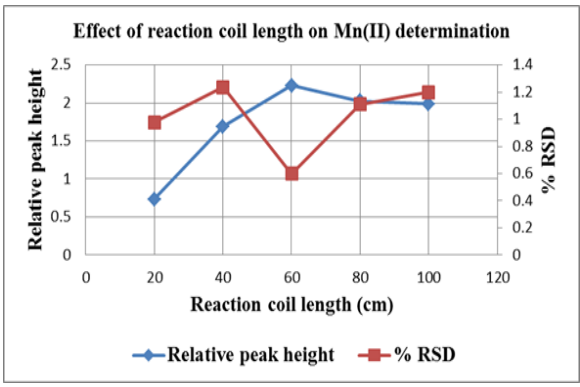

Figs. 4.5 (a) and 4.5 (b) confirmed the length of the reaction coil as 60 cm.

Peak height	RC L (cm)	% RSD
1.021	20	1.041
2.221	40	0.988
2.835	60	0.478
2.146	80	1.014
1.745	100	0.978

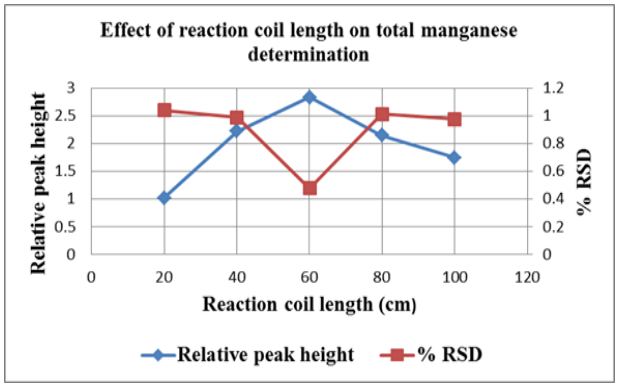

Figure 4.5 (b) RC L on total Mn determination.

Effect of reaction coil internal diameter (i.d) on Mn(II) and total Mn determination.

Peak height	RC i.d (mm)	% RSD
2.094	0.025	2.029
2.695	0.03	0.957
3.11	0.64	1.33
2.878	0.76	0.815

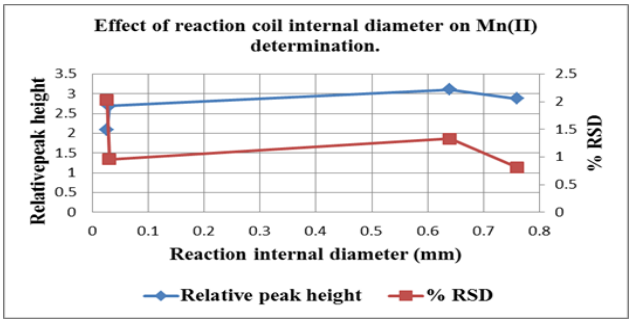

Figure 4.6 (a) RC i.d on Mn(II) determination.

Peak height	RC i.d (mm)	% RSD
2.763	0.025	1.963
2.941	0.03	1.021
3.054	0.64	0.947
2.855	0.76	0.581

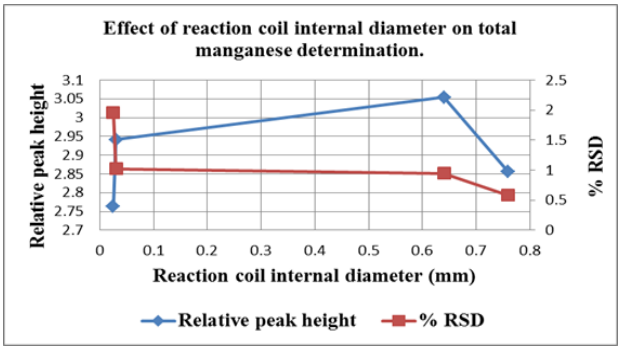

Figure 4.6 (b) RC (i.d) on total Mn determination.

0.76 mm was computed to be an ideal internal diameter for the reaction coil for this analysis as shown in Figs. 4.6 (a) and 4.6 (b).

4.4.1.3. Effect of sample volume.

Effect of sample (S) volume on Mn(II) and total Mn determination.

Peak height	(S) volume µL	% RSD
0.654	60	0.98
0.674	120	1.15
0.719	180	0.76
0.733	240	0.43
0.768	300	0.82

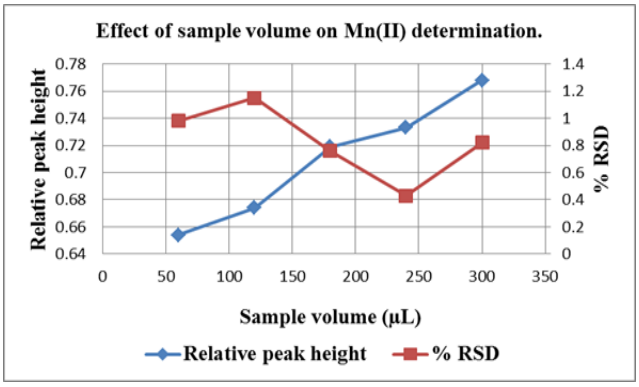

Figure 4.7 (a) Sample volume on Mn(II) determination.

Peak height	(S) volume µL	% RSD
1.259	60	1.051
1.275	120	0.974
1.284	180	0.73
1.311	240	0.497
1.290	300	0.811

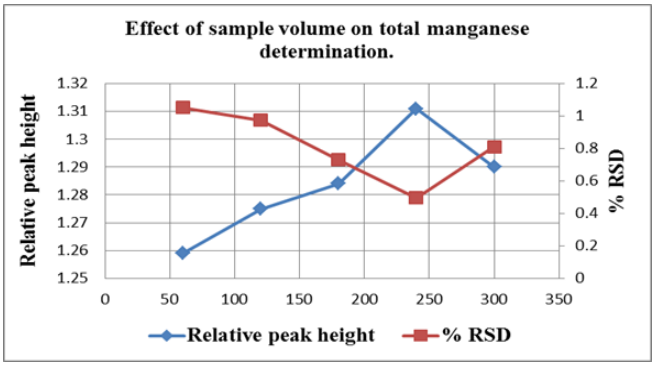

Figure 4.7 (b) (S) volume on total Mn determination.

The ideal sample volume identified for this analysis was 240 µl and was computed from Figs. 4.7 (a) and 4.7 (b).

4.4.1.4. Effect of colour reagent volume.

Effect of colour reagent volumes on Mn (II) and total Mn determination.

Peak height	PAR volume (µL)	% RSD
0.613	60	0.683
0.635	120	0.87
0.669	180	0.713
0.685	240	0.926
0.666	300	1.224

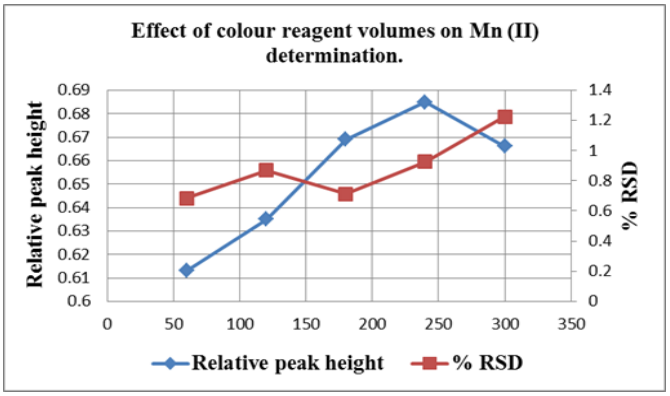

Figure 4.8 (a) PAR volume on Mn (II) determination.

Peak height	PAR volume (µL)	% RSD
0.988	60	0.586
1.143	120	0.984
1.226	180	0.367
1.316	240	0.935
1.336	300	0.748

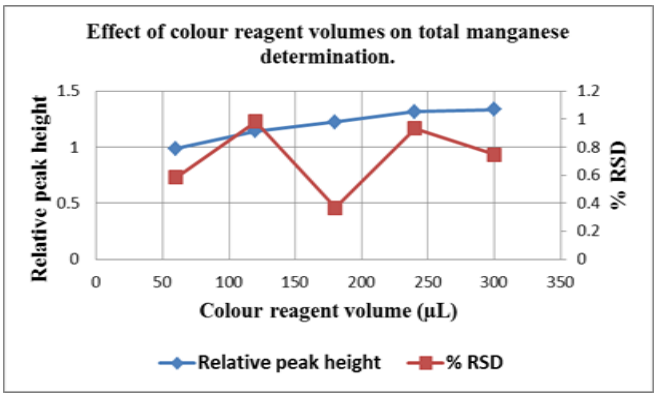

Figure 4.8 (b) PAR volumes on total Mn determination.

From Figs. 4.8 (a) and 4.8 (b) it was concluded the the most appropriate volume for the colour reagent (PAR) that sould be used is 180 µl.

4.4.2. Optimum Chemical parameters.

It is important to optimize the chemical parameters bearing in mind the economical use of reagents. The effect of PAR concentration was studied over the range 10^{-1} to 10^{-5} mol/L. 1 X 10^{-5} mol/L was identified from Figs. 4.9 (a) and 4.9 (b). The ascorbic acid concentration was

evaluated over the range (0.02 - 1.02) % where 1% was the optimum concentration shown in Fig. 4.11.

4.4.2.1. Effect of colour reagent concentration.

Effect of colour reagent (PAR) concentration on Mn(II) and total Mn determination.

Peak height	PAR (mol/L)	% RSD
0.568	$1X\ 10^{-6}$	0.957
0.659	$1\ X\ 10^{-5}$	0.234
0.733	$1\ X\ 10^{-4}$	0.724
0.748	$1\ X\ 10^{-3}$	1.065

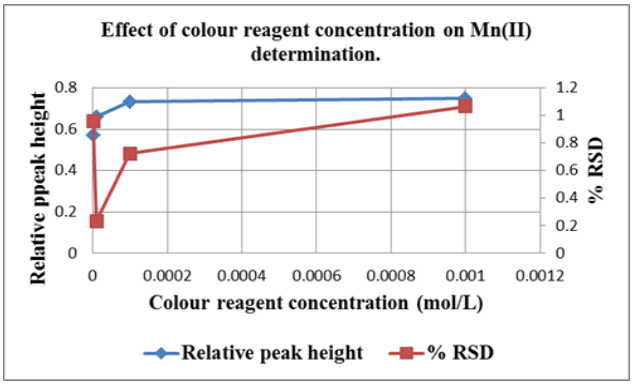

Figure 4.9. (a) PAR concentration on Mn(II) determination.

Peak height	PAR (mol/L)	% RSD
0,957	0.000001	0.698
1.235	0.00001	0.241
1.818	0.0001	0.921
1.246	0.001	1.298

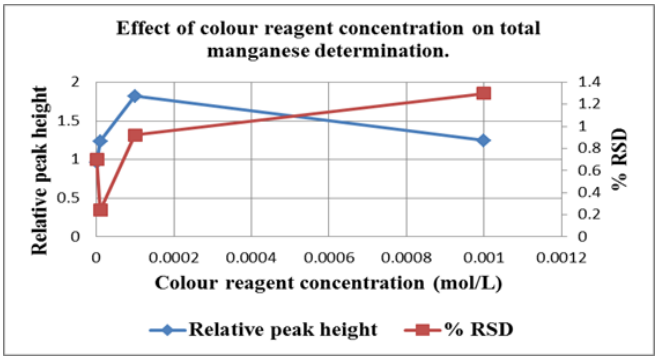

Figure 4.9. (b) PAR concentration on total Mn determination.

4.4.2.2. Influence pH.

Effect of pH on Mn(II) determination

Peak height	pH	% RSD
1.588	10.4	1.214
1.632	10.6	1.235
1.643	10.8	1.125
1.778	11.0	0.985
2.148	11.2	0.796
2.024	11.4	0.974
1.867	11.6	1.221

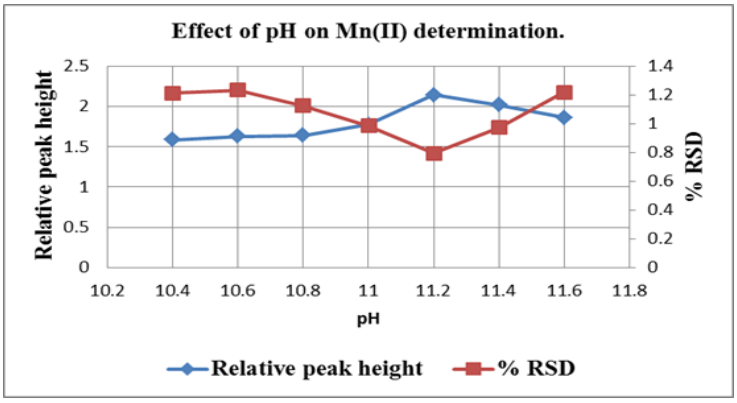

Figure 4.10 (a) Effect of pH on Mn(II) determination.

The buffer pH was varied from pH 10.5 to pH 11.5 and a pH 11.2 was chosen for this system as displayed in Figs. 4.10 (a) and 4.10 (b).

Peak height	pH	% RSD
1.013	10.4	1.245
1.421	10.6	1.281
1.601	10.8	1.297
1.841	11.0	1.011
2.931	11.2	0.684
2.664	11.4	0.971
1.776	11.6	1.235

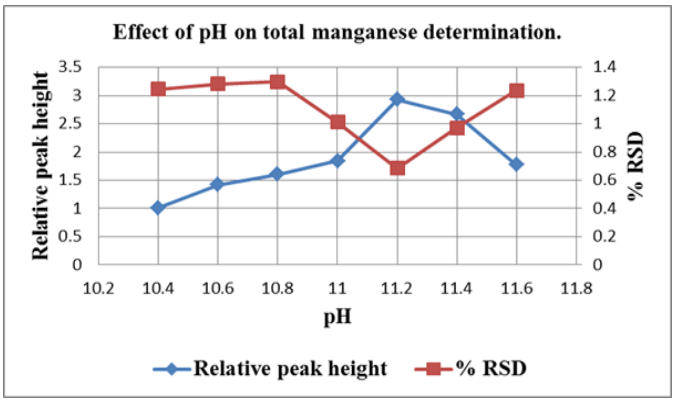

Figure 4.10 (b) Effect of pH on total Mn determination.

4.4.2.3. Ascorbic acid concentration.

Effect of ascorbic acid concentration on total manganese determination

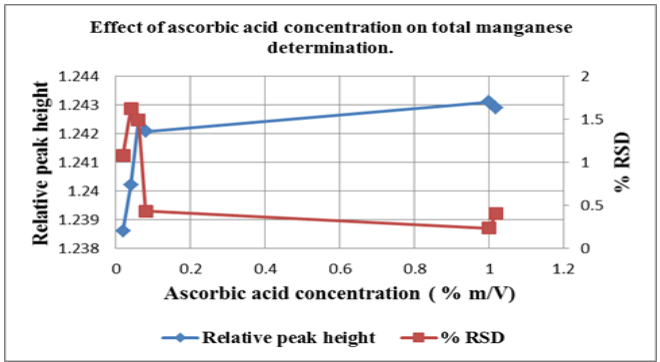

Peak height	Ascorbic acid (% m/V)	% RSD
1.2386	0.02	1.08
1.2402	0.04	1.62
1.2425	0.06	1.49
1.24207	0.08	0.43
1.2431	1.00	0.23
1.2429	1.02	0.40

Figure 4. 11 ascorbic acid concentrations on total Mn determination.

Fig. 4.11 shows the ideal ascorbic acid concentration as 1%.

4.5. Method evaluation.

In this work, the proposed method was subjected to critical evaluation with respect to parameters such as precision, linearity, accuracy, limit of detection, sample interaction, interferences with foreign ions, frequency of sampling, and recovery. The response for the spectrophotometric speciation of Mn(II) and Mn(VII) was obtained using the optimum conditions by employing the standard working solutions of Mn(II) and Mn(VII), respectively.

4.5.1. Linearity.

The linearity of the proposed SIA system was determined. All the other preliminary exercises yielded results that when computed could be determined to adhere to Beer's lambert law within the range (0.20–1.0) mg/L for both Mn(II) and total Mn. This is displayed in Fig.4. 12

Linear curve for total Mn and Mn(II).

Peak height Mn (II)	Peak height (Total Mn)	Concentration (mg/L)
0.6011	1.1671	0.2
0.8023	1.4721	0.4
1.0431	1.7698	0.6
1.245	2.0711	0.8
1.4544	2.4109	1

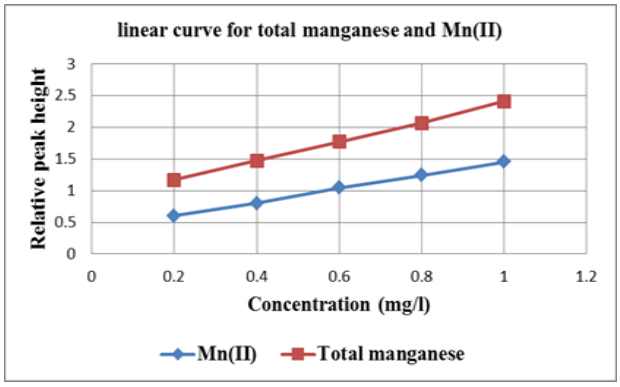

Figure 4. 12 Linear curve for total manganese and Mn(II).

The regression output indicating the relationship between the response and the concentration is given by the following:

Table 4.2. Regression output for Mn(II) and total Mn.

	Mn(II).	Total Mn
Constant	0.38439	0.8522
Std. Err. of Y - Estimated	0.0110	0.0145
R squared	0.9992	0.9994
No. of observations	5	5
Degrees of freedom	3	3
X. coefficient	1.0737	1.5433
Std. Err. of coefficient	0.0174	0.0224

4.5.2. Accuracy, recovery, precision and detection limit.

The accuracy of the proposed SIA system was first evaluated and validated by determining the

recovery of Mn(II) and Mn(VII) from known quantity of Mn(VII) to real samples with predetermined Mn(II) and Mn(VII), this was done in essence to follow the recovery

percentage of spiked samples (Table 4.4). Synthetic samples with known concentrations of the two manganese species as shown in Table 4.5 are also determined. Both these trials yielded very good recovery over 99 %.

As can be determined from the results in Table 4.3 the results of the proposed SIA system compare very well with those obtained a standard titration method for both species as well as AAS for total Mn. The % RSD was 0.27% for Mn(II) and 0.34% for total Mn. The detection limit (DL) for both Mn(II) and total Mn was calculated as from Chapter 3. The detection limits were 0.005 mg/L for Mn(II) and 0.008 mg/L for total Mn.

4.5.3. Sample frequency.

The sample frequency was 119 s per cycle.

4.5.4. Interferences.

If any chemical species was to complex with PAR then there will be less concentration of PAR available to react with the Mn (II).

Chemical masking of Fe and Al was achieved by a 0.1 mol/L NaF in the PAR reagent solution. Potential interferences from the other ions (Table 4.6) were negligible as their cocentrations were very low in the real water samples under investigation.

Table 4.3 Comparison of results from proposed SIA method, AAS, and the titration method

Sample	Proposed SIA method	AAS	Titration

	Mn(II) mg/L	Mn(VII)mg/L	Total Mn mg/L	Mn(II)mg/L	Mn(VII)mg/L
Mutshedzi	0.020 ± 0.002	0.063 ± 0.004	0.085 ± 0.002	0.017 ± 0.049	0.060 ± 0.038
Blesbok	0.018 ± 0.003	0.054 ± 0.006	0.076 ± 0.008	0.020 ± 0.041	0.052 ± 0.042
Crocodile	0.022 ± 0.001	0.083 ± 0.002	0.110 ± 0.006	0.021 ± 0.032	0.080 ± 0.042
Grootvlei	0.031 ± 0.007	0.096 ± 0.003	0.133 ± 0.004	0.028 ± 0.038	0.091 ± 0.031
SE1	0.411 ± 0.005	-	0.415 ± 0.011	0.395± 0.032	-
SE3	0.635 ± 0.003	0.038 ± 0.002	0.0675±0.052	0.625 ± 0.041	0.035 ± 0.022
SE4	1.022 ± 0.003	0.027 ± 0.002	1.050 ± 0.002	1.022 ± 0.019	0.026 ± 0.018

SE1, SE3 and SE4 are sample obtained from the pharmaceutical research laboratory from University of Pretoria.

Table 4.4: Recovery results after spiking with 0.2 mg Mn (VII).

Sample	Mn(VII) mg/L	Expected Mn(VII) mg/L	Recovered Mn(VII) mg/L	% Recovery
Blesbok	0.054	0.254	0.252	99.21
Grootvlei	0.096	0.296	0.295	99.66
SE1	-	0.200	0.198	99.00
SE3	0.038	0.238	0.236	99.16
SE4	0.027	0.227	0.226	99.56

Table 4.5. Recovery studies from synthetic samples by SIA method.

Added mg/L	Recovered mg/L

Mn(II)	Mn(VII)	Mn(II)	Mn(VII)
0.02	-	0.021± 0.004	-
0.06	1.20	0.059 ± 0.003	1.198 ± 0.004
0.12	1.00	0.198 ± 0.003	1.001 ± 0.002
0.16	0.16	0.160 ± 0.002	0.161 ± 0.004
1.00	0.12	1.001 ± 0.003	0.120 ± 0.003
1.20	0.06	1.198 ± 0.003	0.058 ± 0.002
-	0.02	-	0.020 ± 0.003

Table 4.6 interferences [19].

Species	Interference factor[a]
Ni(II)	1
Cui(II)	1
Hg(II)	1
Al(III)	0.99
Zn(II)	0.96
Cd(II)	0.97
Fe(III)	0.93
Co (II)	1.11

[a]An interference factor of 1.00 means there is no interference within 1 %, and anything above this values have a marked influence on the final value of the analyet.

4.5.5. Statistical evaluation.

From the statistical evaluation it was concluded that there is a very good correlation between the proposed SIA method and the two standard methods being AAS. For Mn(II) the $t_{calculated}$ = 2.20, and $t_{tabulated}$ = 2.447 while for total Mn $t_{calculated}$ = 0.036 and $t_{tabulated}$ = 2.571. Therefore, in both instances $t_{calculated} < t_{tabulated}$ meaning there is no signicant difference between the proposed SIA and AAS methods. The linear range was 0.20–1.0 mg/L for both Mn(II) and total Mn as per data from table of Fig. 4.12.

4.6. Conclusions.

An on-line sequential injection analysis system with spectrophotometric detection using 4-(2-pyridylazo) resorcinol was carried out for the speciation of Mn(II) and Mn(VII) as computed from total Mn. The sampling frequency is 30 determinations per hour. Chemical masking of Fe and Al was achieved by on-line addition of a 0.1 mol/l NaF solution were necessary [20]. The proposed system yielded results that compare very well with standard methods. 180 µL is very economic for reagents. There is no need for separation of the sample prior to the analysis rendering it a convenient procedure.

The proposed SIA method can be accepted as an analytical method for the speciation of Mn(II) and Mn(VII) with its good analytical performance displayed in Table 4.3, with comparable results to AAS. Recovery studies gave a high percentage Table 4.5.

4.7. References.

1. J. Meija, Atomic weight of the elements 2013 "(IUPAC Technical Report)". Pure and Applied Chemistry 88(3) (1998) pp 265.
2. W. Robert, Handbook of Chemistry and Physics. Boca Raton, Florida: Chemical Rubber Company Publishing, pp 110.
3. A.G. Minerals, Trace Elements and Human Health, Life Sciences Press: Tacoma (WA), (1996).
4. S. Bleich, D. Degner, B. Bandelow, A. Riegel, J.M. Maler, E. Ruther, J. Kornhuber, Ger. J. Psychiatry 3 (2000) pp 14.
5. K. Eder, A. Kralik, M. Kirchgessner, Biol. Trace Elem. Res. 55 (1996) pp 137.
6. D.G. Barceloux, J. Toxicol. Clin. Toxic. 37 (1999) pp 293.
7. H. Paquet, N. Clauer, Soils and Sediments: Mineralogy and Geochemistry, Springer, Berlin, (1998).
8. M.D. Cooper, P.K. Winter, I.M. Kolthoff, P.J. Elving, Treatise on Analytical Chemistry. Part II. Analytical Chemistry of the Elements, Vol. 7, Interscience, New York, (1962) pp 427.
9. I.M. Kolthoff, E.B. Sandell, E.J. Meehan, S. Bruckenstem, Qualitative Chemical Analysis, 4th Ed., Macmillan, London, (1969).
10. I.M. Kolthoff, R. Belcher, Volumetric Analysis, Vol. 111, Interscience, New York, (1957).
11. H.A. Laitinen, Chemical Analysis, McGraw-Hill, New York, (1960).
12. G.H. Jeffery, J. Bassett, J. Mendham, R.C. Denney, Vogel's Textbook of Quantitative Chemical Analysis, 5th Ed., Longman, Essex, UK, (1987).
13. L.J. Mallini, A.M. Schiller, Limnol. Oceanogr. 38 (1993), pp 1290.
14. M. Kamburova, Talanta 46 (1998), pp 1073.
15. N. Maniasso, E.A.G. Zagatto, Anal. Chim. Acta 366 (1998) pp 87.

16. M.F. Gine, E.A.G. Zagatto, H.B. Filho, Analyst 104 (1979) pp 371.

17. J.F. van Staden, L.G. Kluever, Anal. Chim. Acta. 350 (1997) pp 15.

18. U.G. Gaokar, M.C. Eshwar, Mikrochim. Acta 11 (1982) pp 247.

19. I.M. Kolthoff, E.B. Sandell, E.J. Meehan, S. Bruckenstem, Qualitative Chemical Analysis, 4th Ed., Macmillan, London, (1969).

20. G.D. Christian, Analytical Chemistry, 5th Ed., Wiley, New York, (1994).

CHAPTER 5

Simultaneous determination of Chromium (III) and Chromium (IV) by sequential injection analysis system

5.1. Introduction.

Chromium (Cr) has an atomic number of 24 and was discovered in 1797 by Louis Nicolas Vauquelin, it is a steely gray, lustrous, hard and brittle metal with its name derived from the Greek word “chroma” meaning colour [1]. It does not occur in nature as a free metal, but only as chromite ore. It has oxidation states in the range (Cr^{0} to $Cr^{6+)}$ and the most abundant has the atomic mass of 51.941 at 83.8 %. It has a Standard atomic weight of 51.996 μ with an electron configuration [Ar] $3d^{5}4s^{1}$, melting point 2180K, and a boiling point of 2944 K [2].

5.1.1. Application.

It is mainly used in the manufacture of stainless steel, surface coating and preservation of wood [3-5]. Chromite and chromium oxide are used in blast furnaces, cement kilns and metal casting [5]. Many of its compounds are used as catalysts and widely used to produce magnetic tapes for audio tapes and cassettes. Various chromium compounds are used as dyes and production of synthetic rubies [6].

5.1.2. Biological role.

Cr^{3+} is an essential element while Cr^{6+} is carcinogenic [7-9]. It also helps in the treatment of depression and polycystic ovary syndrome [10]. It has several biological roles such as growth, cholesterol control, and sugar level control [11-13].

5.1.3. Further chemistry of chromium and its speciation.

Chromium is naturally abundant, in other words, it is found in plants, water, soild, rocks, volcanic dusts and gases, and so on. The chromium species that is commonly found in water include the chromate (CrO_4^{2-}), cationic chromium (III) hydroxo-compounds ($Cr(OH)_2^{+}$) and organically bound or colloidally sorbed Cr (III) [10–12].

Elmahadi et al. used algae for chromium speciation analysis [13]. Several techniques for chromium speciation were carried out as through, human erythrocytes, Saccharomyces cerevisiae, and by microbore anion exchange column [14-16]. Some of the common methods for chromium speciation and the use of chemiluminiscence detector have been clearly outlined [17- 20]. FIA chromium speciation has also been demonstrated [21].

In this work, SIA with a single detector was proposed. The system operates by first measuring the amount of Cr (VI) species present, then followed by oxidizing the Cr (III) to its Cr(VI) via Cr (IV) to be determined as total chromium. The chosen spectrophotometric method relies on the specific reaction of diphenylcarbazide (DPC) with Cr (VI) [23]. The reaction is best conducted in acidic media where it gives an intense red–violet colour due to the formation of a complex cation which can be monitored at a wavelength of 548 nm. The reliability of the reaction is further enhanced as the ligand can only react very slightly with other transition metals to give a different colour to the Cr (VI) complex, thereby minimizing the risk of interferences.

5.2. Experimental.

5.2.1. Reagents and solutions.

A stock standard Cr (VI) solution (1000 mg/L) was prepared by dissolving 2.8288 g of potassium dichromate (Merck) in de-ionised water and quantitatively diluting to IL with de-ionised water. A stock standard Cr(III) solution was prepared similarly from 5.1123 g of chromium(III) chloride hexahydrate (Merck). Working standard Cr(III) solutions in the range 0.50–30.00 mg/L and working standard Cr(VI) solutions between 0.10 and 25.00 mg/L were prepared from the standard stock solutions. 98 % H_2SO_4 (Holpro Analytics) was used to prepare the 0.20 mol/L carrier solution. A 0.025 g/L Ce(IV) solution was prepared in 0.20

mol /L H_2SO_4. A solution of 2.5 g/L was prepared by first dissolving in the minimum amount of ethanol and diluting with a 0.20 mol/L H_2SO_4 to a litre of solution.

5.2.2 Sample preparation.

Each of the liquid samples used here was directly analysed without a prior preparation. A minimal amount of 6% (v/v) HCl was utilized to dissolve 10 tablets from the pharmaceutical formulation using controlled heating. When needed, more acid was added into the solution to allow for complete dissolution of the sample. A 50 mL of chloroform ($CHCl_3$) was employed for the extraction of the organic phase using a separating funnel, and this step was repeated twice. To achieve a complete separation, an additional 50 mL $CHCl_3$ was added to the aqueous layer and left overnight. The aqueous layer was collected and made up to volume with 0.20 mol/ L H_2SO_4 in a 100 mL standard volumetric flasks. These solutions were diluted to the working ranges with a 0.20 mol/L H_2SO_4.

5.3. Instrumentation.

The sequential injection system used for this work was assembled as in Fig. 1.7 with appropriate adjustment. The design of this system allows the simultaneous determination of Cr(VI) and total chromium. In essence from this set up it is then possible to calculate the concentration of Cr (III). Port 1 is the sample, port 2 diphenyl carbazide, then port 3 to the detector. This is followed by carrier (H_2SO_4) port 4, then sample at port 5, Ce(IV) port 6, port 7 oxidation coil, port 8 diphenyl carbazide and port 9 to the detector.

sample ←	**DPC** ←	**detector** →	**Wash carrier** ←	**sample** ←	**Ce(VI)** ←	← **mixing** →	**DPC** ←	**detector** →
3 s	**2 s**	**25 s**	**4 s**	**3 s**	**3 s**	**15 s**	**2 s**	**19 s**

Figure 5.1 Summary of pump action and period.

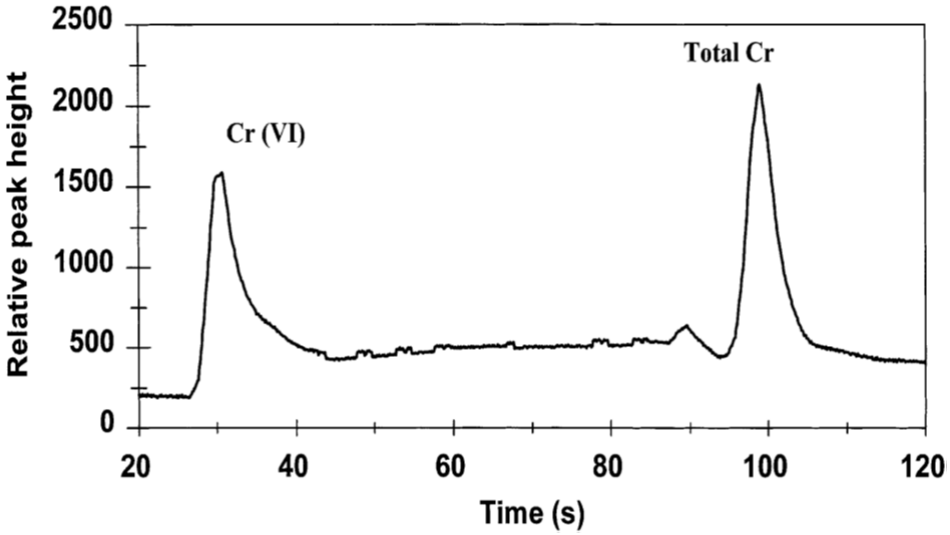

Figure 5.2. Peak profile of Cr(VI) and total chromium.

Fig. 5.1 shows the summary of pump action and period for this speciation and Fig. 5.2 clearly shows the well resolved and the distinct peaks for Cr(VI) and total Cr respectively. The two different peaks emerge at different times which are consistent to the design of the system as displayed in Table 5.1.

Table 5.1. SIA sequence for Cr(III) total chromium speciation for one cycle

Time (s)	Pump	Valve	Description
0	Off	Sample	Pump stops, select sample stream (valve position 1)
2	Reverse		Draws up sample solution
4	Off		Pump stops
5		Advance	Select DPC (valve port 2)

6	**Reverse**		**Draws up DPC**
9	**Off**		**Pump stops**
10		**Advance**	**Valve advances to new position (valve port 3)**
11	**Forward**		**Pump stacks of zones to detector**
35	**Off**		**Pump stops**
36		**Advance**	**Valve advances to new position(valve port 4)**
37	**Reverse**		**Draws up carrier stream**
41	**Off**		**Pump stops**
42		**Advance**	**Valve advances to new position (valve port 5)**
43	**Reverse**		**Draws up sample**
45	**Off**		**Pump stops**
46		**Advance**	**Valve advance to new position (valve port 6)**
47	**Reverse**		**Draws up Ce(IV) solution**
50	**Off**		**Pump stops**
51		**Advance**	**Valve advances to new position (valve port 7)**
52	**Forward**		**Forward mixture (Ce(VI) and sample) through port 7 into oxidation coil**
59	**Off**		**Pump stops**
60	**Reverse**		**Draws (oxidation product) into holding coil**
70	**Off**		**Pump stops**
71		**Advance**	**Valve advances to new position (valve port 8)**
72	**Reverse**		**Draws up DPC**
75	**Off**		**Pump stops**
76		**Advance**	**Valve advances to a new position (port 9)**
77	**Forward**		**Forward mixture (oxidation product and DPC) to detector**
119	**Off**		**Pump stops**
120		**Home**	**valve moves to home position**

5.4. Optimisation, results and discussion.

All the data given (relative peak heights) and % R.S.D. in the optimization of the physical and chemical parameters are the mean values from 10 successive determinations. All the optimisation steps were carried out with a chosen Cr (VI): Cr (III) ratio of 1:1 as 10 mg/L for each.

5.4.1. Physical parameters.

5.4.1.1. Flow rate.

Optimisation of flow rates for Cr(VI) and total Cr.

Peak height	Flow rate mL/min	% RSD
0.4476	2.70	1.114
0.5896	3.00	1.240
0.7735	3.30	0.645
0.8147	3.60	0.897
0.9964	3.90	1.138

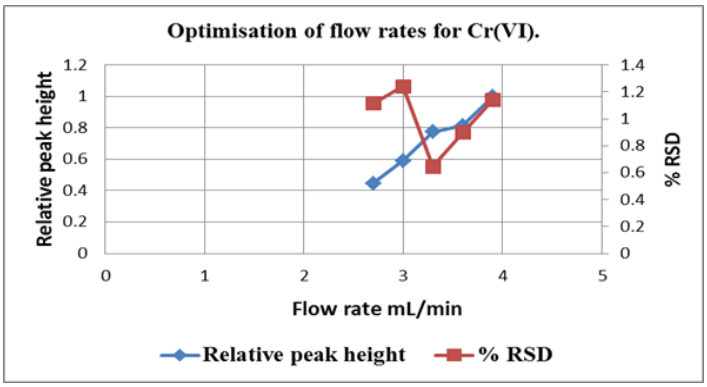

Figure 5.3 (a) Optimisation of flow rates for Cr(VI).

Peak height	Flow rate mL/min	% RSD
0.7089	2.70	1.213
0.8786	3.00	1.033
0.9224	3.30	0.722
1.2344	3.60	0.897
1.9679	3.90	1.277

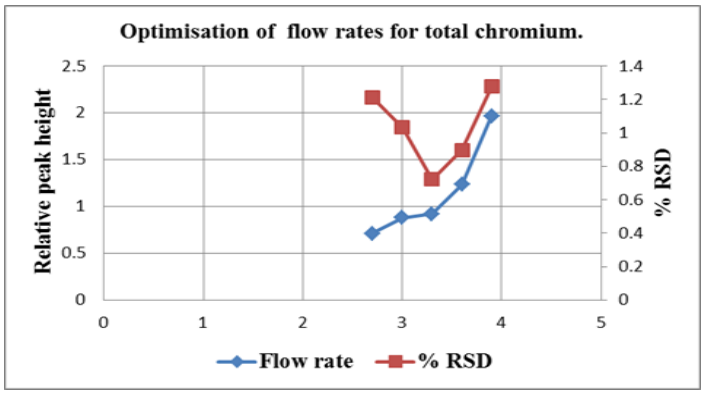

Figure 5.3 (b) Optimisation of flow rates for total Cr.

Figs. 5.3 (a) and 5.3 (b) displays the optimisation of the flow rate and 3.30 mL/min.

5.4.1.2. Sample and reagent volumes.

The stoichiometric mole ratio for the reaction between Cr (VI) and DPC is 2:3 [24]. Different sample and reagent volumes were tested to establish the one that will be optimal for this analysis.

Optimisation of sample volumes for Cr (VI) and total Cr.

Peak Height	Sample volume (µL)	% RSD
0.4866	60	1.096
0.7338	120	0.583
1.0983	180	0.870
1.2334	240	0.588
1.3485	300	1.201

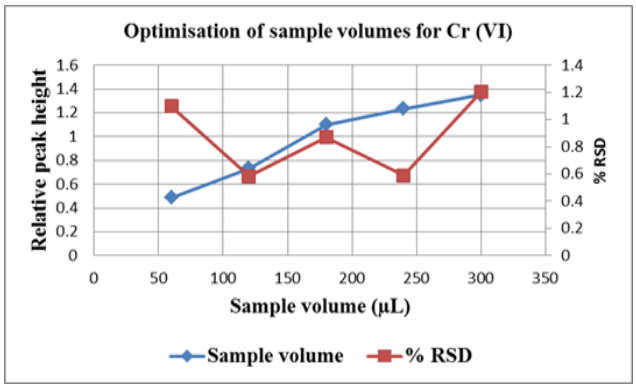

Figure 5.4 (a) Optimisation of sample volumes for Cr (VI).

Peak Height	Sample volume (µL)	% RSD
0.5124	60	2.342
1.2422	120	1.472
1.5348	180	0.870
1.9634	240	0.632
2.4651	300	1.195

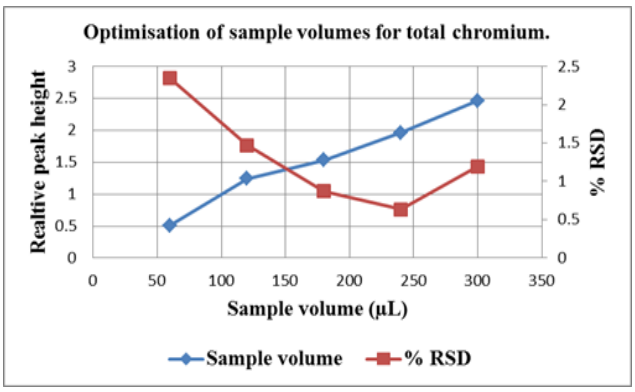

Figure 5.4 (b) Optimisation of sample volumes for total Cr

Form Figs. 5.4 (a) and 5.4 (b) computations of results showed that the ideal sample volume for this determination is 240 µL.

Optimisation of colour reagent (DPC) volumes for Cr(VI) and total Cr.

Peak height	DPC volume (µL)	% RSD
0.4221	40	1.932
0.7459	80	2.02
0.8352	120	0.998
1.2384	160	0.658
0.9232	200	1.021

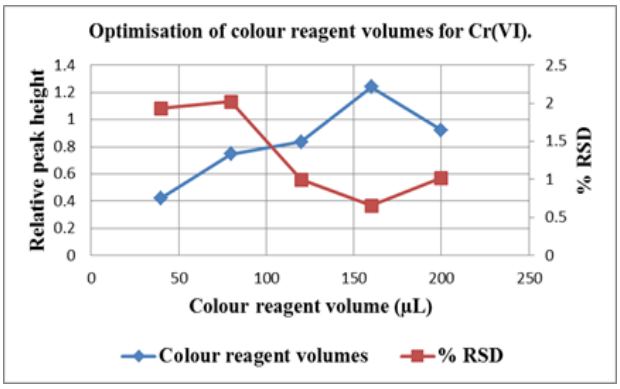

Figure 5.5 (a) Optimisation of DPC volumes for Cr(VI).

Peak height	DPC volume (µL)	% RSD
0.5346	40	2.114
0.8738	80	0.895
1.3668	120	1.233
2.0627	160	0.864
1.8652	200	1.021

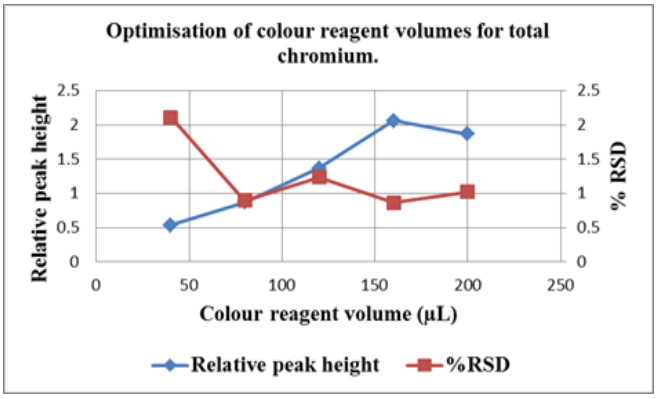

Figure 5.5 (b) Optimisation DPC volumes for total Cr.

A volume of 160 µL for DPC as observed from Figs. 5 .5 (a) and 5.5(b) was the one chosen for this analysis.

5.4.1.3. Holding coil internal diameter and length.

A holding coil with a length of 3.0m and an internal diameter of 1.02mm was the one that was chosen for this analysis after several lengths and internal diameters were evaluated. This combination was quite suitable for this analysis as shown in Figs. 5.5 (a) and 5.5 (b).

Optimisation of holding coil internal diameters for Cr(VI) and total Cr.

Peak height	(HC) i.d	% RSD
2.1227	1.65	1.635
1.8226	1.6	1.898
1.5133	1.14	0.7614
1.2011	1.02	0.3861
0.9836	0.76	0.7481

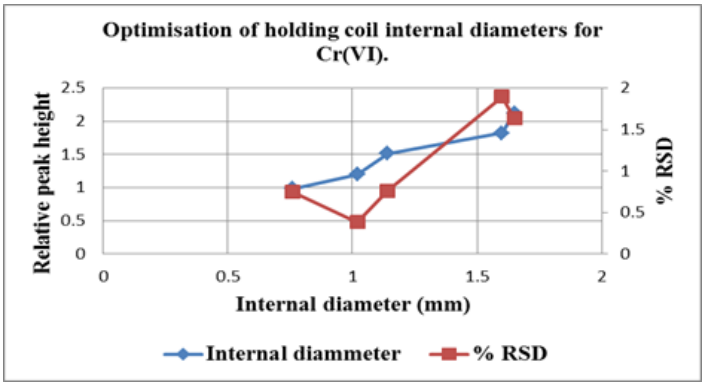

Figure 5.6 (a) Optimisation holding coil i.d for Cr(VI).

Peak height	(HC) i.d	% RSD
3.1207	1.65	1.585
2.6136	1.6	1.877
2.1285	1.14	0.7584
1.6255	1.02	0.4634
1.2184	0.76	0.8112

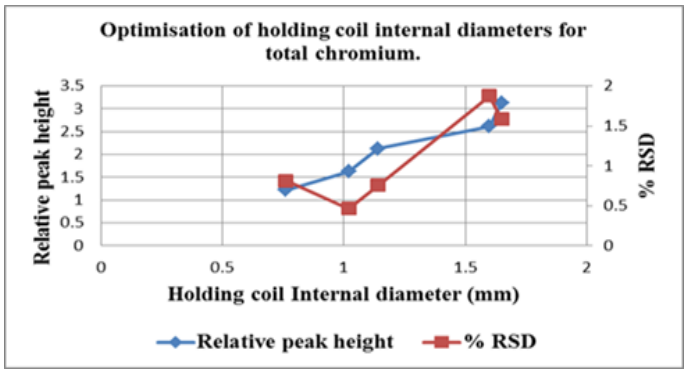

Figure 5.6 (b) Optimisation holding coil i.d for total Cr.

Figs. 5.6 (a) and 5.6 (b) for optimisation holding coil internal diameter was 1.02 mm.

Optimisation of holding lengths (L) for Cr(VI) and total Cr.

Peak height	HC L (m)	% RSD
0.884	1.5	0.998
2.116	2.0	0.894
1.789	2.5	0.918
2.0858	3.0	0.458
2.1763	3.5	1.360

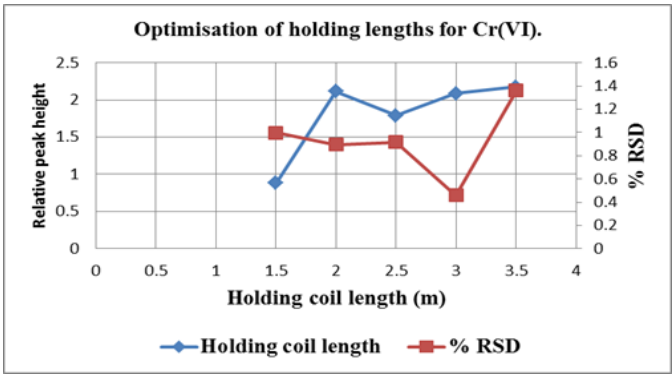

Figure 5.7 (a) Optimisation of holding lengths for Cr(VI).

Peak height	HC L (m)	% RSD
1.2085	1.5	0.887
2.3251	2.0	0.924
1.8491	2.5	0.949
2.1132	3.0	0.464
2.2481	3.5	1.385

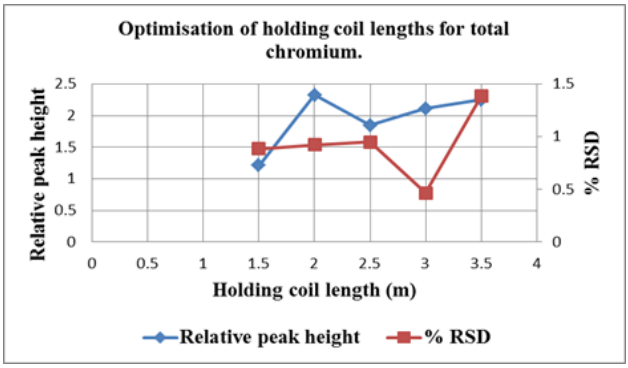

Figure 5.7 (b) Optimisation (HC) lengths for total Cr.

Holding coil length that was optimised from Figs. 5.7 (a) and 5.7 (b) is 3m.

5.4.1.4. Influence of oxidation coil temperature.

The reaction between Ce(IV) and Cr(III) is temperature dependent. This oxidation product was directly proportional to the increase in temperature. A series of temperatures from 25˚C to 90 ˚C were evaluated. From 80 ˚C to 90 ˚C gas bubbles formed at such a rate that results became erratic. From 40 ˚C to 65 ˚C the increase in response was slight. This led to the choice of 45 ˚C as the optimum temperature since it gave the best precision as shown in Fig. 5.8

Optimisation of temperature on total chromium determination.

peak height	Temperature ºC	% RSD
2.7781	40	2.115
2.8703	45	0.928
2.9986	50	1.977
3.0114	55	1.358
3.0235	60	1.767
3.1553	65	1.865

Figure 5.8. Optimisation of temperature on total Cr.

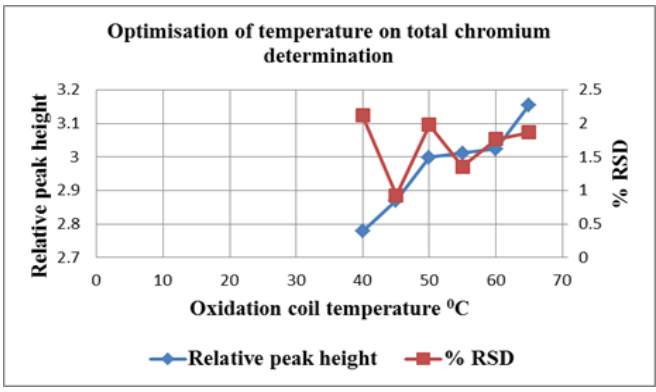

5.4.1.5. Influence of diameter and length for oxidation coil.

The dimensions of the oxidation coil play an important role in the residence time and therefore oxidation efficiency of Cr(III) to Cr(VI) and thus the determination of total chromium. The length of the oxidation coil should allow the maximum oxidation efficiency of Cr(III) after complete mixing of Ce(IV) and Cr(III).

5.4.1.6. Influence of reaction coil length and internal diameter on Cr(IV) and total Cr.

The reaction coil has a more pronounced effect on zone penetration and product dispersion. A reaction coil with a length of 0.6m and an internal diameter of 1.14 mm gave the best response and precision as shown in Figs. 5.9 (a) and 5.9 (b).

Influence of reaction coil (OC) lengths on Cr (VI) and total Cr determination.

Peak height	RC (L) (m)	% RSD
0.758	0.6	0.379
0.8984	0.8	1.285
1.0583	1	1.355
1.6116	1.2	1.190
1.5537	1.8	1.848

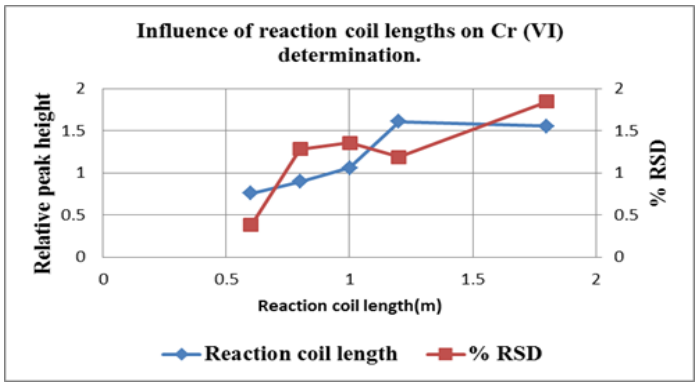

Figure 5.9 (a) RC lengths on Cr (VI) determination

Peak height	RC (L) (m)	% RSD
0.9462	0.6	0.517
1.1224	0.8	1.311
1.3488	1	1.402
1.6526	1.2	1.887
1.5241	1.8	1.935

Figure 5.9 (b) RC lengths on total Cr determination.

A reaction coil length of 0.60m was chosen from results shown by Figs. 5.9 (a) and 5.9 (b).

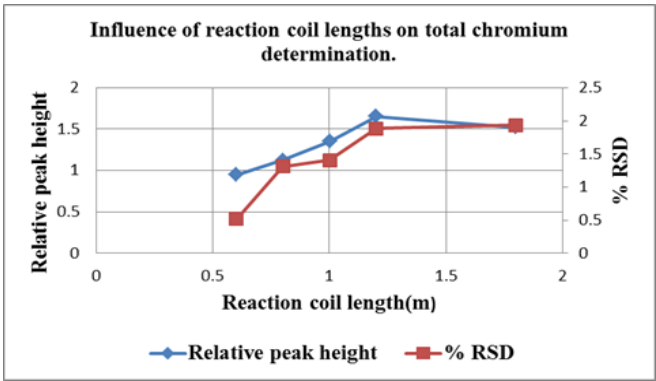

Influence of reaction coil internal diameter on Cr (VI) determination.

Peak height	RC i.d (mm)	% RSD
1.2981	0.025	0.761
1.4876	0.03	1.358
1.7611	0.114	0.431
1.414	0.76	1.485

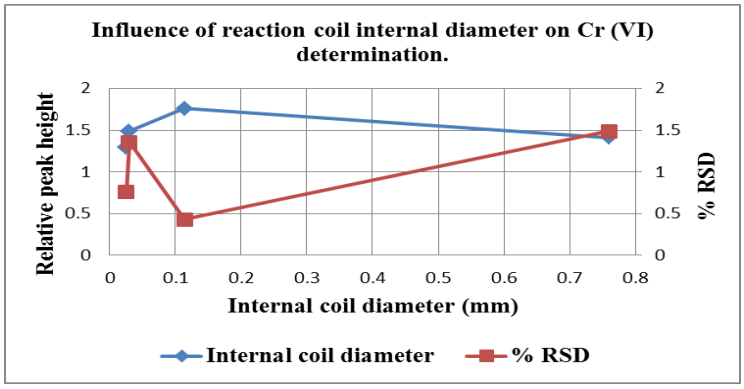

Figure 5.10 (a) Influence of RC (i.d) on Cr (VI) determination.

Peak height	RC i.d (mm)	% RSD
1.6859	0.025	0.853
1.5966	0.03	1.225
1.9641	0.114	0.561
1.7522	0.76	1.654

Figure 5.10 (b) RC (i.d) on total Cr determination.

A 0.114 mm diameter gave the best results as per Figs. 5.10 (a) and 5.10 (b) it was chosen.

5.4.1.7. Oxidation coil physical parameters.

The physical parameters of the oxidation coil are of utmost importance to the determination of the total chromium. The system would then be used to determine the concentration of total chromium (original Cr(VI) + the product of Cr(III) oxidation and by appropriate calculation then Cr(III) can be calculated.

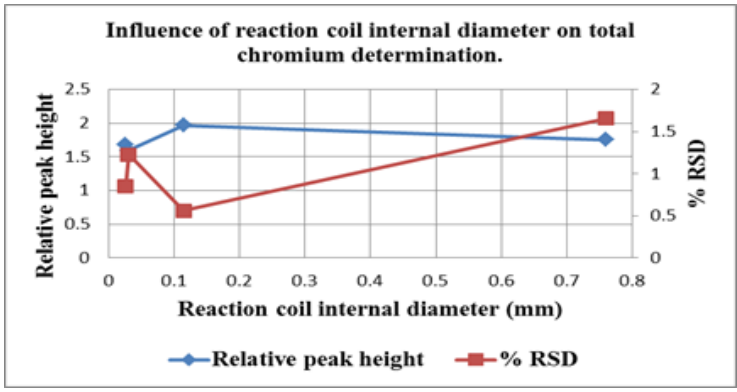

Influence of oxidation coil (OC) internal diameter on Cr(VI) and total Cr determination.

Table 5.2 Preliminary evaluation of oxidation coil length and internal diameter.

Oxidation Coil length(m)	Internal diameter of oxidation coil (mm)				
		0.025	0.03	0.64	0.76
		Cr(III)	Cr(III)	Cr(III)	Cr(III)
0.2	Peak height	0.386	0.409	0.635	0.663
	% RSD	3.15	2.33	2.65	2.43
0.4	Peak height	0.411	0.532	0.656	0.717
	% RSD	3.18	2.88	2.22	1.99
0.6	Peak height	0.402	0.627	0.768	0.8911
	% RSD	2.44	2.08	1.38	0.862
0.8	Peak height	0.433	0.735	0.832	1.191
	% RSD	2.18	2.33	0.93	0.641
1.0	Peak height	0.565	0.668	0.798	1.089
	% RSD	2.96	2.86	1.65	0.88
1.2	Peak height	0.448	0.598	0.777	0.978
	% RSD	3.18	2.95	3.13	2.11

Table 5.2 gives preliminary results for the optimisation of coil length and diameter for the speciation of chromium.

Influence of oxidation coil internal diameter on Cr(VI) and total Cr determination.

Peak height	i.d	% RSD
0.443	0.025	2.27
0.724	0.03	2.18
0.832	0.64	0.84
1.197	0.76	0.73

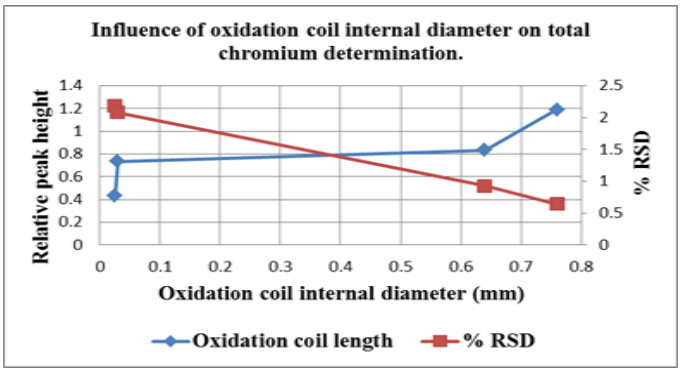

Figure 5.11 OC (i.d) on total Cr determination.

Fig. 5.11 confirms 0.076 cm as the preferred oxidation coil internal diameter.

Influence of oxidation coil length on total Cr. Determination.

Peak height	OC (L) (cm)	% RSD
0.386	0.2	3.15
0.411	0.4	3.18
0.402	0.6	2.44
0.433	0.8	2.18
0.565	1.0	2.96
0.448	1.2	3.18

Figure 5.12. OC (L) on total Cr determination.

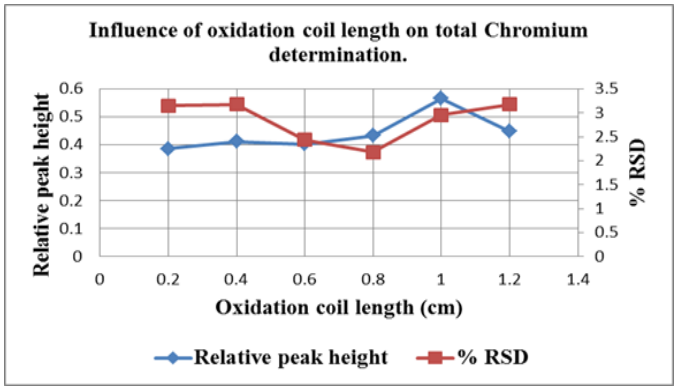

Fig. 5.12 gave oxidation coil length as 0.8 m.

5.4.2. Chemical parameters.

The Diphenyl carbazide (DPC) concentration was optimized by studying its effect on the sensitivity for the determination of chromium for both chromium (VI) and total chromium. The quest is to minimise reagents volumes yet achieving the best sensitivity.

5.4.2.1. Influence of colour reagent concentration on chromium speciation.

Influence of colour reagent concentrations on Cr(VI) determination.

Peak height	DPC g/0.1L	% RSD
1.1344	0.062	2.076
1.4865	0.124	1.965
2.3877	0.186	1.291
2.4246	0.248	0.675
2.4153	0.31	1.822

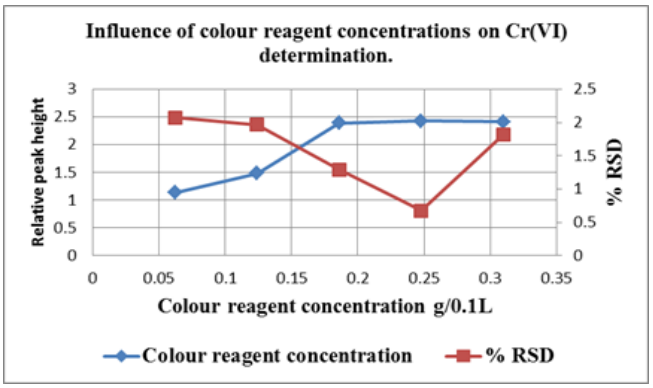

Figure 5.13 (a) DPC concentrations on Cr(VI) determination.

The best results were obtained from 0.248 g/0.1L as shown in Figs. 5.13 (a) and 5.13 (b)

Influence of colour reagent concentrations on total chromium determination.

Peak height	DPC g/ 0.1L	% RSD
0.4225	0.062	2.005
0.5386	0.124	1.684
0.7648	0.186	1.386
0.8114	0.248	0.664
0.9326	0.31	2.31

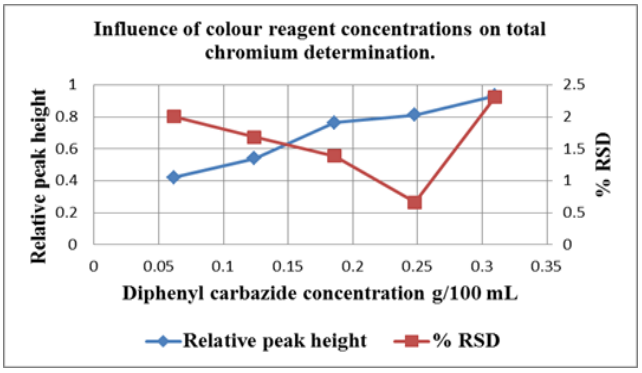

Figure 5.13 (b) DPC concentrations on total Cr determination.

5.4.2.2. Influence of H_2SO_4 concentration on chromium speciation.

Oxidation of Cr(III) with Ce(IV) to Cr(VI) occurs in an acidic medium. Ce(IV) concentrations were studied over the range (0.05–0.30) g/L. The most reliable with a concentration of 0.2 g /L as shown in Figs. 5.14 (a) and 5.14 (b).

Influence of H_2SO_4 concentration on Cr(VI) and total Cr determination.

Peak height	[H_2SO_4] mol/L	% RSD
0.8971	0.05	0.985
1.1931	0.10	1.324
1.5341	0.15	0.896
1.8335	0.20	0.683
1.0981	0.25	0.935
0.8202	0.30	1.458

Figure 5.14 (a) H_2SO_4 concentration on Cr(VI) determination.

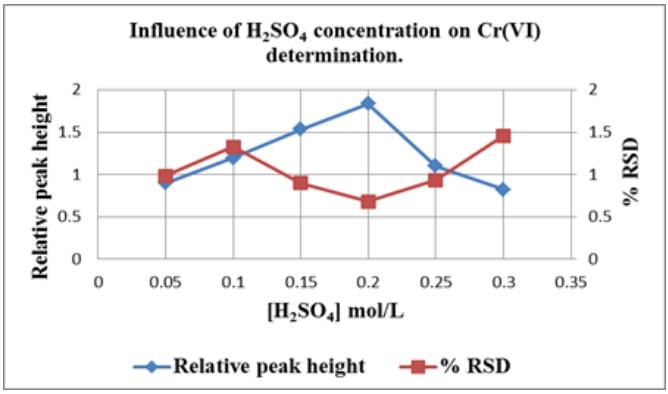

0.2 mol/L gave the best results as observed in Fig. 5.13 (a) and 5.13 (b).

Influence of H_2SO_4 concentrations on total chromium.

Peak height	[H_2SO_4] mol/L	% RSD
1.2865	0.05	1.213
1.3562	0.10	1.482
1.78225	0.15	0.987
2.0972	0.20	0.732
1.3667	0.25	1.109
1.1975	0.30	1.516

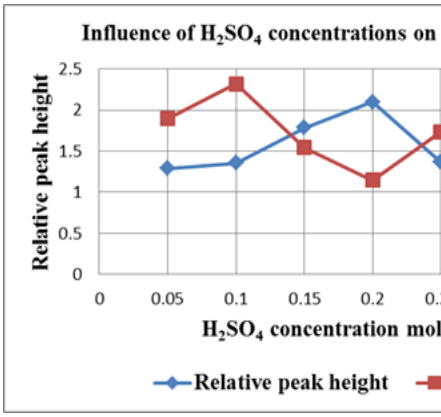

Figure 5.14 (b) [H_2SO_4] on total Cr.

5.5. Method evaluation.

First, a calibration graph was plotted for each species, and the linear range was determined to be between 0.2 and 1.0mg/L for Cr(III) and total chromium. Fig. 5.15 shows the regression output which indicates the relationship between the response (peak height) and the concentration of the target analyte.

Linear curves for (Cr(VI) and total Cr.

Cr(VI)	Total Cr.	Concentration

0.9331	1.1436	0.2
1.2017	1.6348	0.4
1.5011	2.1346	0.6
1.8106	2.6401	0.8
2.1009	3.1308	1

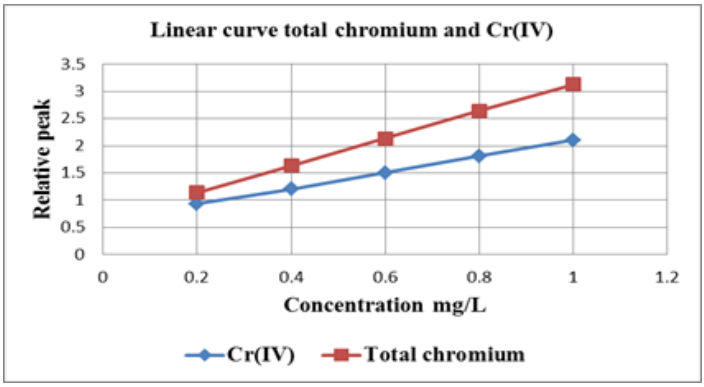

Figure 5. 15. Linear curve (Cr(VI) and total chromium.

	Regression Output: Cr(VI)	Regression Output: Total Cr.
Constant	0.6016	0.655
Std Err of Y Est	0.0219	0.0463
R Squared	0.99993	0.99996
No. of Observations	5	5
Degrees of Freedom	3	3
X Coefficient(s)	1.503	2.453
Std Err of Coef.	0.001	0.001

Equation $H_1 = 1.503[\text{Cr(IV)}] + 0.6016$

Equation $H_2 = 2.453[\text{Total Cr}] + 0.655$

where H_1 and H_2 are the relative peak heights for Cr(VI) and Cr(III) with concentrations given as mg/L. To validate the accuracy of the proposed SIA system, the SIA results were compared with those well-established and standard methods, including titrimetry and AAS. Table 5.3 showed statistical comparison between the proposed SIA system and standard methods to establish the reliability of the results from the SIA system. At the 95% confidence level

$t_{tabulated}$ = (2.78) t calculated = (0.464) for Cr(VI) and for total Cr ttabulated = 2.78 with tcalculated = 0.469). In both instances tcalculated < t tabulated, statistically, there is no significant difference between the two techniques for total chromium and Cr(VI) meaning the methods are highly comparable. It is seen from Table 5.3 that the results depict a very good correlation with those from the standard methods, with a good precision (> 0.7%). The % recovery of Cr(III) from the real samples was also determined by spiking samples with Cr(III) and then determining the total Cr(III).

Table 5.4 showed that a 99% recovery with low RSD (0.64%). The proposed system was further validated by recovery tests of different amounts of Cr(III) and Cr(VI) from synthetic aqueous samples containing matrix species present in real samples and the results obtained are given in Table 5.5. As expected, good recovery and RSD value of 0.64% were observed. The estimated 3σ limit of detection was 0.042 mg/L for the Cr(III) and 0.023 mg/L for the total Cr, while the sample interaction was ±1.1% at a sampling rate of 30 samples/h. Although the adopted DPC method is quite sensitive and almost specific for Cr (VI) when conventional manual procedure is adopted, it should however be noted that there are several other chemical species that could form a complex with DPC [30]. Interferences are may occur via two sources: where one species forms complexes with the DPC and where the interferent reduces Cr(VI) to Cr(III) [31]. Andrade et al. [30] observed a more pronounced interference from some species for the direct Cr(VI)–DPC reaction in FIA compared to the manual method. To assess the level of interference, different complex with DPC and shows a positive interference as indicated in Table 5.6 that may pose a problem if the concentration of iron(III) in real samples rises too high. However, a comparison of the proposed SIA system with standard methods (titrimetry and AAS) shows that the effect of Fe(III) for the real samples tested is negligible. For Hg(II) and V(V) which may cause some problems, interstingly showed neglible or no interferences in the tested samples.

5.6. Results.

Table 5.3. Simultaneous determination of Cr(III) and Cr(VI) in real samples.

Sample	SIA method		Standard methods [10,11]		
				Total chromium mg/L	
	Cr(III) mg/L	Cr(VI) mg/L	Cr(VI) mg /L	Titrimetric	AAS
SE1	0.313 ± 0.002	1.174 ± 0.007	1.160 ± 0.013	1.479 ± 0.017	1.495 ± 0.008
SE2	0.132 ± 0.001	1.318 ± 0.008	1.297 ± 0.014	1.434 ± 0.016	1.451 ± 0.005
SE3	0.125 ± 0.001	0.679 ± 0.004	0.668 ± 0.005	0.790 ± 0.006	0.812 ± 0.004
SE5	0.212 ± 0.001	2.683 ± 0.017	2.636 ± 0.022	2.886 ± 0.024	2.901 ± 0.012
Bree river	0.851 ± 0.005	0.643 ± 0.004	0.585 ± 0.007	1.498 ± 0.011	1.534 ± 0.004
Chechassuer	0.263 ± 0.001	0.234 ± 0.001	0.108 ± 0.014	0.488 ± 0.007	0.542 ± 0.002
Demiskraal-kanal	1.230 ± 0.007	1.066 ± 0.006	1.086 ± 0.013	2.276 ± 0.028	2.308 ± 0.010
Driel barrage	1.893 ± 0.009	0.422 ± 0.002	0.396 ± 0.005	2.328 ± 0.028	2.341 ± 0.010
GBR-mond	0.708 ± 0.003	0.266 ± 0.001	0.273 ± 0.009	0.978 ± 0.009	0.981 ± 0.004
Mutshedzi dam	0.892 ± 0.004	0.586 ± 0.003	0.565 ± 0.006	1.395 ± 0.015	1.506 ± 0.008
Bettaway adult's own [a]	49.35 ± 0.288	_	_	48.58 ± 0.656	49.36 ± 0.214
Bettaway family's own [a]	24.276 ± 0.155	0.026 ± 0.003	0.026 ± 0.001	24.250 ± 0.269	24.28 ± 0.103

Table 5.4. Recovery studies from synthetic samples with appropriate addition of Cr (III) and Cr(VI) as indicated.

Added mg/L		Recovered mg/L		
Cr(VI)	Cr(III)		Cr(VI)	Cr(III)
0.00	1.00		0.00	0.98
		% RSD	-	0.61
0.20	0.80		0.19	0.79
		% RSD	0.63	0.55
0.40	0.60		0.39	0.60
		% RSD	0.64	0.52
0.60	0.40		0.60	0.38
		% RSD	0.64	0.63
0.80	0.20		0.8	0.19
		% RSD	0.59	0.56
1.00	0.00		0.99.	-
		% RSD	0.63	-

Table 5.5. Recovery studies from real samples spiked with 0.4 mg/L Cr(III).

Sample i.d	Cr(III) (mg/L)	Expected Cr(III) (mg/L)	Recovered Cr(III) (mg/L)	% Recovery
SE2	0.1318	0.5318	0.5267	99.04
SE5	0.2123	0.6123	0.6088	99.43
Bree rivier	0.8512	1.2512	1.2479	99.74
Driel barrage	0.1893	0.5893	0.5779	98.07
Chechasseur	0.0380	0.4380	0.4307	98.33

Table 5.6. Statistical evaluation of SIA method and standard AAS method for Cr (VI).

Cr(VI) ppm						
		SIA	Standard Method	*Di*	*Di*- D	$(Di- D)^2$
1.	SE1	1.1736	1.1598	0.0138	0.0081	0.000066
2.	SE3	0.0679	0.0668	0.0011	-0.0046	0.000021
3.	Bree river	0.0663	0.0585	0.0078	0.0021	0.0000
4.	Driel barrage	0.0422	0.0396	0.0026	-0.0031	0.0000
5.	Bettaway family's own	0.0132	0.0098	0.0034	-0.0023	0.0000

Table 5.7. Statistical evaluation of SIA method and standard AAS method for total Cr.

Total Chromium ppm						
		SIA	AAs	*Di*	*Di*- D	$(Di- D)^2$
1.	SE1	1.4868	1.4788	-0.0080	0.2081	0.0433
2.	SE3	0.0804	0.0790	-0.0014	0.2147	0.0461
3.	Bree river	0.9175	0.8978	-0.0197	0.1964	0.0386
4.	Driel barrage	0.2315	0.2328	-0.0013	0.2148	0.0461
5.	Bettaway family's own	24.54	23.49	-1.05	-0.8339	0.6954

Table 5.8. Particular chemical species with interference factor [19].

Species	Interference factor[a]
Co(II)	0.96
Cu(II)	0.92
Fe(II)	1.02
Fe(III)	1.28
Hg(II)	0.76
Ni(II)	0.95
Mo(VI)	0.95
V(V)	1.27
MnO_4	0.94

[a]An interference factor of 1.00 means no interference within 1%, a factor greater than 1.00 means an enhancement and a factor less than 1.00 means a depression of the expected value [21]

Table 5.9. Influence of interference type and concentration [19].

Species	Tolerance level mg/L	Added interferent mg/L	Interference factor	Range in samples mg/L
Co(II)	200	10	0.96	0.001-0.060
Cr(III)	100	10	1.26	0.008- 0.045
Cu(II)	100	10	0.92	0.031- 0.078
Fe (II)	100	10	1.02	4.80-7.98
Fe(III)	100	10	1.28	5.32- 8.35
Hg (II)	200	10	0.76	0.007- 0.014
Ni(II)	150	10	0.95	0.040-0.790
Mo(VI)	200	10	0.95	0.009- 0.021
V(v)	100	10	1.27	0.016- 0.058
*MnO_4	75	10	0.94	0.300-3.00

*** Azide was successfully used for masking MnO_4.**

5.7. Conclusions.

The proposed SIA system for the speciation analysis of Cr(II) and Cr(VI) yielded results that are comparable with those of the standard methods. Statistical evaluation showed that there are no significant differences between the proposed system and standard methods. 30 samples per hour are acceptable. Interferrences of MnO_4 could be easily eliminated by the use of Azide. The linear range is (0.1-1.0) mg/L as shown in Fig. 5.15. SIA method and AAS yield similar results from Table 5.6. There is also good recovery shown in Table 5.5.

5.8. References.

1. E.A. Brandes, H.T. Greenaway, H.E.N. Stone "Ductility in Chromium". Nature. 178 (587) (1956) pp 587.
2. E. Nakayama, T. Kuwanato, S. Tsunibo, H. Tokoro, Fujiwara, Anal. Chim. Acta 130 (1981) pp 401.
3. M. Hiraide, A. Mizuike, Z. Fresenius. Anal. Chem. 335 (1989) pp 924.
4. R.A. Anderson, Clin. Physiol. Biochem. 4 (1986) pp 31.
5. J. Versieck, R. Cornelis, Trace Elements in Human Plasma or Serum, CRC Press, Boca Raton, (1989).
6. E.A. Garcia, D.B. Gomis, Analyst 122 (1997) pp 899.
7. A. Maquieira, H.A.M. Elmahadi, R. Puchades, Anal. Chem.,66 (1994) pp 1462.
8. C. Robles, A.J. Aller, J. Anal. Chem. At. Spectrom. 9 (1994) pp 871.
9. A. Maquieira, H.A.M. Elmahadi, R. Puchades, J. Anal. Chem. At. Spectrom. 11 (1996) pp 99.
10. A. Maquieira, H.A.M. Elmahadi, R. Puchades, Analyst 121 (1996) pp 1623.
11. T.L. Mullins, Anal. Chim. Acta 165 (1984) pp 97.
12. A. Knochel, G. Weseloh, Fresenius J. Anal. Chem. 363 (1999) pp 533.
13. Y. Madrid, C. Cabrera, T. Perez- Corona, C. Camara, Anal. Chem., 67 (1995) pp 750.
14. H.A.M. Elmahadi, G.A. Greenway, J. Anal. Chem. At. Spectrom. 9 (1994) pp 547.
15. B. Neidhart, S. Herwald, C. Lippmann, B. Straka-Emden, Z. Fresenius Anal. Chem. 337 (1990) pp 853.
16. H. Bag, A.R. Turker, M. Lale, A. Tunceli, Talanta 51 (2000) pp 895.
17. S. Saverwyns, K. van Hecke, F. Vanhaecke, L. Moens, R. Dams, Fresenius J. Anal. Chem. 363 (1999) pp 490.

18. Y. He, M.L. Cervera, M.I. Garrido-Ecija, M. de la Guarda, Anal. Chim. Acta 421 (2000) pp 5765.
19. A. Gaspar, C. Sogor, J. Posta, Fresenius J. Anal. Chem. 363 (1999) pp 480.
20. Y.K. Chau, Analyst 117 (1992) pp 571.

CHAPTER 6.

Bromine, bromide speciation by sequential injection analysis with spectrophotometric detection.

6.1. Introduction into bromine/ bromide chemistry.

Bromine (Br) was discovered by Carl Jacob Lowig in 1825 [1] with an average atomic number of 34, and an atomic mass of 79.904 g. Its name bromine was derived from the ancient Greek word "*bromos*" meaning strong smelling. It is the only non-metallic fuming red-brown liquid with bleaching characteristics. Free bromine does not occur in nature, but only occurs as colourless crystalline mineral salts. It has a boiling point of 332.0 K , melting point of 265.8 K and density of 4050 kg/ m^3 [1].

6.1.1. Isotopes.

There are at about 23 known radio isotopes known which range from ^{67}Br to ^{98}Br. The two most stable isotopes are ^{79}Br and ^{81}Br at 50.69 % and 49.31 % respectively. The common oxidation states are: $(HBr)^0$, $(Br_2)^0$, $(BrCl)^0$, $(BrF_3)^{-2}$, $(BrF_5)^{-4}$ and $(BrO_4)^{-7}$.

6.1.2. Applications.

Bromine is used as, flame retardants, production of polyethylene, poly vinylchloride and as anti-engine knocking agents. It is also used in the photographic industry, insecticide, pesticide and water purification [2-4]. It is also plays important roles in the medical field. [5]. Many drugs are formulated as bromide or hydrobromide salts [6].

Several methods have been used for both bromide and bromine determination. Titration, amperometry, inductively coupled plasma/mass spectrometry; X-ray fluorescence and neutron activation are some of the most common methods for total bromide determination [7-13]. An ion-selective electrode has been used for bromide determination [14]. Various procedures have been used for their speciation [15-19]. A combination of separation and element-selective detection is typically required for this kind of analysis.

The aim of this chapter was to develop an on-line method for the simultaneous determination of bromine and bromide (computed from bromine + bromide oxidised to bromine) with SIA and phenol red. The peak profile from this procedure displays two distinctive peaks, one for the bromine and the other for the total bromine this is shown in Fig. 6.3. The bromide concentration is then calculated by subtraction of bromine from total bromine. The procedure is carried out by sequentialy aspirating equal quantities of the sample. The first aspiration was executed for the determination of bromine and the second aspiration for the oxidation by chloramine T and consequent estimation of total bromine.

6.2. Experimental.

6.2.1. Reagents and standard solutions.

All solutions were analytically prepared with deionised water.

6.2.1.1. Bromine stock solution.

A 1000 mg/L bromine stock solution was prepared by appropriate dilution of the 99 % Br_2 (Fluka) bromine solution. This solution was standardised by iodometric titration [20, 21]. The stock solution was diluted accordingly to prepare solutions within the linear range.

6.2.1.2. Bromide stock solution.

A 100 mg/L bromide solution was prepared by dissolving 0.1489 g of KBr (Analar) in a litre of de-ionised water. Standard working solutions within the linear range were prepared by suitable dilution of the stock solution.

6.2.1.3. Sodium acetate/acetic acid buffer solution.

A pH 5.2 buffer was prepared by adding 39 mL of a 2 mol/L sodium acetate and 11mL of a 2 mol/L acetic acid solution followed by appropriate adjustment of the pH and finally diluting to 500 mL with de-ionised water.

6.2.1.4. Chloramine T solution.

Chloramine T (sodium-chloro- *p* -toluenesulfonamide trihydrate; 0.1 g) was dissolved in the minimal amount of de-ionised water and quantitatively diluted to 100 mL with buffer solution to prepare a 0.1% (m/v) solution.

6.2.1.5. Phenol red solution.

Phenol red solution (0.02%) was prepared by dissolving 0.02 g of phenol red in ethanol and finally diluting quantitatively to 100 mL with the acetate buffer solution.

6.2.2. Instrumentation.

A schematic flow diagram of the proposed SIA system for the speciation of bromine and bromide is the adaptation of the one from Chapter 1 with adjustments outlined in section 6.4. The length and size of the holding coil was 300cm with an i.d. of 1.02 mm, the oxidation coil was 80 cm long with an i.d. of 0.76 mm and the reaction coil was 60 cm in length with an i.d.

of 0.76 mm. A UV light source (Desaga, Heidelberg, Germany) supplying 15–20 W at 366 nm was used for irradiation.

6.2.3. Sample preparation.

The effluent samples analysed contain no solid particles and were analysed directly without any filtering or conditioning. The analysis of samples is done on-line by the proposed SIA process analyser, so there is no need for sample preservation. The real-time monitoring is one of the major advantages of the proposed SIA system. The proposed SIA system also served as a screening procedure, because if the concentration of any one of the two analyte species is greater than the linear range, the species is diluted into the linear range and feeds again into the system.

6.3. Operation of the system.

Table 6. 1 gives the sequence of the series of steps that are followed for a single complete cycle for the determination of bromine and total bromine, hence speciation of bromine and bromide. This speciation analysis procedure was carried out by first determining bromine. This was done by the aspiration of sample followed by the aspiration of the phenol red colour reagent through port 1 and port 2, respectively. These were stacked into zones within the holding coil before the product was forwarded to the detector through port 3 for the determination of bromine.

A wash solution (buffer) was aspirated through port 4. This was followed by the subsequent aspiration of the same amount of the sample through port 5 which was then mixed with Chloramine T (from port 6) to oxidise bromide to bromine through port 7 the oxidation

product was mixed with phenol red (port 8) and determined as total bromine when propelled through port 9 to the detector depicted as a summary in Fig. 6.1.

The product between phenol red and bromine was monitored at 590 nm. Fig. 6.2 displays the peak profiles for bromine and total bromine. The bromide concentration is given by the difference between total bromine and bromine. The reaction coil was irradiated with a UV light source (to catalyse the bromination of phenol red to bromophenol blue) according to:

Bromine + phenol red ⟶ violet product

UV radiation

sample ←	Phenol red ←	Detector →	Acetate buffer ←	sample ←	Chloramine T solution ←	← mixing →	Phenol red ←	detector →
2 s	3 s	24 s	4 s	2 s	3 s	15 s	2 s	119 s

Figure Figure 6. 1. Summary of the bromine, bromide speciation SIA system.

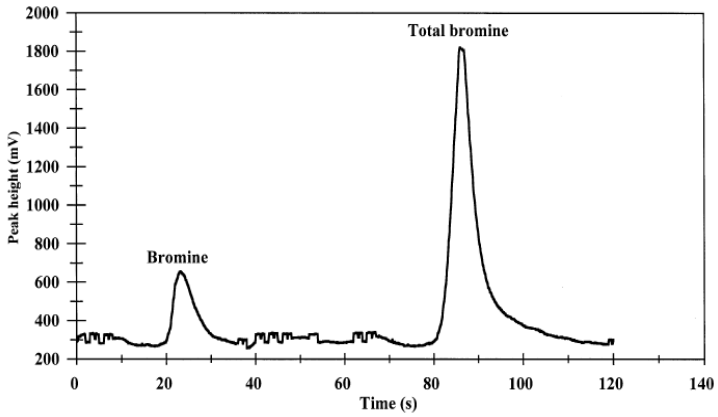

Figure 6. 2. Peak profile of bromine and total bromine determination.

Table 6.1. One cycle for bromine, total bromine speciation

Time(s)	Pump	Valve	Description
0.0	Off	Sample	Pump stops, select sample stream (valve position 1)
2.0	Reverse		Draws up sample solution
4.0	Off		Pump stops
5.0		Advance	select phenol red (valve port 2)
6.0	Reverse		Draws up phenol red
9.0	Off		Pump stops
10.0		Advance	valve advances to new position (valve port 3)
11.0	Forward		Pump stacks of zones to detector
35.0	Off		Pump stops
36.0		Advance	Valve advances to new position(valve port 4)
37.0	Reverse		Draws up acetate buffer
41.0	Off		Pump stops
42.0		Advance	Valve advances to new position (valve port 5)
43.0	Reverse		Draws up sample.
45.0	Off		Pump stops
46.0		Advance	Valve advance to new position (valve port 6)
47.0	Reverse		Draws up Chloramine T solution
50.0	Off		Pump stops
51.0		Advance	Valve advance to new position(valve port 7)
52.0	Forward		forward mixture [chloramine T and sample] trough port 7
59.0	Off		Pump stops
60.0	Reverse		Draws (oxidation product) into holding coil
70.0	Off		Pump stops
71.0		Advance	Valve advances to new position (valve port 8)
72.0	Reverse		Draws up phenol red
75.0	Off		Pump stops
76.0		Advances	Valve advances to a new position (port 9)
77.0	Forward		forward mixture (oxidation product and phenol red) to detector
119.0	Off		Pump stops
120.0		Home	Valve moves to home position.

6.4. Optimisation, results and discussion.

The optimisation steps were carried out using a sample containing equal amounts (2 mg/L) of bromine and bromide. The operation of the proposed SIA system as depicted in Fig. 6.1 can be divided into three key sections and the final computation section, which are:

i. Determination of bromine,
ii. Oxidation of bromide to bromine,
iii. Determination of total bromine,
iv. Calculation of bromide concentration from total bromine.

A key factor of the proposed SIA system is the interdependence of the three sections on each other for optimum performance. It is therefore of crucial importance that this should be taken into account when shared parameters are optimised for higher sensitivity and precision.

6.4.1. Physical parameters.

One part of the performance of a SIA system is linked to the optimisation of physical parameters as these dictate the rate, period and extent of mixing of the reagents. Physical parameters determine the degree of dispersion and penetration as reagent, sample and product zones are propelled to the detector along the flow conduits of the system.

6.4.1.1 Influence of holding coil length and internal diameter.

From Figs. 6.3 (a) and 6.3 (b) show the optimised holding coil length was computed to be 3m.

Influence of holding coil lengths on bromine determination and total bromine.

Peak height	HC (L) m	% RSD
0.5137	1.5	2.24
0.8346	2.0	2.02
1.0231	2.5	1.84
1.2543	3.0	0.64
1.3754	3.5	1.21

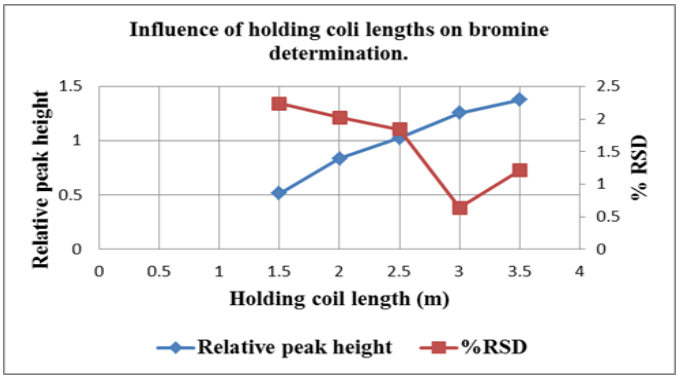

Figure 6.3 (a) HC (L) on bromine determination.

Peak height	HC (L) m	% RSD
0.7855	1.5	2.36
0.9776	2.0	1.96
1.2434	2.5	1.74
1.5247	3.0	0.58
1.8132	3.5	1.32

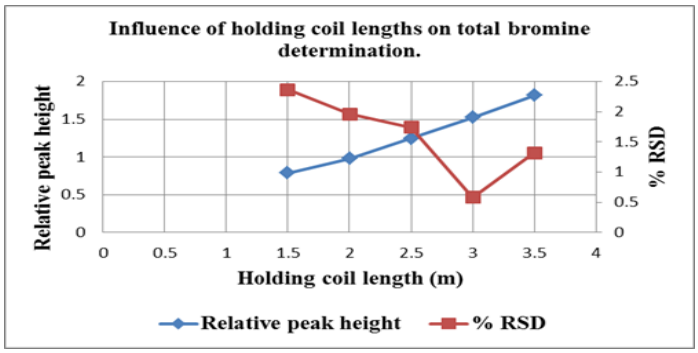

Figure 6.3 (b) HC (L) on total bromine determination.

Optimisation of (HC) internal diameter (i.d) for bromine and total bromine determination.

Peak height	(HC) i.d mm	% RSD
0.7778	1.65	1.85
0.9646	1.6	1.08
1.1219	1.14	0.761
1.3028	1.02	0.385
1.5933	0.76	0.831

Figure 6.4 (a) HC (i.d) on bromine determination.

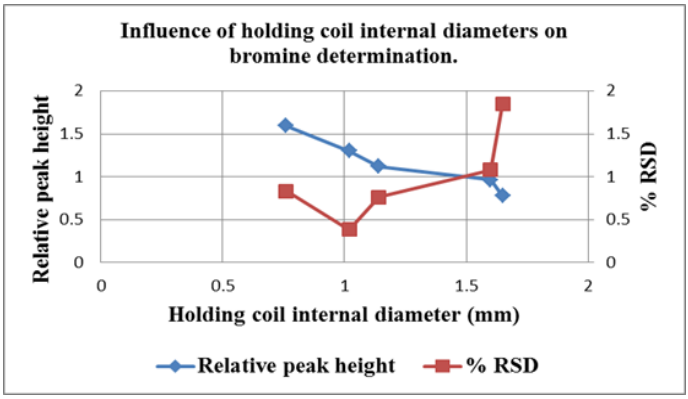

The optimised holding coil internal diameter is 1.02 mm displayed in Figs. 6.4 (a) and 6.4 (b).

Peak height	(HC) i.d (mm)	% RSD
0.9127	1.65	2.06
1.3556	1.6	1.13
1.5085	1.14	0.83
1.7221	1.02	0.42
1.9482	0.76	0.91

Figure 6.4 (b) HC (i.d) on total bromine determination.

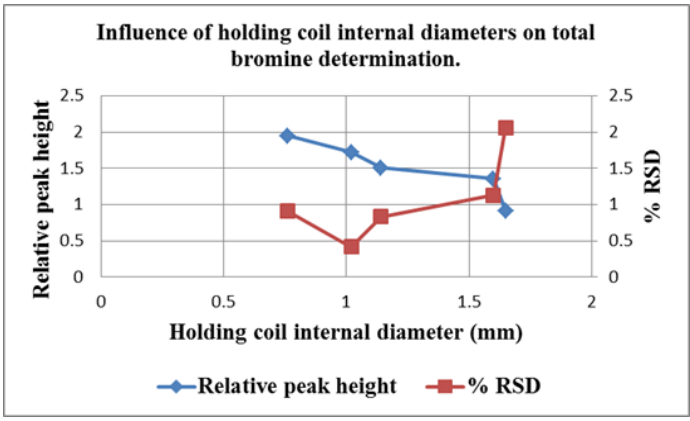

6.4.1.2. Influence of reaction coil (RC) length and internal diameter.

The length of the reaction coil was varied between (0.20 and 1.20) m and the internal diameter between (0.25 and 1.02) mm. This is where the product to be monitored is generated. It must allow the maximum colour production to increase the sensitivity without compromising the analytical performance of the system.

Influence of reaction coil lengths on bromine determination.

Peak height	(RC) L (m)	% RSD
0.6884	0.2	0.975
0.7244	0.4	1.063
0.8021	0.6	0.546
0.7996	0.8	0.799
0.7011	1.0	1.864
0.8552	1.2	0.988

Figure 6.5 (a) RC (L) on bromine determination.

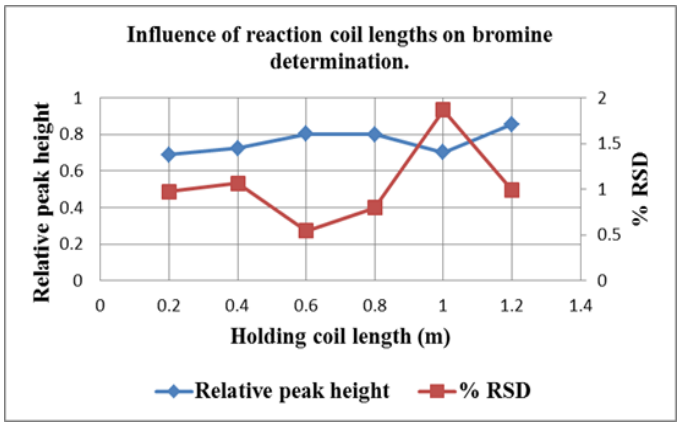

Figs. 6.5 (a) and 6.5 (b) gave optimised reaction coil length as 0.60 m.

Peak height	(RC) L mm	% RSD
0.9118	0.2	0.886
1.1922	0.4	1.244
1.5448	0.6	0.621

1.7686	0.8	0.912
1.9321	1.0	1.804
0.8552	1.2	1.975

Figure 6.5 (b) (RC) (L) on total bromine determination.

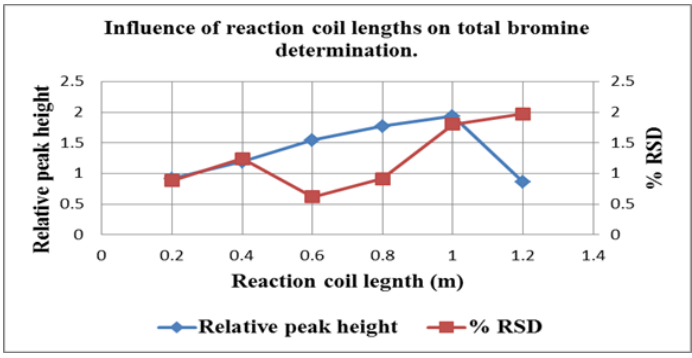

Influence of reaction coil internal diameters on bromine and total bromine determination

Peak height	(RC) i.d mm	% RSD
0.6881	0.025	0.896
0.8476	0.03	1.285
1.0975	0.64	2.284
1.1986	0.76	0.637

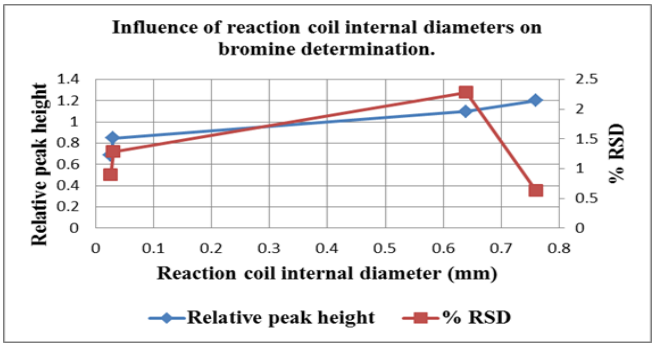

Figure 6.6 (a) RC (i.d) on bromine determination.

Peak height	(RC) i.d mm	% RSD
0.8758	0.025	0.925
1.1083	0.03	1.283
1.3246	0.64	2.314
1.5977	0.76	0.582

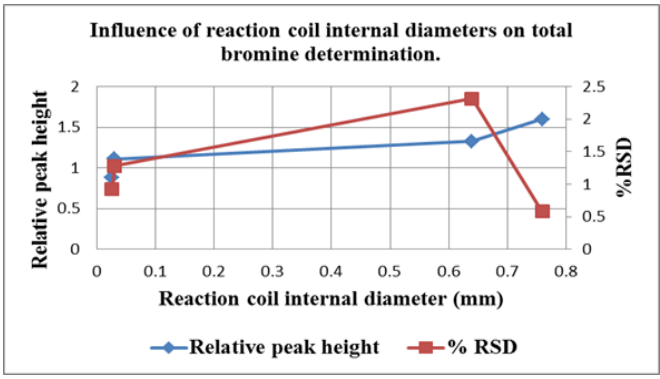

Figure 6.6 (b) RC (i.d) on total Br determination.

From Figs.6.6 (a) and 6.6 (b) the rection coil internal diameter determined to be ideal was 0.76 mm.

6.4.1.3. Influence of oxidation coil length and diameter.

Evaluation of the parameters of the oxidation coil revealed that a length of 0.80 m and an internal diameter of 0.76 mm gave an optimum oxidation of bromide to bromine with the best precision. The oxidation coil provides the area in which bromide is oxidised to produce the bromine that is added to the initial bromine content to form the total bromine. This has a critical influence on the determination of the total bromine. It must allow sufficient production of bromine for quantitative determination.

Influence of oxidation coil (OC) lengths and internal diameter total bromine determination

Peak height	(OC) L m	% RSD
1.8509	0.6	1.331
2.6542	0.8	0.543
2.0644	1	1.673
1.4965	1.2	0.956

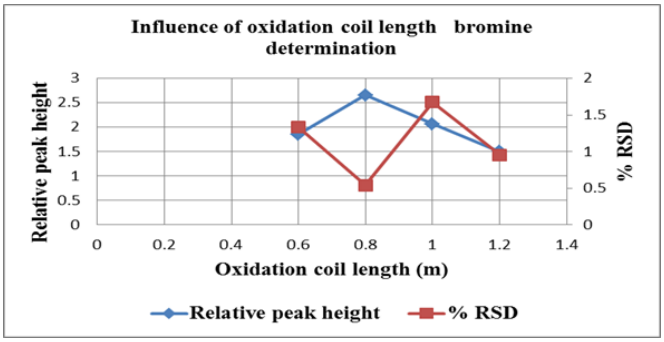

Figure 6.7 (a) OC (L) on Br determination.

Peak height	(OC) L m	% RSD
0.6868	0.025	0.933
1.0074	0.03	1.498
1.4233	0.64	1.851
1.9854	0.76	0.618

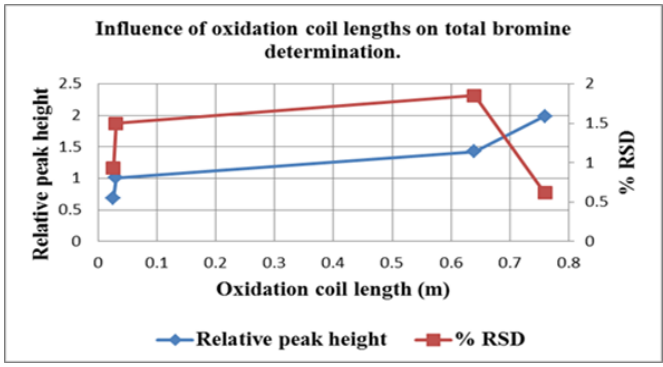

Figure 6.7 (b) OC length on total Br determination.

Figs. 6.7 (a) and 6.7 (b) gives the optimised oxidation coil length as 0.8 m and as a length of 0.76 m would work well when computed to 0.8 to match with that for Br determination.

6.4.1.4. Influence of sample volume and flow rate.

The flow rate determines the contact period between the sample and chromogen, sample and the oxidising reagent and finally has an influence on the dispersion of the product zone. The influence of the flow rate on all the above mentioned was evaluated for flow rates between 1 and 6 mL /min and it was found that a flow rate of 3.8 mL/min satisfied both the oxidation step and the colour development stages for both species regarding response and precision. With this study any flow rate lower than 3.8 mL/ min resulted in peaks that were not fully resolved and sample carry over was very high. Flow rates above 4mL/ min limited oxidation of the analyte to bromine, gave a lower response and together with a reduced dispersion a decrease in precision.

In order to be economical with the use of the reagents it was essential to optimise the sample and colour reagent volumes without compromising the quality of the results. This step was done bearing in mind that the required volumes must still produce sufficient colour for monitoring and still be within the confinement of the minimal detectable limit of both species. Both volumes were evaluated between 180 and 420 μL and the results obtained are displayed in Figs. 6.8 (a) and 6.8 (b) and 180 μL was chosen. The pattern followed to optimise these parameters was to keep the volume of one constant and then vary the other one. This was done for five volume sizes. The optimum volumes that were chosen for further work are 180 μL for both sample and colour reagent.

Influence of sample volumes on bromine determination.

Peak height	S vol. (µL)	% RSD
0.8685	180	0.36
0.9348	240	1.17
0.9556	300	2.13
0.9866	360	2.11
0.9932	420	1.18

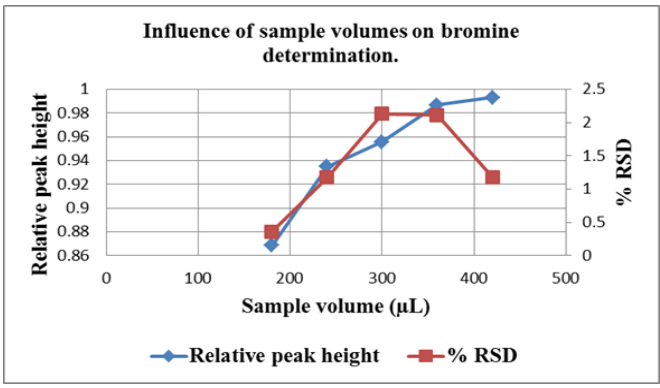

Figure 6.8 (a**)** Sample volumes on bromine determination.

Influence of sample volumes on total bromine determination**.**

Peak height	S vol.(µL)	% RSD
0.9574	180	0.41
0.9768	240	1.21
1.0111	300	1.33
1.1347	360	0.97
1.2204	420	2.31

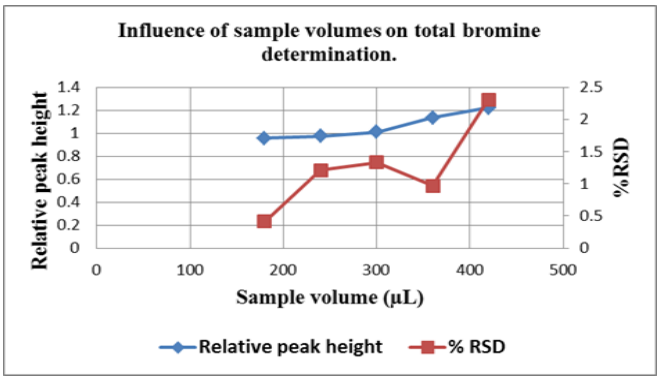

Figure 6.8 (b) Sample volumes on total Br determination.

Influence of phenol red (P.red) volume on Br and total Br

Peak height	(P. red) (µL)	% RSD
0.8653	180	0.36
0.8841	240	2.33
0.9901	300	1.98
1.0138	360	2.02
1.1212	420	1.68

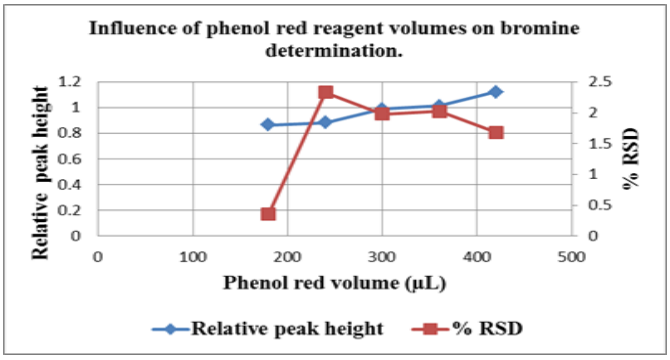

Figure 6.9 (a) (P. red) volumes on Br determination.

Figs. 6.9 (a) and 6.9 (b) gave phenol red volume as 180 µL which was the lowest investigated.

Influence of colour reagent volumes on total bromine determination.

Peak height	(P.red) (µL)	% RSD
0.9574	180	0.41
0.9816	240	1.11
1.0111	300	1.37
1.1668	360	1.75
1.3098	420	2.17

Figure 6.9 (b) (P.red) volumes on total (Br) determination.

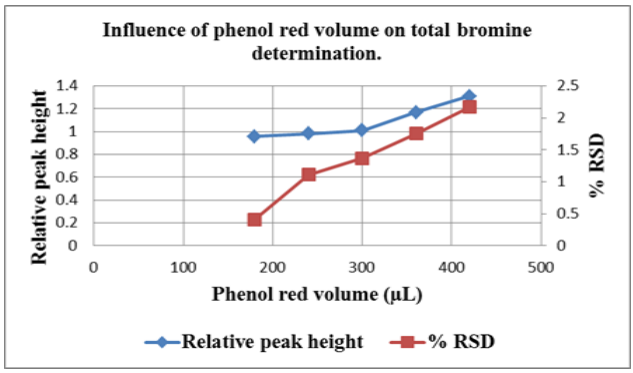

Influence of flow rates on Br and total Br determination

Peak height	Flow rate mL/min	% RSD
0.4096	1.4	1.1
1.2467	2.2	1.3
0.8585	3	1.42
1.4221	3.8	0.513
0.9017	4.6	1.02
0.7551	5.4	1.39
0.5898	6.2	1.78

Figure 6.10 (a) Flow rates on bromine determination.

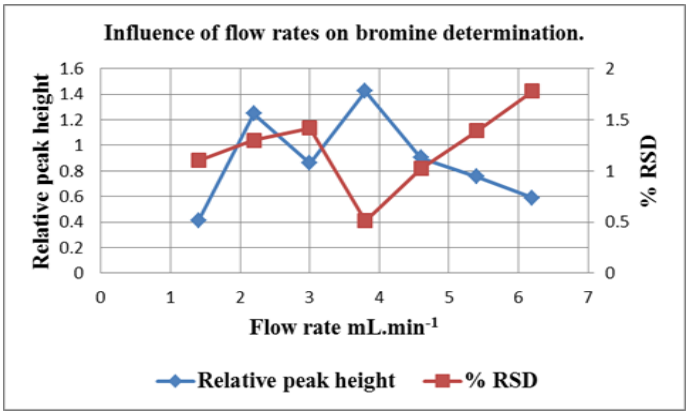

Peak height	Flow rate mL/min	% RSD
0.6113	1.4	1.26
1.0985	2.2	1.53
1.2325	3	1.42
2.5356	3.8	0.62

1.2248	4.6	0.87
0.9317	5.4	1.45
0.6113	1.4	1.26

Figure 6.10 (b) Flow rates on total bromine determination.

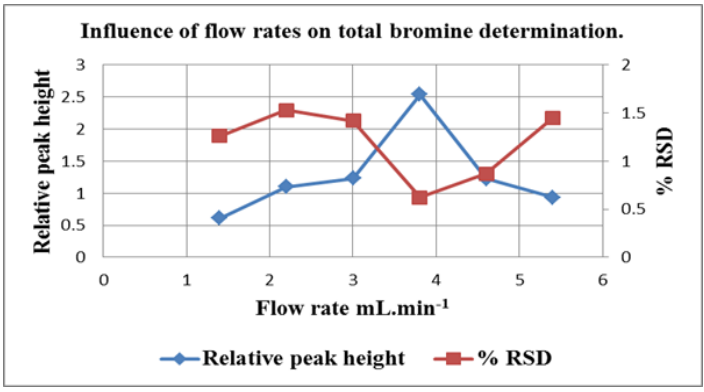

Figs. 6.10 (a) and 6.10 (b) confirmed 3.8 mL/min as the best flow rate.

6.4.2. Chemical parameters.

Influence of phenol red, chloramine T concentrations, and buffer pH.

These are the parameters that will have a significant bearing on the detection limit and the linear range of the method. Reagent concentrations must be such that they are not wasted while striving to get the best sensitivity. Preliminary experiments showed that concentrations of 0.4% (m/v) for Chloramine T and 0.1% (m/v) for Phenol Red tended to compress the linear range and decreased the limit of detection.

6.4.2.1. Chloramin T concentration. [Chloramin T]

It was observed that the rates of colour development and subsequent decay are dependent on the concentration of Chloramine T. Excess Chloramine T tends to bleach out the bromophenol blue. The influence of Chloramine T was studied over the range 0.05 to 0.25% (m/v) and the results obtained are outlined in Fig. 6.11. A concentration of 0.1% (m/v) was the most consistent and reliable with a best precision (RSD=0.51%) and this concentration was chosen for further work.

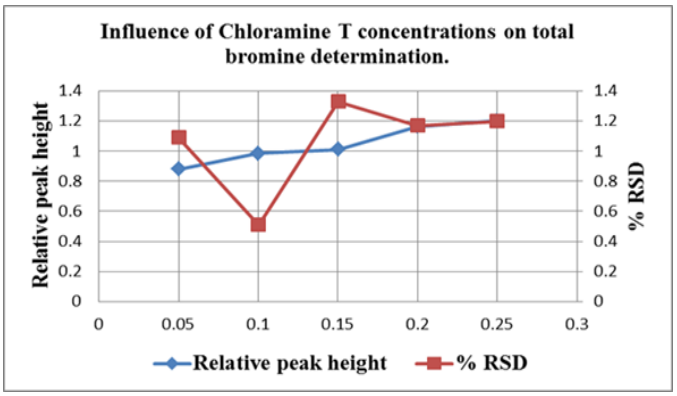

6.11 [Chloramine T] on total bromine determination.

Peak height	[Chloramine T] (m/v)	% RSD
0.8798	0.05	1.09
0.9864	0.1	0.51
1.0113	0.15	1.33
1.1635	0.2	1.17
1.2024	0.25	1.20

6.4.2.2. Phenol Red concentration.

The effect of the phenol red concentration for both the determination of bromine and total bromine was studied over the range (0.005 and 0.025) % (m/v). The results obtained in Figs. 6. 12 (a) and 6.12 (b) revealed a best response and precision with a concentration of 0.02% (m/v) and this concentration was used for further work. The pH is very critical as it dictates and enhances the specificity of this method and aids in eliminating interferences.

Peak height	[P. red]	% RSD
0.6331	0.005	2.01
0.6609	0.01	0.98
0.6913	0.015	1.19

0.8314	0.20	0.38
0.8321	0.25	0.78

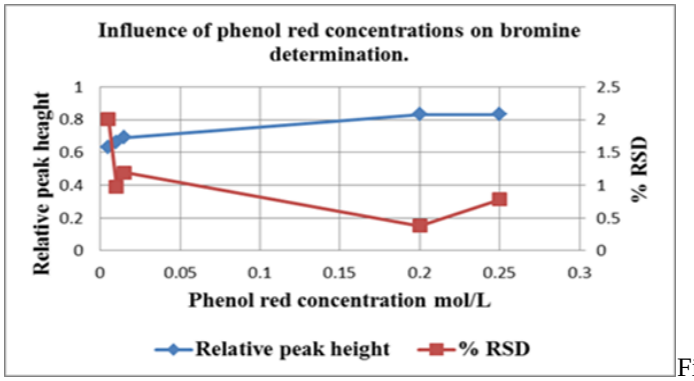

Figure 6.12 (a) [P.red] on Br determination.

Influence of phenol red concentrations [mol/L] [P.red] on Br and total Br determination

Peak height	[P.red]	% RSD
0.7101	0.005	2.11
0.7511	0.01	1.98
0.8334	0.015	1.34
0.9645	0.020	0.47
0.9667	0.025	0.86

Figure 6.12 (b) [P.red] on total Br determination.

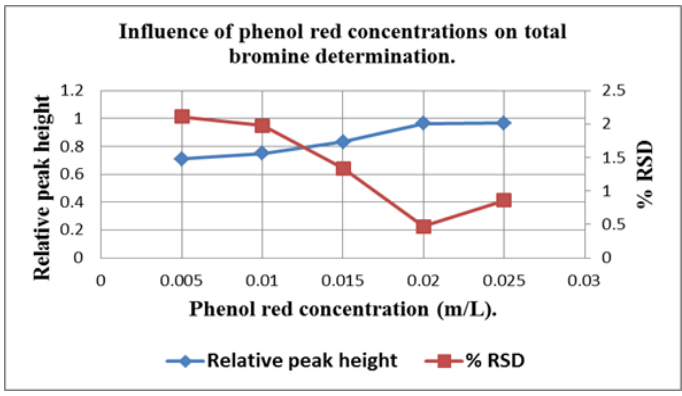

6.4.2.3. Influence of pH

The pH should create an optimum environment to satisfy the criteria required for the reactions in all three key sections of the proposed SIA system. The reaction between bromine and phenol red and the oxidation of bromide to bromine with Chloramine T are both pH dependent. The influence of sodium acetate/acetic acid buffer pH was evaluated between 4.8 and 5.6 and a buffer pH of 5.2 as shown in Figs. 6.13(a) and 6.13 (b) gave the best response and precision and was chosen for further work.

Influence of pH variations on Br and total Br determination

Peak height	pH	% RSD
0.7881	4.8	0.97
0.8135	5	0.61

0.8426	5.2	0.36
0.8388	5.4	1.35
0.8177	5.6	2.15

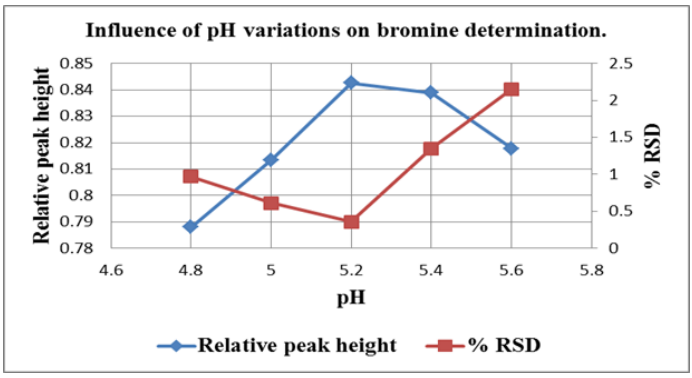

Figure 6.13 (a) pH variation on Br determination

Peak height	pH	% RSD
1.2087	4.8	1.35
1.2236	5	1.09
1.3568	5.2	0.48
1.2559	5.4	1.01
1.2487	5.6	0.89

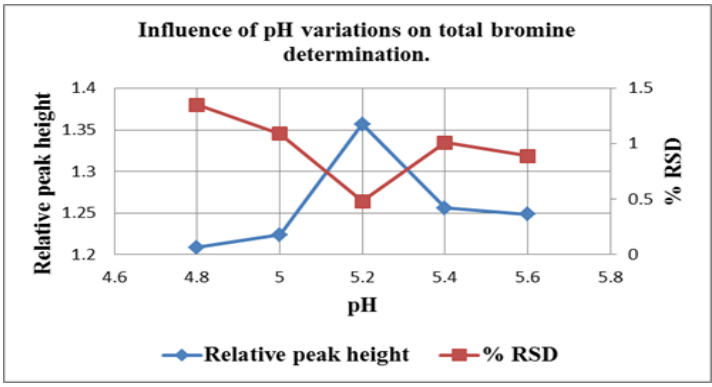

Figure 6.13 (b) pH variations on total bromine determination.

6.5. Method evaluation.

The proposed method underwent rigorous tests with regard to linearity, precision, accuracy, detection limit, sample frequency and interaction, interferences and percentage recovery. This was done to determine its applicability and reliability for on-line analysis. These tests were carried out under the optimum operational conditions. Linearity studies were first carried out for the individual species and then followed by studying their behaviour in the presence of each other. The bromine and bromide solutions were prepared by keeping one species constant while varying the other. The regression output for bromine and total bromine are given as follows:

	bromine	Total bromide

Constant	0.9474	2.0597
Std Err of Y Est	0.0198	0.0396
R Squared	0.9997	0.9996
Observations	5	5
Degrees of Freedom	3	3
X Coefficient(s)	1.4190	0.1025
Std Err of Coef.	0.001	0.001

$H_{bromine} = 1.4190C + 0.9474$; $r^2 = 0.9997$ *(*n = 10*)* and

$H_{total\ bromin} = 0.1025C + 2.0597$; $r^2 = 0.9996$ *(*n = 10*)*

Where H is the peak height in mV, C the concentration in mg/L and n is the number of repetitions. The calibration curve for the proposed SIA system method was found to be linear between (0.2 -1.0) mg/L for bromine and total bromine. The accuracy of the proposed SIA system was first evaluated and validated by determining the recovery of bromine and bromide from synthetic samples with known concentrations of the two species in varying amounts.

Calibration curves for bromine and total bromine

mg/L	Bromine peak	total bromide peak
0.2	0.9331	1.1436
0.4	1.2017	1.6348
0.6	1.5011	2.1346
0.8	1.8106	2.6401
1.0	2.1009	3.1308

Figure 6. 14. Calibration curves for bromine and total bromine.

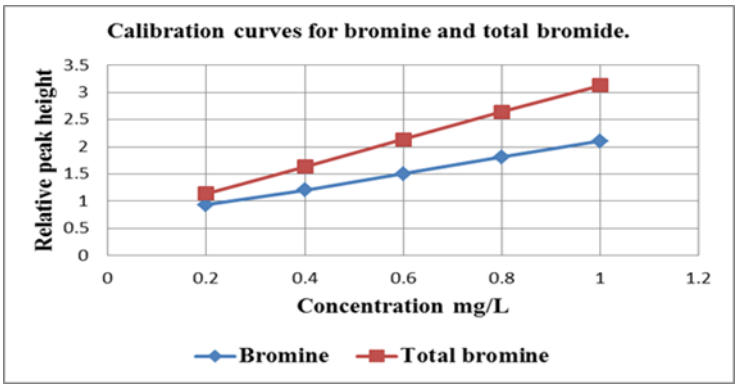

The results displayed in Table 6.2 show a recovery of

better than 97 % and indicates that the proposed SIA system is suitable for speciation of the two species. Real samples from effluent streams were also evaluated for both bromine and bromide and the results are given in Table 6.3. The accuracy of the proposed SIA system was therefore also validated by comparing the results obtained for real effluent stream samples with those from well-established and standard methods [22, 23]. It is evident from Table 6.3 that the results showed a good correlation with the standard methods. Real water samples with predetermined bromide values were spiked with 0.500 mg/L bromide, it is clear from Table 6.4 that the results matched with the expected values with a recovery of between (97–99.5) percent. Repeating each determination ten times and comparing consecutive determinations tested the precision of the proposed methods. The % RSD was 0.8% for bromine and 0.7% for total bromine. The calculated detection limits are 0.6mg/Lfor bromine and 0.4 mg/L for total bromine. This was improved by the irradiation of the reaction coil with a UV lamp at 366 nm and 15–20W.

The proposed system is able to monitor bromine and total bromine at a rate of 30 samples per hour with a sample carry-over of less than 1.1%. The phenol red method is adopted as the standard method for the monitoring of bromine and bromide in water [23]. $t_{calculted}$= 1.874. $t_{calculated}$ ((0.5673) < $t_{tabulated}$ = (2.26). At 95 % confidence level $t_{calculated}$ < $t_{tabulated.}$ Therefore, the two methods yield similar results.

Table 6.2. Results from synthetic samples as bromine: bromide ratio.

Added		Recovered	
Bromine (mg/L)	Bromide (mg/L)	Bromine (mg/L)	Bromide (mg/L)
0.00	1.00	-	0.9 ±0.003
0.20	0.80	0.17 ±0.001	0.78 ±0.006

0.40	0.60	0.38 ±0.009	0.59 ±0.004
0.60	0.40	0.61 ±0.013	0.38 ±0.004
0.80	0.20	0.77 ±0.007	0.18 ± 0.009
1.00	0.00	0.96 ±0.005	-

Table 6.3 Comparison of results by SIA and standard method from effluent streams.

Sample	Proposed SIA system		Standard titration method [23]	
	Bromine (mg/L)	Total bromide (mg/L)	bromine (mg/L)	Total bromide (mg/L)
S1	31.02 ± 0.002	634.69 ± 0.013	30.68 ± 0.023	633.70 ± 0.020
S2	16.71 ± 0.003	486.92 ± 0.008	15.25 ± 0.008	487.01 ± 0.011
S3	14.96 ± 0.012	476.99 ± 0.005	13.05 ± 0.017	478.04 ± 0.007
S4	43.96 ± 0.003	1203.80 ± 0.002	42.56 ± 0.004	1204.58 ± 0.012
S5	11.60 ± 0.007	535.07 ± 0.003	10.86 ± 0.006	533.96 ± 0.005

Table 6.4 Recovery studies (Recovery after adding 0.500 mg bromide) to real samples.

	Bromide concentration (mg/L)	

Sample	Original	Recovered	Expected	% Recovery
S1	603.67 ±	588.10	604.17	97.34
S2	470.45 ±	468.60	470.95	99.5
S3	462.03 ±	455.36	462.53	98.45
S4	1160.19 ±	1147.69	1160.69	98.88
S5	523.47 ±	519.25	523.97	99.10

Table 6.5 Table (Influence of interferences added as 20 mg/L for 4.0 mg/L of bromine.)

Species	Interference factor[a] [24,25]
Cl	1.28
Ammonia	0.89
Bicarbonate	0.97
Organic material	0.96
Rhodamine	0.98
Hydroxylamine	0.94
Silver	0.91
Iodine	095

[a] An interference factor of 1.00 means no interference, and a factor greater than 1.00 means an enhancement and a factor of less than 1.00 means a depression of the expected value. Table 6.5 shows the extent of interferences by that method.

6.6. Conclusions.

Statistical evaluation showed that there are no significant differences between the proposed system and standard methods with a sample frequency of 30 samples per hour with a carry over of less than 1.1% as displayed in Table 6.3. The method saves time and reagent, and is simple to assemble with very inexpensive instrumentation compared to other competing methods. Recovery studies from Table 6.2 for synthetic samples and Table 6.4 for real samples gave a high recovery of over 96 %.

6.7. References.

1. M.E. Weeks, "The discovery of the elements: XVII. The halogen family". Journal of Chemical Education. 9 (11), (1932). pp 1915.
2. J.F. Mills, (Bromine: in Ullmann's Encyclopedia of Chemical Technology. Weinheim: Wiley (2002). VCH Verlag.
3. M.J. Dagani, H.J. Barda, T.J. Benya, D.C. Sanders, (2005), "Bromine Compounds", Ullmann's Encyclopedia of Industrial Chemistry, Weinheim: Wiley-VCH,
4. M.I. Brebu, T. Bhaskar, K. Murai, A. Muto, Y. Sakata, M.A. Uddin, Chemosphere. Aug; 56(5): (2004) pp 433.
5. E.D. Weil, S. Levchik, A Review of Current Flame Retardant Systems for Epoxy Resins J. Fire Sci.22 (2004), pp 25.
6. G.S. Paulekuhn, J.B. Dressman, C. Saal, J. Med. Chem., 50 (26) (2007, pp 6665

7. W.Z. Hu, S.A. Cao, M. Tominaga, A. Miyazaki, Anal Chim Acta 322, (1996), pp 43.

8. T. Tomiyasu, Y. Taga, H. Sakamoto, N. Yonehara, Anal Chim Acta 319, (1996),pp199.

9. H. Yonehara, S. Akaike, H. Sakamoto, M. Kamada, Anal Sci 4, (1988), pp 273.

10. M.J. Fishman, M.W. Skougstad, Anal Chem 35, (1963), pp 146.

11. G.S. Pyen, M.J. Fishman, A.G. Hedley, Analyst, 105, (1980), pp 657.

12. P.I. Anagnostopoulou, M.A. Koupparis, Anal. Chem. 58, (1986), pp 322.

13. M.L. Dow, Journal of the Association of Official Analytical Chemists, 53, (5), (1970) pp 1040.

14. J.F. van Staden, Analyst, 112, (1987), pp 595.

15. J.L.P. Pavon, C.G. Pinto, B.M. Cordero, J.H. Mendez, Anal Chem, 62, (1990), pp 2405.

16. A.N. Araujo, J.L.F.C. Lima, A.O.S.S. Rangel, Analyst, 114, (1989), pp 1465.

17. M.D. Luque de Castro, Talanta, 33, (1986), pp 45.

18. J. Marcos, A. Rios, M. Valcarcel, Trends Anal Chem 11, (1992), pp 373.

19. J. Marcos, A. Rios, M. Valcarcel, Anal Chim Acta, 261, (1992), pp 489.

20. N.W. Barnett, C.E. Lenehan, S.W. Lewis, Trends Anal Chem, 18, (1999), pp 346.

21. D.C. Harris, Quantitative Chemical Analysis. Freeman, New York, (1999), pp 433.

22. W.J. Williams, Hand book of anion determination. Butterworth, London, (1997).

23. D.F. Boltz, J.A. Howell, Colorimetric determination of nonmetals. Wiley, New York.

24. D.R. Jones, Anal. Chim. Acta, 271 (1993), pp 315.

25. G.D. Christian, Analytical chemistry, 5th edn, Wiley, (1994), pp 34.

CHAPTER 7

Sequential injection analysis of α-amylase and β-amylase by spectrophotometric detection

7.1. Introduction

Enzymes are biomolecules responsible for cells' function at normal temperature [1]. They are widely used in food processing and the manufacture of beverages. They are biological catalysts used to control texture, appearance and nutritive value of food as well as to generate desirable flavors and aromas [2]. They have become very important in clinical and industrial uses [3]. Amylases are enzymes, which, in the presence of water, will convert large molecules of starch to sugar units. There are mainly three types of amylases the, alpha, beta

and gamma amylase [3].

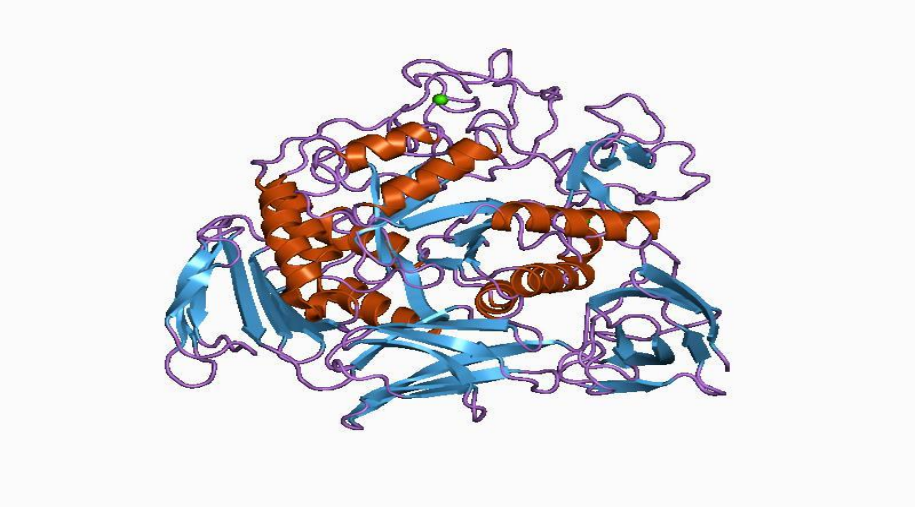

Figure 7. 1. alpha amylase [4].

Fig. 7.1 is the thre dimensional structure of α-amylase.

The alpha amylase (EC 3.2.1.1, 1, 4-α-D glucan glucano-hydrolase, endoamylase) hydrolyzes starch, glycogen, and related polysaccharides by randomly cleaving internal α-1.4-glucosidic linkages yielding glucose and maltose [4]. α-amylase is an important industrial enzyme. It is used as an additive in detergents, the liquefaction of starch, and the proper formation of dextrin in baking [5-6].

Alpha amylase produces alcohol and also saccharin and glucose which are used in the sweet factory and breweries [7-9]. It can be used for clinical diagnosis of, pancreatitis, parotitis and occlusion of the pancreas [10, 11] and also dental carries are enhanced [12].

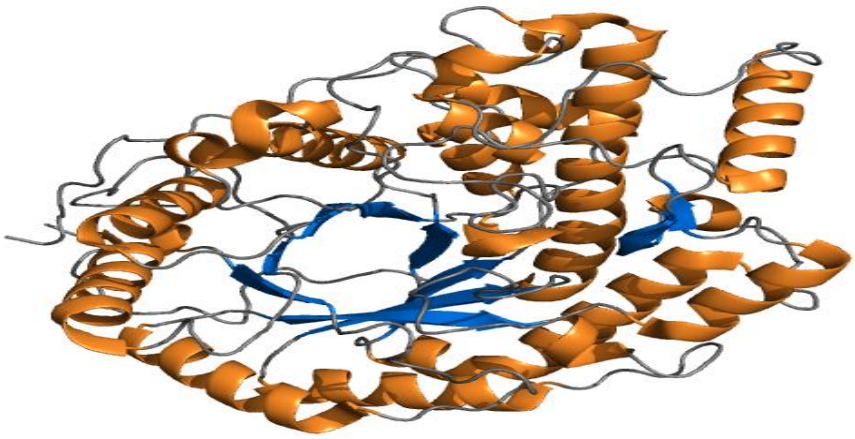

Figure 7. 2. Beta amylase [4].

Fig. 7.2 is the three dimensional structeure of β-amylase.

Beta amylase (EC 3.2.1.2) is an exo-enzyme forms successive maltose units from the non-reducing end of a polysaccharide chain by hydrolysis of α-1.4-glucan linkages. Since it is unable to bypass branch linkages in branched polysaccharides the hydrolysis is incomplete and a macromolecular limit dextrin remains. The beta amylases are exclusively from vegetable or are of microbial in origin [13]. The technological importance of beta amylase is in the brewing, distilling, and baking industries, where starch is converted into fermentable sugar [14-17].

Because of the importance of amylase action in clinical and different industries it is important to develop reliable methods that can be used for the assay of α-amylase and β-amylase. A large number of valuable methods have been described for the assay of amylase [18-24]. The aim of this chapter was to adapt SIA for (α / β)-amylase activity determination. The method is based on the adaptation of the method by Bernfeld for diastatic activity determination of (α /β)-amylase [25]. This will be achieved by specific inhibition of β- amylase by $SnCl_2$ [26], then determine α-amylase. The Specific inhibition of α amylase by acarbose (precose) allowing the determination of β amylase activity [27].

7.2. Experimental

7.2.1. Reagents and standard solutions.

All solutions were prepared by using de-ionised water from a modulab system (Continental Water Systems, San Antonio, TX). All solutions were degassed before they were used. Chromogenic reagent, 1g of 3.5 dinitrosalysilic acid (Fluka. Bucsh SG, Switzerland) was dissolved in 20 ml of 2 mol/l NaOH solution, followed by the addition of sodium-potassium tartrate and diluted to 100 ml with de- ionised water. The solution was protected from CO_2 by fitting an air tight cap. If this was not done the NaOH would react with either CO_2 or O_2 and affect the quality of this solution. It was also advisable to use freshly prepared solutions to avoid inconsistency.

7.2.1.1. Buffer.

9.470g of Na_2HPO_4 and 9.208g of NaH_2PO_4 (Merck, Germany) were individually dissolved in sufficient de-ionised water and then each diluted to 1 L. For a 500 mL phosphate buffer (A) 200 mL of Na_2HPO_4 were mixed with 300 ml of NaH_2PO_4 and 2.3g of dried NaCl then adjusted to pH 6.89. For a 500 mL phosphate buffer (B) it followed the same prepararion and then adjustment to pH 4.80.

7.2.1.2. Starch.

For α-amylase 0.270g of dry starch (Merck, Germany) were mixed with 200 mL of buffer (A) and for β-amylase buffer (B) was used in the same amounts as for α-amylase. The two solutions were then individually boiled gently for 1 min. The solutions were then cooled to room temperature. The respective buffer was used for dilution and to make to the 400 mL

mark.

For the α-amylase working standard solutions, α-amylase from (Bacillus licheniformis, 2.0 U/mg) (Fluka, EC 3.2.1.1, Buchs, Switzerland) solution were prepared by addition of the appropriate mass of the pure α-amylase to a specific volume of de-ionised water to prepare a standard stock solution 0.05 FAU (fungal amylase unit). The range (0.01-0.04) FAU solutions were obtained by appropriate serial dilutions by deionised water.

The same range of concentrations for the β-amylase activity concentrations were prepared exactly in the same manner as for α -amylase. FAU is the amount of enzyme that hydrolyses 5.26 g of starch per hour [28]. The conversion of starch by the α- amylase activity to maltose is 0.95 and therefore the amount of maltose formed is 4.997 g/h [21]. 1 SIGMA unit liberates 1 mg of maltose from starch in 3 min at pH 6.9; therefore 0.02g maltose per hour. The factor between FAU and SIGMA units is therefore 1 FAU= 249.85

7.2.1.3. Experimental.

Figs 7.3 and 7.4 displays the flow diagram of simultaneously analyzing both alpha amylase and beta amylase. For α-amylase and for β-amylase the samples are prepared in 1 %. $SnCl_2$ and 1 % acarbose, respectively.

Sample preparation is outlined in Figs. 7.3 and 7.4, [22].

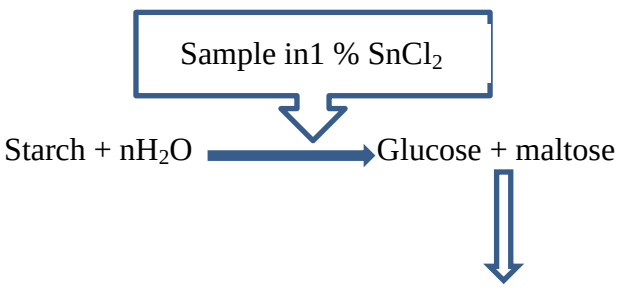

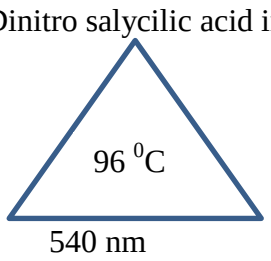

Figure 7. 3. This is the pathway for α-amylase hydrolysis at pH 6.8.

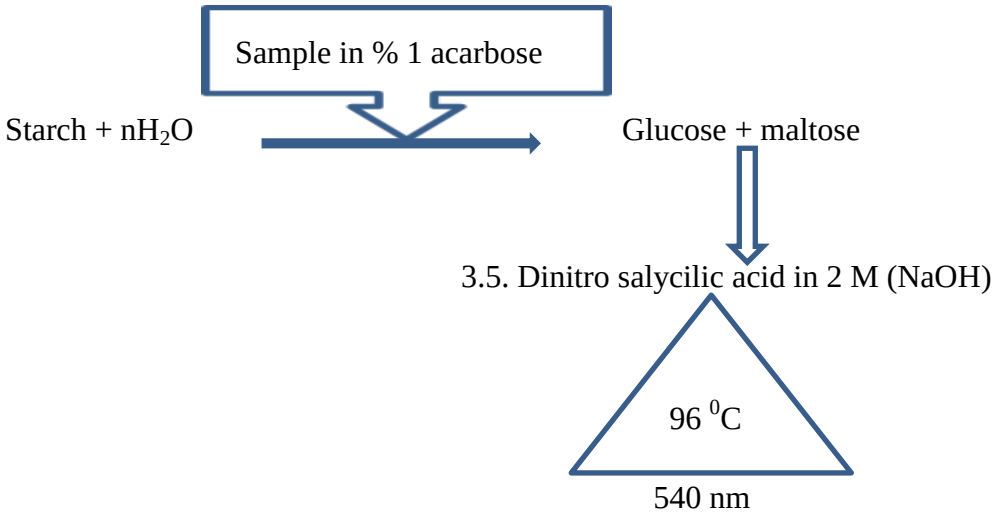

Figure 7. 4. This is the pathway for β-amylase hydrolysis at pH 4.7

7.3. Instrumentation.

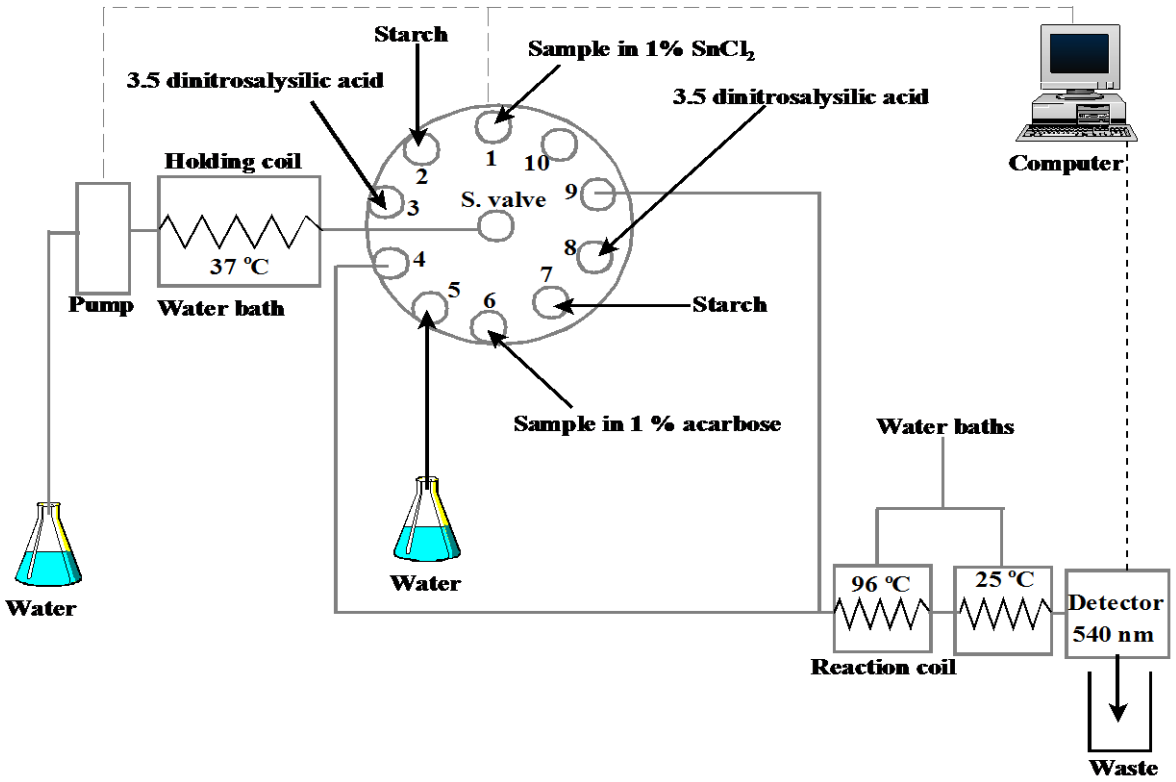

Figure 7. 5. Sequential injection analysis system for simultaneous α-amylase and β-amylase.

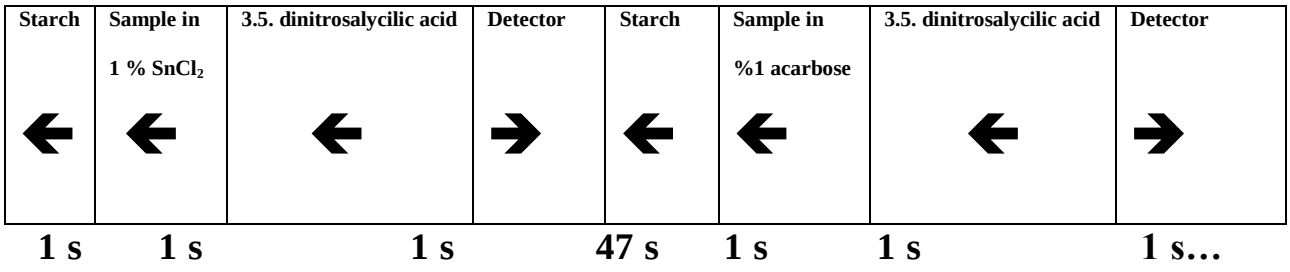

Figure 7. 6. Summary of sequence for simultaneous α-amylase and β-amylase determination.

Fig. 7.5 shows the scheme followed for (α/β)-amylase speciation this was adapted from Fig. 1.7 in Chapter 1. Fig. 7.6 shows the summary of the steps involved with the timming and direction of the pump.

Table 7.1 One cycle of the SIA system for α-amylase and β-amylase speciation.

Time(s)	Pump	Valve	Description

0.0	**Off**	**Sample**	**Pump stops, select starch stream (valve position 1)**
3.0	**Reverse**		**Draws up starch solution in buffer (A)**
4.0	**Off**		**Pump stops**
5.0		**Advance**	**Select sample in 1 % $SnCl_2$ (valve port 2)**
6.0	**Reverse**		**Draws up sample**
7.0	**Off**		**Pump stops**
8.0		**Advance**	**Valve advances to new position (valve port 3)**
9.0	**Reverse**		**Draws up 3.5 dinitrosalysalic acid solution**
10.0	**Off**		**Pump stops**
11.0		**Advance**	**Valve advances to new position(valve port 4)**
12.0	**Forward**		**Forward mixture through reaction coil to detector**
59.0	**Off**		**Pump stops**
60.0		**Advance**	**Valve advances to new position (valve port)**
61.0	**Reverse**		**Draws up carrier solution**
62.0	**Off**		**Pump stops**
63.0		**Advance**	**Valve advance to new position (valve port 6)**
64.0	**Reverse**		**Draws up sample in 1 % acarbose solution**
65.0	**Off**		**Pump stops**
66.0		**Advance**	**Valve advance to new position(valve port 7) buffer (B) starch)**
67.0	**Reverse**		**Draws up 3.5 dinitrosalysalic acid solution**
68.0	**Off**		**Pump stops**
69.0		**Advance**	**Valve advance to new position (valve port 8)**
70.0		**Forward**	**Forward mixture through reaction coil to detector**
129.0	**Off**		**Pump stops**
130.0		**Home**	**Valves resume first position**

7.4. Operation of the system.

Table 7.1 give the sequence of the series of steps that are followed for the single complete cycle for the quantitative determination of both (α/β)-amylase activity. This is carried out by differential inhibition of the β amylase activity by $SnCl_2$ in the presence of $CaCl_2$ in buffer (A) and by specific inhibition of α-amylase by acarbose (precose) in buffer (B). The profile of this determination is displayed in Fig. 7.7 through distinct peaks for α-amylase and β-amylase respectively.

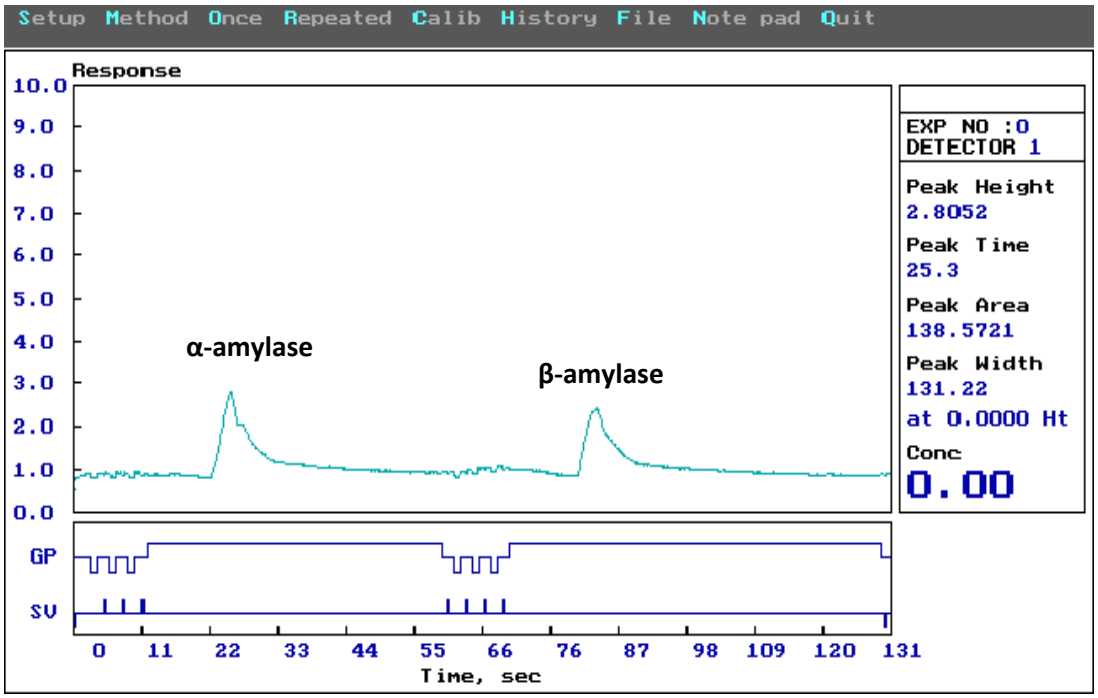

Figure 7. 7. α-amylase and β-amylase profile.

7.5. Optimisation, results and discussion.

Preliminary evalution of different ratios for (α-amylase: β-amylase) such as 1:2, 1:3 and swapping them were carried out. For the optimization part of the enzyme ratio, the enzymes concentration ratios used was 0.02: 0.02 FAU as (α-amylase: β-amylase). This set-up allows equal volumes to undergo the same chemical manipulation.

7.5.1. Physical parameters.

7.5.1.1. Effect of holding coil lengths and internal diameters on α-amylase and β- amylase determination.

Figs. 7.8 (a) and 7.8 (b) show evaluation of this parameter and the results was 300 cm for the holding coil.

Influence of holding coil length on α-amylase determination

Peak height	HC L (m)	% RSD
2.0039	1.5	2.32
1.9985	2.0	2.02
2.3862	2.5	1.84
4.1876	3.0	0.58
3.6657	3.5	1.66

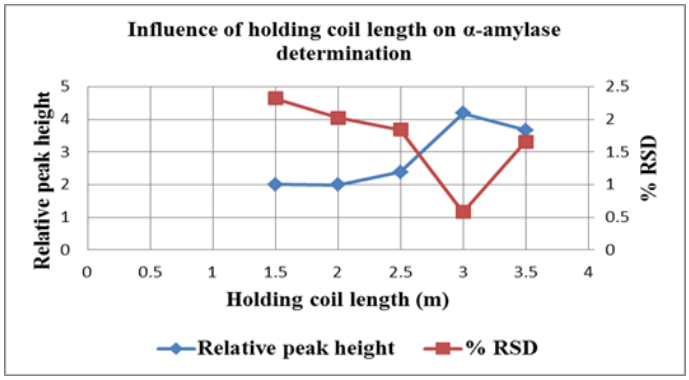

Figure 7.8 (a) Holding coil length on α-amylase determination.

Influence of holding coil length on β – amylase determination

Peak height	HC L (m)	% RSD
1.9881	1.5	2.24
1.7844	2.0	1.96
2.2918	2.5	1.87
3.8296	3.0	0.63
3.5867	3.5	1.58

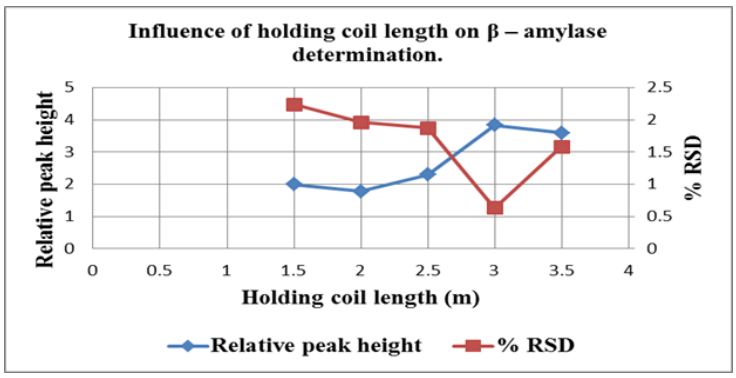

Figure 7.8 (b) Holding coil length on β-amylase determination.

7.5.1.2. Influence of hydrolysis coil lengths and internal diameter.

The parameters for the hydrolysis coil were evaluated at 38 ^{o}C. The results of the hydrolysis coil length and diameter optimization step are well illustrated in the table and figure below. This is the most important part of the simultaneous analysis of α-amylase and β-amylase. It is the part where the actual breakdown of starch producing the maltose which is the biochemical molecule that serves as the bases of the determination step. This exercise confirmed the following values in that they yielded appreciable peak heights accompanied Figs. 7.9 (a) and 7.9 (b) gave 80 cm for the hydrolysis coil length.

Influence of hydrolysis coil lengths on α–amylase determination.

Peak height	Hydrolysis coil L (cm)	% RSD
1.7659	40	1.99
2.9437	60	1.96
3.3841	80	0.6
2.7588	100	1.84
2.5933	120	1.93
1.8981	160	2.01

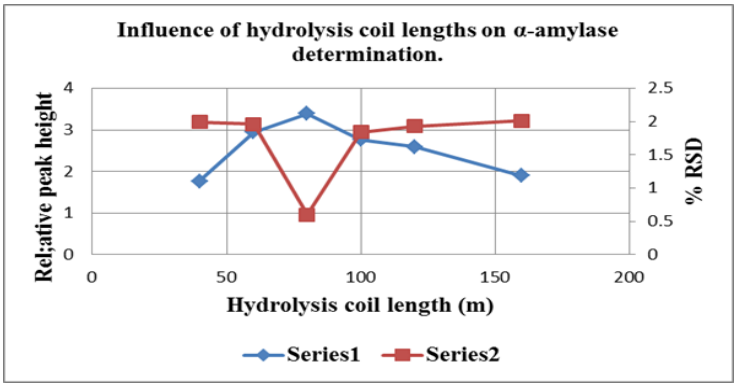

Figure 7.9 (a) hydrolysis coil lengths on α-amylase determination.

Influence of hydrolysis coil length on β-amylase determination.

Peak height	Hydrolysis coil length (cm).	% RSD
1.3225	40	1.78
1.9887	60	2.11
2.9746	80	0.930
2.47738	100	1.98
2.18878	120	2.12
1.4868	160	2.59

Figure 7.9 (b)

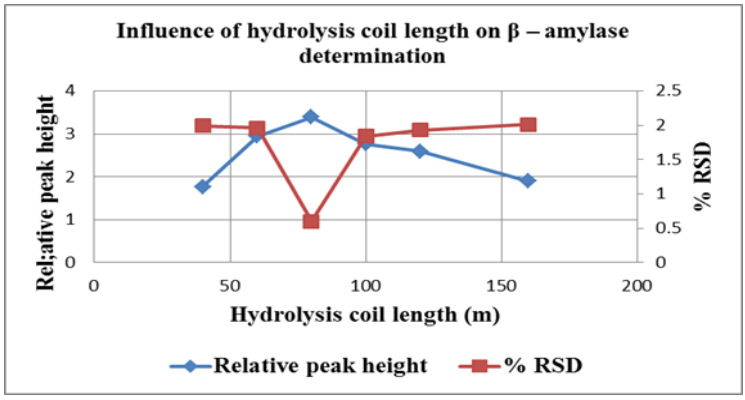

hydrolysis coil L on β-amylase determination.

Influence of hydrolysis coil internal diameter on α-amylase determination.

Peak height	i.d (mm)	% RSD
1.82234	1.65	1.635
2.9658	1.6	1.898
3.6312	1.14	0.7614
2.7619	1.02	0.3861
2.4285	0.89	0.7481

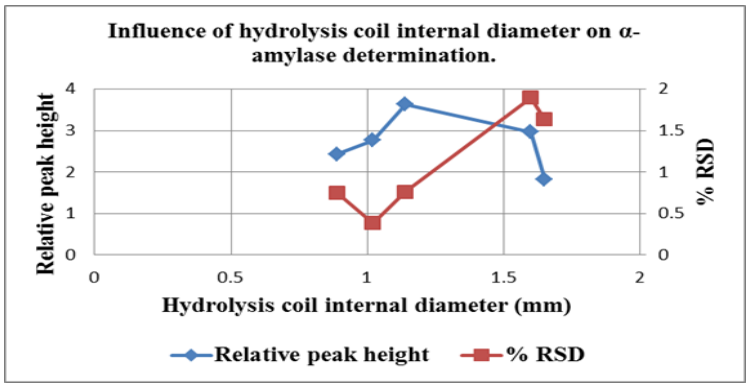

Figure 7.10 (a) hydrolysis coil i.d on α-amylase dermination.

For the hydrolysis coil 1.02 mm gave the best results for the internal diameter optimization as shown in Figs. 7.10 (a) and 7. 10 (b).

Influence of hydrolysis coil internal diameter on β-amylase determination.

Peak height	i.d (mm)	% RSD
1.29851	1.65	1.95
2.0023	1.6	1.79
3.1142	1.14	0.74
2.3822	1.02	0.42
2.2048	0.89	0.92

Figure 7.10 (b) hydrolysis coil i.d on β-amylase determination.

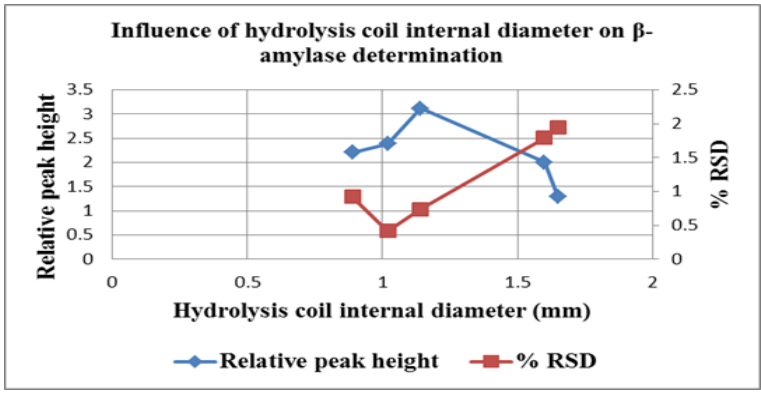

7.5.1.3. Influence of cooling coil lengths and diameters on α-amylase and β-amylase determination.

Effect of cooling curve (CC) length on α-amylase determination.

Peak height	CC (L) (cm)	% RSD
2.2020	20	1.98
2.3967	40	0.86
1.9885	60	1.22
1.7648	80	1.01

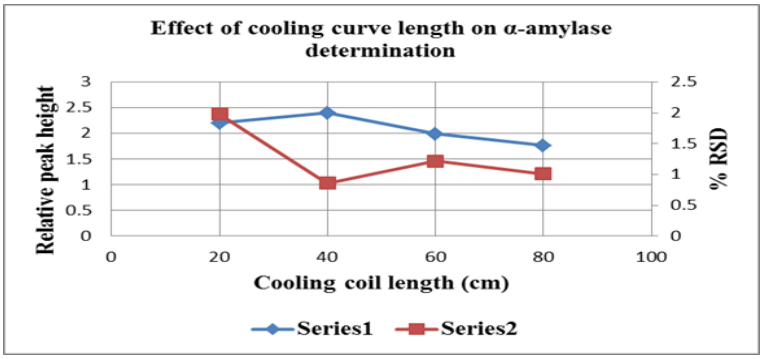

Figure 7.11 (a) cooling coil length on α-amylase determination.

Figs. 7.11 (a) and 7.11(b) confirmed 40 cm as the best length for the cooling coil for both β-amylase and α-amylase determination.

Effect of cooling curve lengths on β-amylase determination.

Peak height	CC (L) cm)	% RSD
2.0198	20	1.76
2.7881	40	0.88
1.8073	60	1.12
1.6324	80	1.31

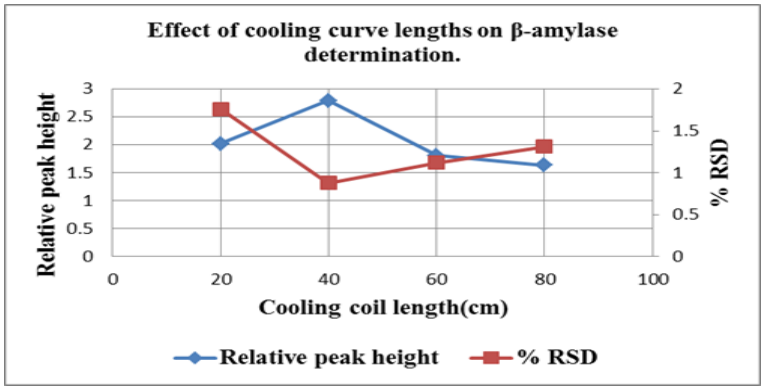

Figure 7.11 (b) cooling coil lengths on β-amylase determination.

7.5.1.4. Effect of reaction coil lengths, internal diameters and temperature variation on α-amylase and β-amylase determination.

Temperature of the reaction coil varied from (88 - 102) ^{0}C. The reaction between maltose and 3.5 dinitrosalycilic acid is temperature dependent.

Effect of reaction coil (RC) temperature on α-amylase determination.

Peak height	Temperature (^{0}C)	% RSD
1.9866	88	1.11
2.4588	92	1.25
3.0185	96	0.88
3.1986	100	1.35
2.9965	104	2.32

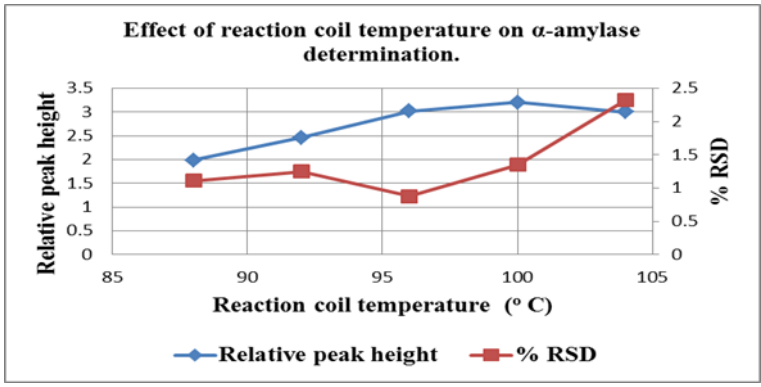

Figure 7.12 (a) RC (^{0}C) on α-amylase determination

From Figs. 7.12 (a) and 7.12 (b) which show the optimization of the reaction coil temperature confirmed 96 ^{0}C as the best temperature.

Effect of reaction coil temperature on β-amylase determination

Peak height	Temperature (^{0}C)	% RSD
1.7924	88	1.34
2.3733	92	1.42
2.90224	96	0.86
2.9852	100	1.77
2.6885	104	2.32

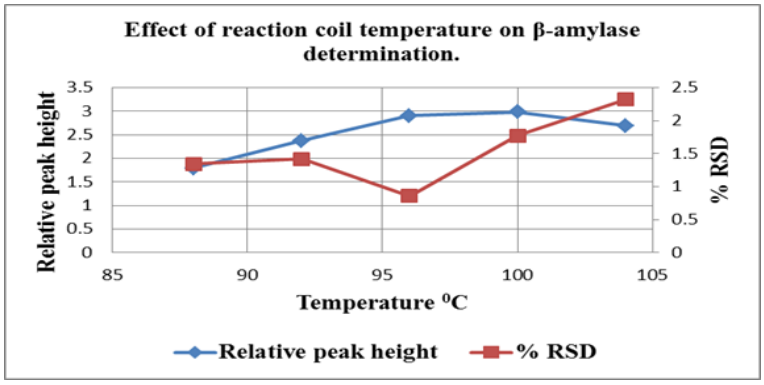

Figure 7.12 (b) RC (^{0}C) on β-amylase determination.

Effect of cooling coil internal diameter on α-amylase determination

Peak height	i.d (mm)	% RSD
1.29851	1.65	1.35
2.0023	1.6	1.98
3.1142	1.14	1.76
2.3822	1.02	1.22
2.2048	0.89	0.72

Figure 7.13 (a) cooling coil (i.d) on α-amylase determination.

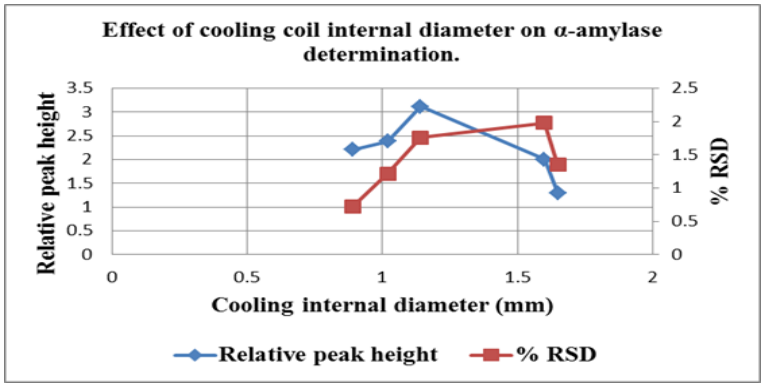

0.89 mm was the best internal diameter for the cooling coil as shown in Fig. 7.13 (a) for α-amylase.

Effect of cooling coil internal diameter on β-amylase determination.

Peak height	i.d (mm)	% RSD
1.1776	1.65	1.95
1.9865	1.6	1.79
2.9857	1.14	0.74
2.0175	1.02	1.12
1.9661	0.89	0.74

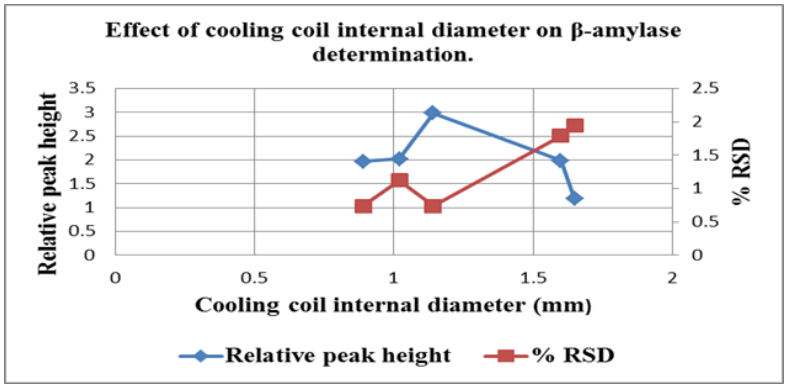

Figure 7.13 (b) cooling coil i.d on β-amylase determination.

1.02 mm was the best internal diameter for the cooling coil as shown in Fig. 7.13 (b) for β-amylase.

7.5.1.5. Effect of flow rate and sample volume on α-amylase and β-amylase determination.

The flow rate that was best suited for this analysis was 3.6 ml/min as displayed in Figs. 7.14 (a) and 7.14 (b).

Effect of flow rate on α-amylase and β-amylase determination.

Peak height	Flow rate mL/min	% RSD
1.3886	2.0	1.87
1.6597	2.8	1.35
2.8756	3.6	0.78
1.9754	4.4	1.48
1.4822	5.2	1.22

Figure 7.14 (a) Effect of flow rate on α-amylase determination.

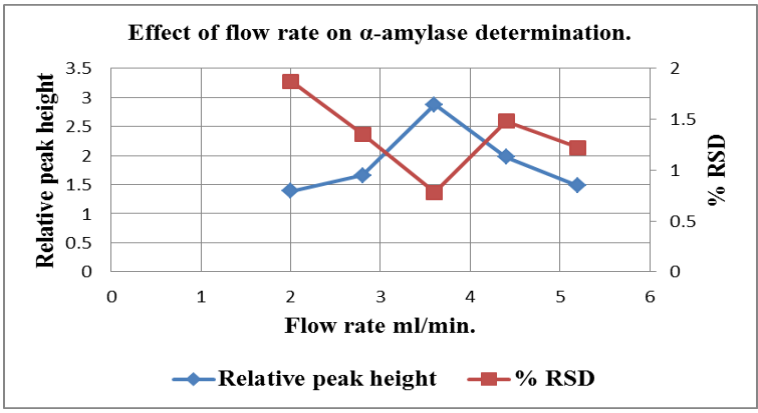

Peak height	Flow rate mL/min	% RSD
1.3548	2.0	1.95
1.5922	2.8	1.42
2.5449	3.6	0.88
1.6834	4.4	1.54
1.4019	5.2	1.36

Figure 7.14 (b) Effect of flow rate on β-amylase determination.

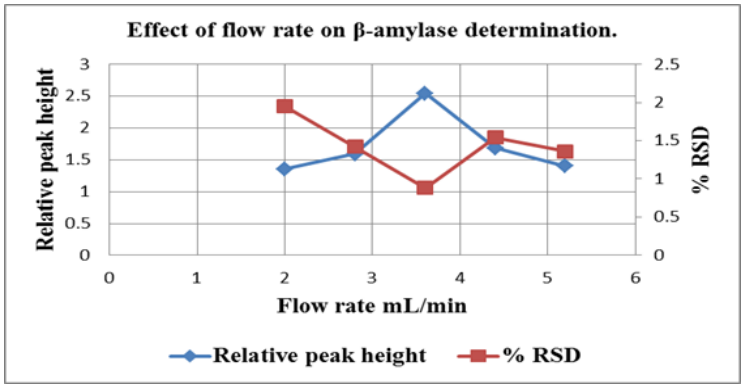

Effect of sample volume on α-amylase determination.

Peak height	Sample volume (µL)	% RSD
1.8685	160	0.58
2.20934	220	1.35
1.9556	280	1.27
2.4566	340	1.09
2.7558	400	1.87

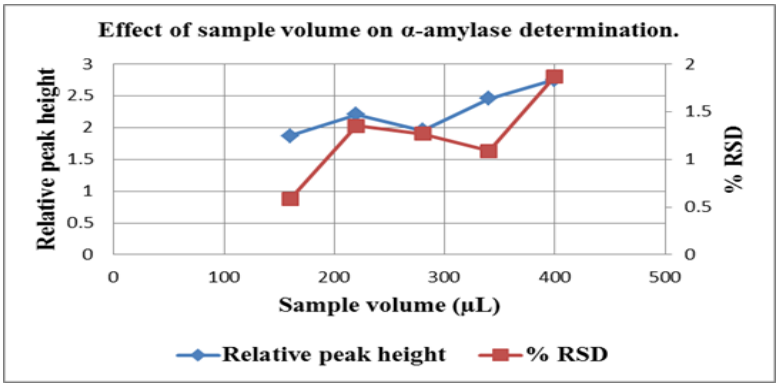

Figure 7.15 (a) sample volume on α-amylase determination.

Effect of sample volume on β-amylase determination.

Peak height	Sample volume (µL)	% RSD
1.6566	160	0.64
1.9764	220	1.47
1.6988	280	1.27
2.1758	340	1.17
2.5987	400	1.78

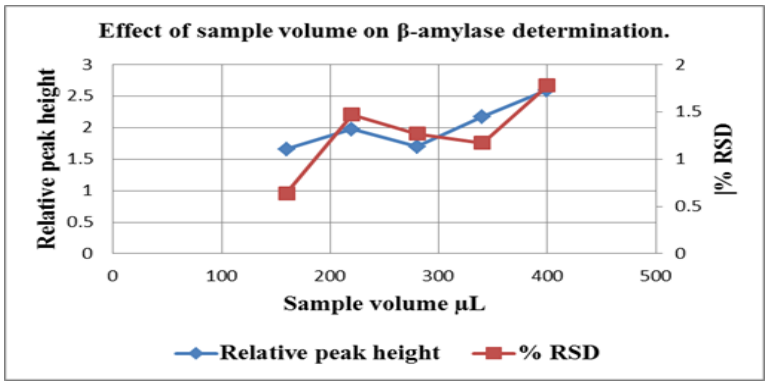

Figure 7.15 (b) sample volume on β-amylase determination.

Figs. 7.15 (a) and 7.15 (b) show that the sample volume optimized to be 160 µL.

Effect of 3.5 dinitrosalycilic acid (DNA) volume on α-amylase determination.

Peak height	3.5. (DNA) µL	% RSD
2.8445	160	0.68
2.3176	220	1.48
1.9887	280	1.37
2.2068	340	1.20
2.5866	400	1.95

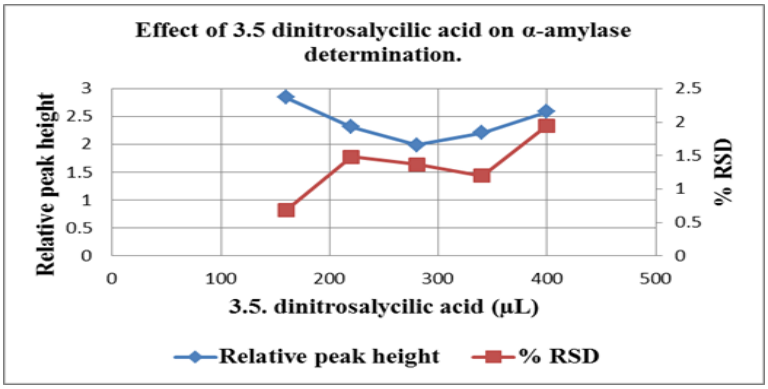

Figure 7.16 (a) (DNA) volume on α-amylase determination.

The volume best suited for this analysis was 160 (µL) of 3.5 dinitrosalycilic acid as shown in Fig. 7.16 (a).

Effect of 3.5 dinitrosalycilic acid volume on β-amylase determination.

Peak height	(DNA) (µL)	% RSD
2.6596	160	0.78
2.1968	220	1.54
1.8695	280	1.15
2.0759	340	0.97
2.3792	400	1.98

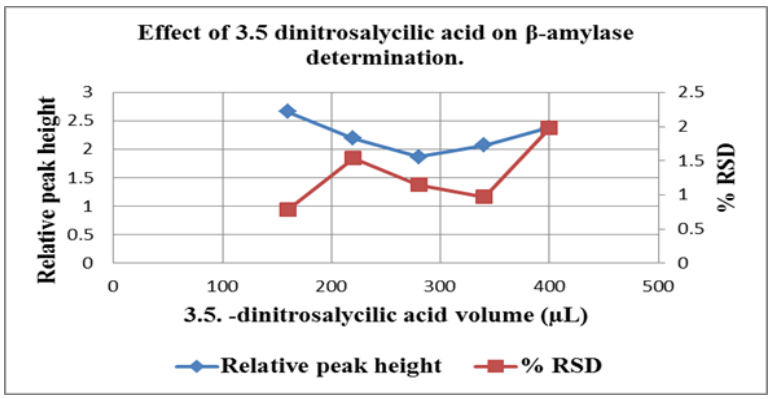

Figure 7.16 (b) (DNA) volume on β-amylase determination.

The volume best suited for this analysis was 160 (µL) of 3.5 dinitrosalycilic acid as shown in Fig. 7.16 (b).

7.5.2. Chemical parameters.

7.5.2.1. (3.5 dinitrosalycilic acid) concentration W/W % on α-amylase and β-amylase.

Effect of 3.5. dinitrosalycilic [DNA] concentration on α-amylase determination.

Peak height	DNA (w/w)%	% RSD
0.8149	0.1	2.01
1.0117	0.15	0.98
3.6885	1	0.75
1.6975	1.5	1.68
1.3098	2.0	1.45

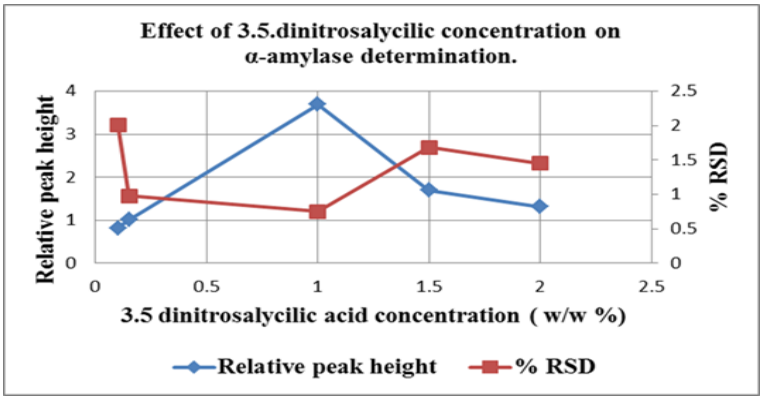

Figure 7.17 (a) [DNA] on α-amylase determination.

1 % 3.5. dinitrosalycilic yielded the best results as shown in Figs. 7.17 (a) and 7.17 (b).

Effect of 3.5. dinitrosalycilic concentration on β-amylase.

Peak height	DNA (w/w %)	% RSD
0.7178	0.1	2.24
0.8876	0.15	1.09
3.1996	1	0.88
1.5586	1.5	1.75
1.2665	2.0	1.38

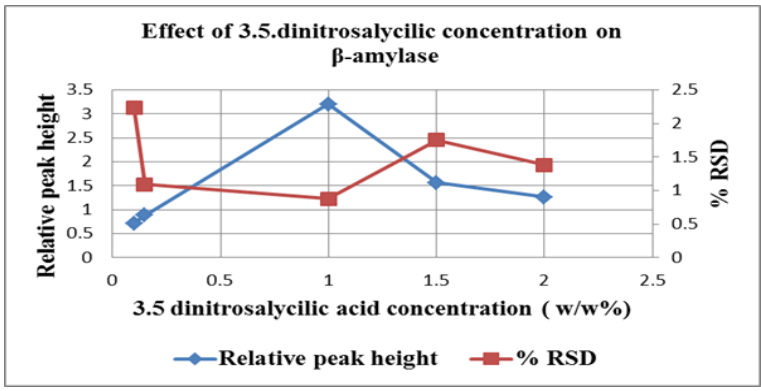

Figure 7.17 (b) [DNA] on β-amylase determination.

7.5.2.2. NaOH concentration.

The concentrations were varied by correlating the appropriate volumes of 2mol/L NaOH to

give the relevant % NaOH given as mass per mass.

Effect of % NaOH on the method sensitivity.

Peak height	% NaOH (m/m)	% RSD
3.2265	0.33	0.87
2.8845	0.66	1.86
1.8019	0.99	1.22
1.0196	1.33	1.09

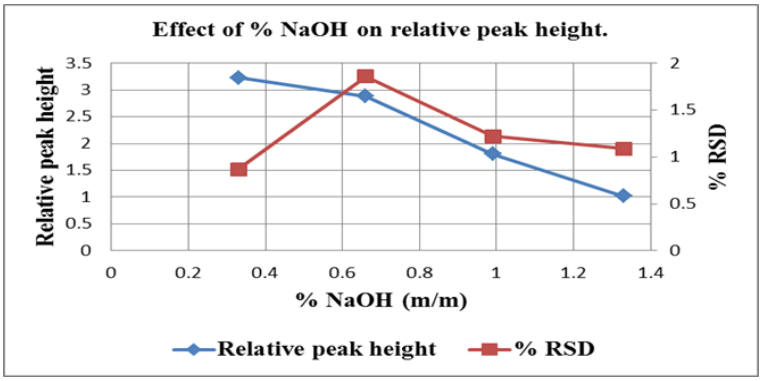

Figure 7. 18. Effect of % NaOH on the method sensitivity.

0.3 % NaOH gave the best sensitivity as per Fig. 7.18.

Effect of starch concentration on α-amylase determination.

Peak height	[Starch] (mol/L)	% RSD
0.6899	0.65	1.09
0.8224	1.30	2.02
1.5896	1.95	1.98
2.7996	2.70	0.68
1.8754	3.35	2.34

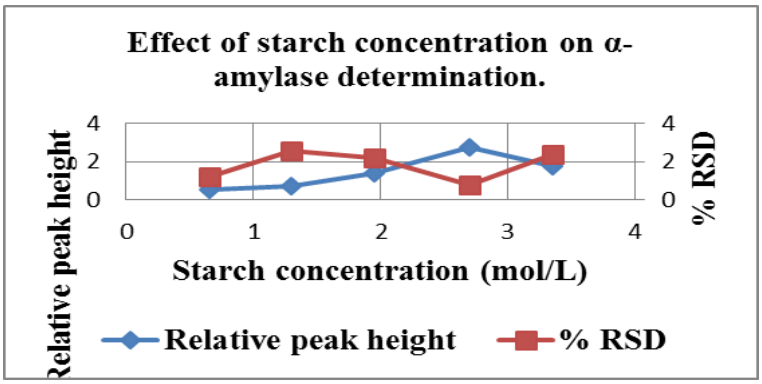

Figure 7.19 (a) [starch] on α-amylase determination.

2.7 mol/L starch proved to be ideal for this analysis as shown in Figs. 7.19 (a).

Effect of starch concentrations on β-amylase determination.

Peak height	[Starch] (mol/L)	% RSD
0.5197	0.65	1.18
0.7089	1.30	2.58
1.3748	1.95	2.18
2.7442	2.70	0.75
1.7361	3.35	2.34

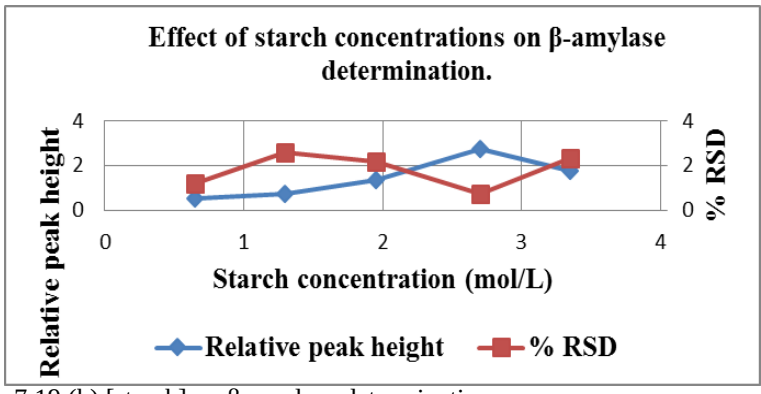

Figure 7.19 (b) [starch] on β-amylase determination.

7.5.2.4. Effect of pH.

Effect of pH on α-amylase and β-amylase determination.

Peak height	pH	% RSD
0.3988	4.89	1.09
0.5831	5.89	2.84
2.7714	6.89	0.76
1.5562	7.89	0.97
0.6218	8.00	1.65

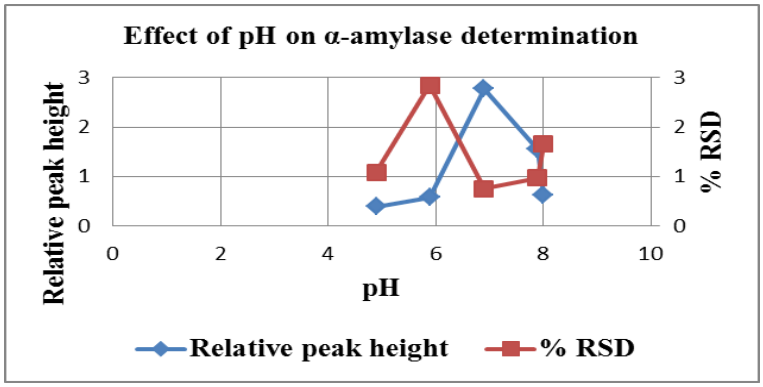

Figure 7.20 (a) Effect of pH on α-amylase determination.

Peak height	pH	% RSD
0.5145	1.80	1.24
0.6544	2.80	2.15
1.7221	4.80	0.78
0.6874	5.80	1.68
0.3896	6.80	2.34

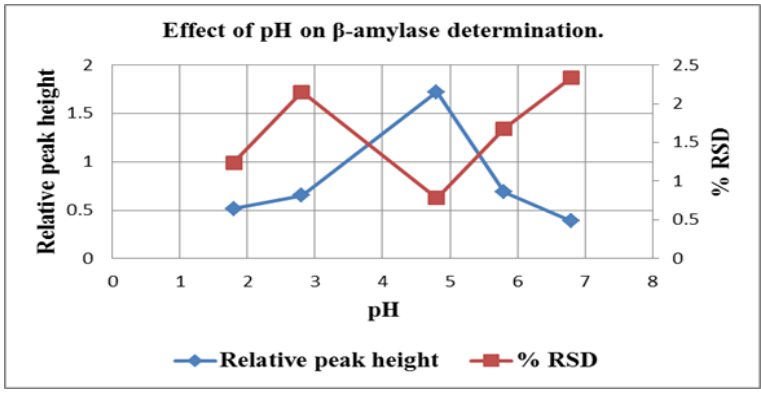

Figure 7.20 (b) pH evaluation for α-amylase for was 6.89.

Figs. 7.20 (b) and 7.20 (b) comfirm pH 4.7 as the ideal pH for both α-amylase and β-

amylase determination.

7.6. Method evaluation.

The proposed method was critically evaluated in terms of the working range as depicted by the linear range, precision, accuracy, detection limit, sample frequency and interaction. Interferences and percentage recovery were also evaluated. All these were done in order to confirm the applicability of the method and how well suited it is, for the simultaneous determination of both α-amylase and β-amylase activities. The ratio used for evaluation was 0.02 FAU (α-amylase) and 0.02 FAU (β-amylase). Linearity was evaluated under optimum conditions for the system. The regression outputs from these analyses are given on Table 7.2 as follows:

Table 7.2 Regression output α amylase and β- amylase.

Activity FAU α-amylase	Activity FAU β-amylase	Relative peak height α-amylase	Relative peak height β-amylase
0.004	0.004	0.1331	0.0981
0.008	0.008	0.5396	0.4409
0.012	0.012	0.9402	0.7698
0.016	0.016	1.3518	1.1324
0.020	0.020	1.7334	1.4285
0.024	0.024	2.1388	1.7989
0.028	0.028	2.5397	2.0985
0.032	0.032	2.9213	2.4457
0.036	0.036	3.3289	2.7509
0.040	0.040	3.6978	3.0977

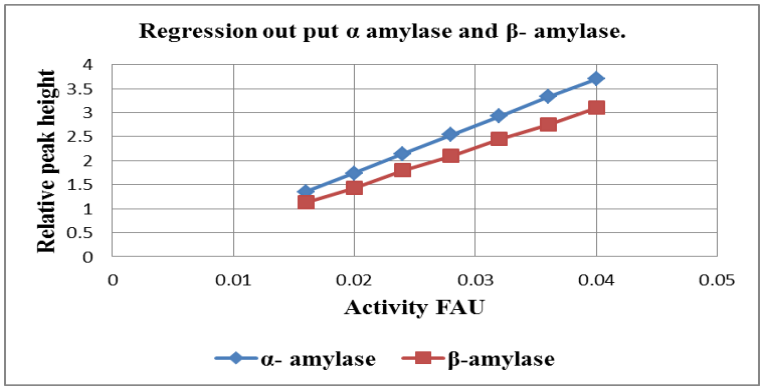

Figure 7.21. Linear curve for α-amylase and β-amylase

	Regression output (α-amylase)	Regression Output (β-amylase)
Constant	0.9286	0.9138
Std Err of Y Est	0.0172	0.0375
R Squared	0.9995	0.9988
No. of Observations	5	5
Degrees of Freedom	3	3
X Coefficient(s)	1.3872	1.3667
Std Err of Coef.	0.001	0.001

$H_{\alpha\ amylase} = 1.3872\ C + 0.9286$; $r^2 = 0.9995$ (n = 10) and

$H_{\beta\ amylase} = 1.3667\ C + 0.9138$; $r^2 = 0.9988$ (n = 10)

The calibration curve for the proposed SIA system method was found to be linear between 0.0154 and 0.0.0460 FAU for both α-amylase and β-amylase as shown in Fig. 7.21. The calculated detection limits were found to be 0.0035 FAU for α-amylase and 0.0038 for β-amylase.

The precision of the method is displayed by the % RSD from Tables 7. 5. The % RSD was

found to be 0.85 and 0.92 for α-amylase and β-amylase activities respectively. The accuracy of the proposed method was checked by spiking known concentrations of the sample with predetermined α- amylase and β -amylase concentrations and then comparing expected values with the determined values, this is given in Table 7.4.

Further comparison of results from this method and the standard methods (Iodine method) gave the performance of the method in terms of precision. Table 7.5 shows that there are slight differences between the results of the two methods. Samples were each spiked with different concentrations of both α-amylase and β-amylase. In all instances the % recovery was more than 90.

Repeating each determination ten times and comparing the consecutive results gave the real precision of the proposed method. One cycle of the determination shows an in built rinsing step that aids in eliminating any sample carry over. There did not seem to be any sign of interferences as a result of sample interaction for each consecutive determination.

Although this step resulted in reducing the number of determinations per given time, it was very important that any determination should be free from sample carry over. The proposed method is able to determine sequentially α-amylase and β-amylase activity at a rate of one sample per 130s.

Statistical evaluation was carried out on the results to determine if the proposed method yielded results that are comparable with the standard iodine method and free from systematic error. The results were closely comparable and with high precission.

Table 7.3 Evaluation of inhibitor type and concentration on α-amylase and β-amylase activity.

Inhibitor Type	Concentration (mol/L)									
	1 X 10^{-3}		**2 X 10^{-3}**		**3 X 10^{-3}**		**4 X 10^{-3}**		**5 X 10^{-3}**	
	Amylase type		**Amylase type**		**Amylase type**		**Amylase type**		**Amylase type**	
	α	**β**	**α**	**β**	**A**	**β**	**α**	**β**	**α**	**β**
	% activity		**% activity**		**% activity**		**% activity**		**% activity**	
$SnCl_2$ *	94	58	91	36	91	21	90	17	90	11
$CuSO_4$	96	76	92	71	91	71	91	68	89	63
EDTA *	96	94	95	80	95	76	92	66	91	62
Precose	14	95	14	95	11	95	11	95	9	93
Ascorbic acid	96	82	95	74	95	60	93	58	92	56
$ZnSO_4$ *	95	39	95	33	93	28	92	23	90	18

∗ The inhibition was investigated in 0.1 % $CaCl_2$ (m/v) and the other as 0.1 % (m/v) inhibitor type.

Table 7.3 gives the % inhibition of the activity of α-amylse and β-amylase by the specific chemical species. This is given as % activity for either α-amylse or β-amylase within the solution spiked with the inhibitor type.

Table 7.4 Displays % Recovery after addition of 0.02 FAU of both (α and β) -amylase.

Sample identity	Original activity FAU		Expected activity FAU		New activity FAU		% Recovery	
	amylase type		amylase type		amylase type		amylase type	
	α	**β**	**α**	**β**	**α**	**β**	**α**	**B**
Malt Wheat	0.034	0.003	0.054	0.023	0.051	0.022	94.0	95.6
Malt sorghum	0.006	0.002	0.026	0.022	0.025	0.023	96.2	104.5
Morvite energy food	0.042	0.005	0.062	0.025	0.063	0.024	101.6	96.0
Sweet potato	0.007	0.108	0.027	0.128	0.026	0.127	96.3	99.2

Table 7.5 determination of (α and β) -amylase activity from real samples.

Sample identity	Proposed SIA method Diastatic activity (FAU)		Iodine method Diastatic activity (FAU)	
	α-amylase	β-amylase	α-amylase	β-amylase
Malt wheat	0.034 ± 0.05	0.002 ± 0.001	0.035 ± 0.012	0.002 ± 0.001
Malt sorghum	0.006 ± 0.001	0.002 ± 0.001	0.006 ± 0.003	0.002 ± 0.001
Energy food Morvite	0.042 ± 0.002	0.005 ± 0.002	0.042 ± 0.004	0.004 ± 0.003
Sweet potato	0.007 ± 0.001	0.096 ± 0.003	0.006 ± 0.001	0.089 ± 0.005

FAU (fungal amylase unit) this is the activity related to the amount of enzyme that hydrolyses 5.26 g of starch per hour. (1FAU = 249.85 sigma).

These samples were chosen because they are commonly used as instant food and for sweet potato it was included as it is a natural vegetable without industrial processing.

7.7. Detection limit.

The detection limits for the method were calculated as similarly to as in Chapter 3. The detection limit for α- amylase determination was calculated to be 0.0046 FAU within a working range of (0.015–0.04) FAU which was the same as for β-amylase.

7.8. Conclusion.

Although the method requires the knowledge of basic chemistry and the understanding of the spectrophotometric protocol, the set-up of this instrumentation is in itself simple and robust. The economics of this procedure is fairly low as minute quantities of reagents are consumed. The rate of analysis is remarkably reduced from 24 hours to within an hour of analysis.

The method showed great versatility during its optimization and yielded a high percentage of precision and reliability. The calculated % RSD was lower than 0.80, an indication of the consistency. This procedure can easily be adapted and can easily be used for on-line clinical analysis and for food quality analysis. Table 7.4 gave a good percentage recovery while Table 7.5 showed the similarity in the results of the iodometric method and the proposed SIA method.

7.9. References.

1. K. Myrback and G. Neumuller, “The enzymes. Chemistry and Mechanism of Action” (JB. Summer and K. Myrback, eds.), Academic Press. New York (1950)

2. J.R. Whitaker, Principles of enzymology for the food sciences, Marcel Dekker, Inc., New York, (1972), pp 391.

3. N. Batlle, J.V. Carbonell, J.M. Sendra, Biotechnolofy and Bioengineering, 67,2, (2000), pp 127

4. C.T. Greenwood, E.A. Milne, Adv. Carbohydr. Chem. 23, (1968), pp 281.

5. T.F. Martinez, M. Diaz, F.J. Moyano, J. of the Science of Food and Agriculture, 82, 4, (2002), pp 398.

6. R. Shinke, Y. Kunimi, H. Nishira, J. Ferm Tech 53(1975), pp 693.

7. I. Nkana, H.G. Muller, J. Cereal Sci. 8 (1988), pp 269.

8. M. Carlsen, J. Nielsen, J. Villadsen, J. Bitechnol. 45 (1996), pp 81.

9. J. Carter, W. Stamples, E. Sinson, Clin. Chem. 19, (1973), pp 686.

10. H. Liang, Q. Wang, M.S. Ruan, J. Chromatogr. Appl. 724 (1999) pp 381.

11. G. Michal, Biochemical Pathways. An Atlas of Biochemistry and Molecular Biology, Wiley, New York, (1999), pp 33.

12. M.D. Luque de Castro, GBF Monographs 14, (1991), pp123.

13. M.S. Karve, N.R. Kale, Indian J. Biochemistry and Biophysics, 118, 4, (1981), pp 132.

14. H.J. Wu, G.Y. Tang, H. Li, Z.D. Li, Sepu. 17, (1999), pp 208.

15. A.W. MacGregor, J.E. Morgan, J. Cereal Sci. 16, (1992), pp 267.

16. T. Moriyama, H. Kikeda, J. Chromatogr. B: Biomed. Appl. 20 (1996) pp 201.

17. R. Schindler, B. Lendl, R. Kellner, Anal. Chim. Acta 366, (1998), pp 35.

18. R.W. Min, C. M. Arlsen, J. Nielsen, J. Villadsen, Biot. Tech. 9 (10), (1995), pp 763.

19. J. Ruzicka, G.D. Marshall, Anal. Chim. Acta 237, (1990), pp 239.

20. J.F. van Staden, H. du Plessis, S.M. Linksy, R.E. Taljaard, B. Kremer, Anal. Chim. Acta 354, (1997), pp 59.

21. J. Ruzicka, G.D. Marshall, G.D. Christian, Anal. Chem. 62, (1990), pp 1861.

22. P. Bernfeld, Enzymology 1, (1955), pp 149.

CHAPTER 8

On-line simultaneous determination of S-and R-perindopril using amperometric biosensors as detectors through FIA and SIA flow systems.

8. 1. Introduction.

Perindopril (aceon) a non-sulfhydryl angiotensin converting enzyme (ACE) inhibitor is used for the treatment of hypertension by inhibiting the renin-angiotensin system [1]. They also modulate sympathetic nervous system activity, increase prostaglandin synthesis, cause vasodilation and mild natriuresis without affecting heart rate and contractility [2].

Perindopril is a dipeptide monoacid monoester with a perhydroindole group with therapeutically active carboxyl side group. It is an orally active and non-thiol prodrug which requires de-esterification to peridoprilat to be used as ACE [2].

Perindopril hydrolyses to form the active derivative that inhibits ACE and the conversion of angiotensin I to angiotensin II; resulting in angiotensin II-mediated vasoconstriction and its subsequent inhibition for aldosterone secretion from the adrenal cortex thus leading to diuresis and natriuresis [3].

It forms an intergral part while in combination with other drugs as one of multiple active ingredients found in Bipreterax (Perindopril + Indapamide), Coversyl Plus (Perindopril +

Indapamide), Preterax (Perindopril + Indapamide) and Prexum Plus (Perindopril + Indapamide). All these are important clinical drugs for hypertension treatment [4].

8.1.1. Chemistry of perindopril [4].

It has a molecular formula is $C_{19}H_{32}N_2O_5$.

With the more pronounced scientific formula as:

IUPAC: Name (2S,3aS,7aS)-1-[(2S)-2-[[(2S)-1-ethoxy-1-oxopentan-2-yl] amino-propanoyl-2,3,3a,4,5,6,7,7a-octahydroindole-2-carboxylic acid

InChI=1S/C19H32N_2O_5/c1-4-8-14(19(25)26-5-2)20-12(3)17(22)21-15-10-7-6-9-13(15)11-16(21)18(23)24/h12-16,20H,4-11H_2,1-3H3,(H,23,24)/t12-,13-,14-,15-,16-/m0/s1

EC Number: 617-394-0

CAS number :82834-16-0

8.1.2. Structure of S /R Perindopril.

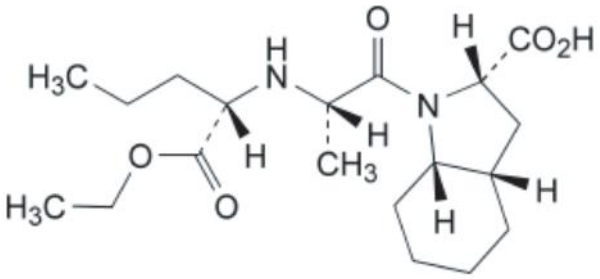

Figure 8. 1. S- Perindopril (S-pdp) [4]

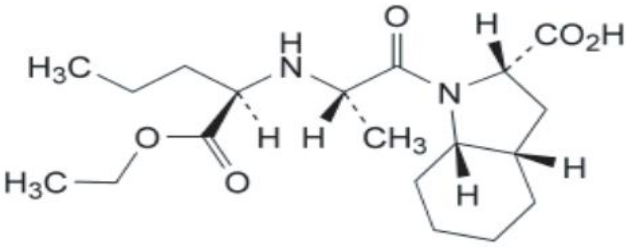

Figure 8. 2. R-Perindopril (R-pdp) [4]

Figs. 8.1 and 8.2 show the structure of S- Perindopril (S-pdp) and R-Perindopril (R-pdp).

8.2. Chiral chemistry and its importance in drug therapy.

Louis Pasteur was the first person to discover chirality [5] which is described as a molecule with exactly the same type and number of atoms but differently arranged in space. They may rotate light polarity and have different biological activity. They are identified as R and S depending on how they rotate the light. Fig. 8.3 shows how the spatial arrangement of the same molecule may differ forming enantiomers. Their activity depends on the other chiral entities within their environment this then requires a more precise technique to quantify these enantiomers.

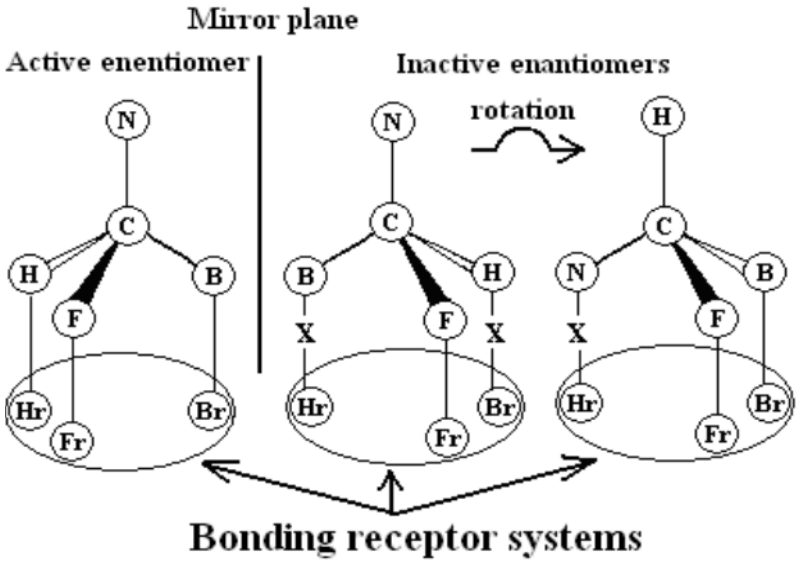

Figure 8. 3. Hypothetical interaction between the two enantiomers of a chiral drug and the biological bonding spots [6].

S-perindopril treats hypertension while R-perindopril does not posse's medicinal activity [7]. It is important to identify and quantify these enantiomers. FIA and SIA may be used as alternatives to chromatographic techniques for discriminating enantiomers. Physical methods and enantioselective immunoassays are popularly used for racemic drugs [8].

FIA and/ or SIA sensors are used for speciation of enantiomers and can thus be easily adapted for the pharmaceutical industry. SIA with its multi-solution handling is best suited for this work and will be the objective of this chapter.

The following types of electrochemical sensors have been used for the discrimination of the enantiomers: potentiometric, enantioselective membrane electrodes, amperometric biosensors, and amperometric immunosensors [9-15].

The separation of enantiomers is carried through by enantioselective membrane FIA/sensor system and they have been already used for the qualitative and quantitative analysis for (S/ R)-pdp (penpndopril) [16, 17]. The aim of this chapter is on the design of FIA and SIA systems for the speciation of the (S/ R)-pdp by coupling with amperometric biosensors. The L- and D-AAOD (amino acid oxidase) were used for the construction of carbon paste based amperometric biosensors because of their high sensitivity [18]. The reactions are represented as:

$$\text{L-amino acid} + O_2 + H_2O \xrightarrow{\textbf{L-AAOD}} \text{keto acid} + NH_3 + H_2O_2$$

$$\text{D-amino acid} + O_2 + H_2O \xrightarrow{\textbf{L-AAOD}} \text{keto acid} + NH_3 + H_2O_2$$

Hydrogen peroxide was measured by the amperometric transducer [19].

8.3. Experimental.

8.3.1. Electrodes design.

Two electrodes, based on graphite paste, were designed as follows: Paraffin oil and graphite powder were mixed in a ratio 1:4 (w/w) to form a graphite paste. 100 mL from each

enzymatic solution (1 mg enzyme/ml in 0.1 mol/L phosphate buffer, pH = 7.0 (Merck)): L-AAOD (E.C. 1.4.3.2. Type I: Crude Dried Venom from Crotalus adamanteus, Sigma) solution and d-AAOD (E.C. 1.4.3.3. Type I: from Porcine Kidney, Sigma) solutions, were respectively added to two separate portions of graphite paste.

Two plastic tips were filled with the corresponding graphite–paraffin oil paste leaving an empty space of 3 to 4 mm, the top part was filled with carbon paste containing the enzyme. The diameter of each sensor was 3 mm. Electrical contact was obtained by inserting a silver wire into the carbon paste. Both electrodes tips were turned into flat surfaces by appropriate rubbing on a fine sand paper. The surface of the electrode was wetted with de-ionized water and then polished with alumina paper (polished strips 30144-001, Orion) before use. The biosensors were stored dry at 4 ˚C.

8.3.2. Apparatus.

A 663 VA Stand (Metrohm, Herisau, Switzerland) in connection with a PGSTAT 20 and software (Eco Chemie version 4.4) was used for all chronoamperometric (E = 650 mV) measurements. A glassy carbon electrode and a calomel electrode served as the counter and reference electrodes in the cell.

8.3.2.1. Flow injection system.

The electrodes were incorporated into the conduits of a FIA as depicted in Fig. 8.4 which had a Carle microvolume two-position sampling valve (Carle No. 2014) containing two identical sample loops. Each loop had a volume of 30 µl. A Cenco peristaltic pump operating at 10 rpm propelled the carrier streams to the manifold system. Tygon tubing (0.51 mm i.d.) was used to construct the manifold, these coils were wound round suitable lengths of glass tubing (15mm i.d.). The sample was injected into a phosphate buffer (carrier stream) at pH = 7.00. A

60 s cycle sampling time was used, giving the system a capacity of about 60 samples per hour.

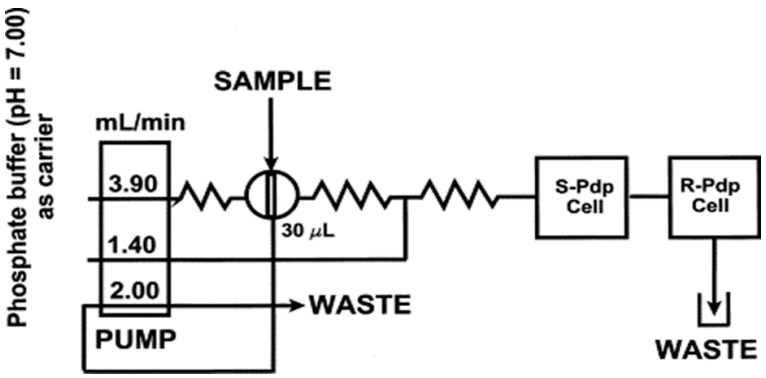

Figure 8. 4. FIA system used for the simultaneous determination for S- and R-pdp.

8.3.2.2. Sequential injection system.

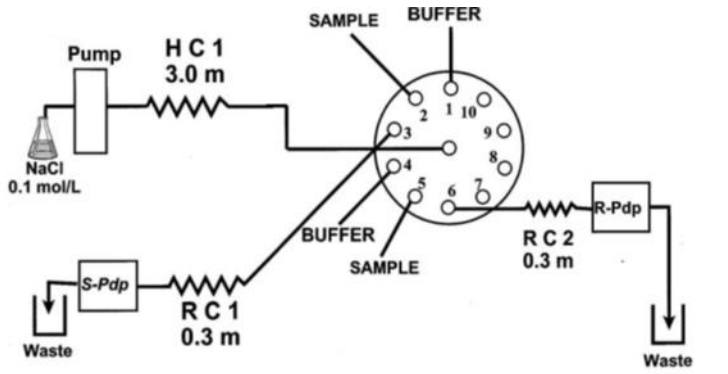

Figure 8.5. SIA system used for the simultaneous determination for S- and R-pdp.

Fig. 8.5 shows the diagram of the SIA system for S- and R-pdp analysis.

Phospahe buffer	sample	S-pdp cell	Phosphate buffer	sample	R-dpd cell
←	←	→	←	←	→
4.5 s	**4.5 s**	**30 s**	**4.5 s**	**4.5 s**	**30.0 s**

Figure 8. 6. Timed sequence for aspiration and forwarding reagents and sample for S- and R-pdp analysis.

The biosensors were incorporated into the conduits of a SIA system and NaCl was used as carrier. The capacity of the system is about 38 samples per hour. The device operating sequence is shown in Table 8.1 and the summarised version shown as Fig.8.6.

Table 8.1. One cycle of the sequential injection system for S- and R-pdp speciation.

Time (s)	Pump	Valve	Description
0 0	**Off**	**home**	**Pump stops, move to port 1(Buffer)**
1.0	**Reverse**	**1**	**Draw up buffer solution**
5.5	**Off**	**home**	**Pump stops, move to port 2 (S-pdp)**
6.5	**Reverse**	**2**	**Draws sample stream (S-pdp)**
11	**Off**	**home**	**Move to port 3**
12	**forward**	**3**	**Pump product to detector**
42	**Off**	**home**	**Select port 4 (buffer)**
43	**Reverse**	**4**	**Draws buffer**
47.5	**Off**	**home**	**Pump stops, select port 5 (R-pdp)**
48.5	**Reverse**	**5**	**Draws sample (R-pdp)**
53	**Off**	**home**	**Pump stops, select port 6 (R-pdp)**
54	**forward**	**6**	**Pump product to detector**
84	**Off**	**home**	**Pump stops,**
85	**Off**	**home**	**Valve return to home**

8.3.3. Reagents and materials.

The S- and R-pdp were supplied by Bristol-Myers Squibb Pharmaceutical Research Institute (Princeton, NJ). Graphite powder of size 1-2µm, synthetic, was supplied by Aldrich (Buchs, Switzerland). Paraffin oil was supplied by Fluka. Phosphate buffer pH = 7.00 was supplied

by Merck (Darmstadt, Germany).

De-ionized water from a Modulab system (Continental Water Systems, San Antonio, TX) was used for all solutions. The S- and R-pdp solutions were prepared from standard S- and R-pdp solutions (1×10^{-2} mol/L), respectively, by serial dilution.

8.4. Results and discussion.

An optimum flow rate of 3.61 mL/min was used to propel the solutions in both flow systems. The timing and flow direction for the SIA system is shown in Fig. 8. 6. It follows from this that in the SIA system, the sample and buffer consumption is only 270 µL each per measurement of S- and R-enantiomer, which is very economical.

8.4.1. The optimum working pH of the amperometric biosensors.

The variation of peak current (measured as relative peak height (H) by using the SIA system) with pH is given in Figs.8.7 and 8.8 for the FIA and SIA systems, respectively. As seen from the graph, the response of the system varied with pH. The optimum pH value for the amperometric biosensor was determined for 40 and 600 nmol/L S-pdp, in the FIA and SIA systems, respectively and for 10 and 80 nmol/L

R-pdp and S-pdp determinations in the FIA and SIA systems with the use of appropriate phosphate buffers. These phosphate buffers were prepared with pH varying between 6.00 and 8.00. For the FIA system, the optimum pH values for the assay of S- and R-enantiomers were found to be 7.0 and between 6.5 and 7.5 (maximum and constant value for the peak height recorded) respectively this was exactly the same for the SIA system, Accordingly, a pH of 7.0 was selected to perform the measurements in both flow systems for the two

enantiomers. The amperometric biosensors/FIA and amperometric biosensors/SIA systems are working at non-equilibrium conditions. Therefore, a major advantage of the flow systems is the repeatable handling of sampling due to the control of the flow pattern.

pH	S-pdp	R-pdp
6	7.4	37.5
6.5	13.4	105.8
7	37.3	106.3
7.5	22.7	106.6
8	16.3	38.3

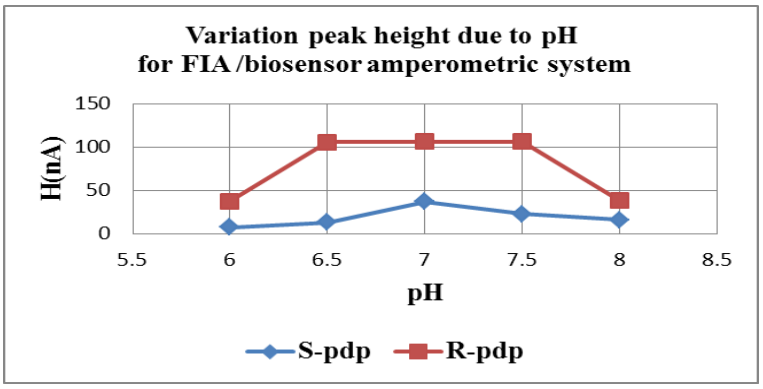

Figure 8 7. pH variation for FIA S-and R-pdp determination

pH	S-pdp	R-pdp
6	0.18	1.02
6.5	1.83	2.23
7	3.92	2.31
7.5	0.96	1.04
8	0.47	0.58

Figure 8 8. pH variation for SIA S- and R-pdp determination

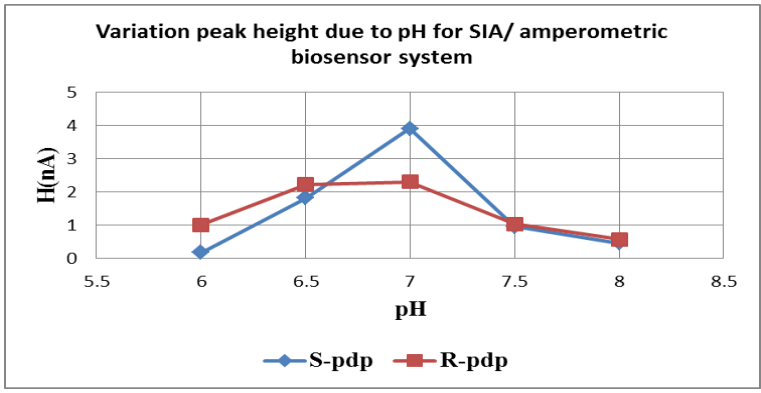

8.4.2. Electrodes response.

The response of both electrodes was determined using chronoamperometric technique (E = 650 mV), using Pt and saturated calomel electrodes as auxiliary and reference electrodes,

respectively at a pH = 7.00 (phosphate buffer). The calibration equations obtained for the amperometric biosensors (n = 10) are as follows:

FIA/amperometric biosensors system:

S-perindopril: H = 20.0 + 0.08c; r = 0.9994

R-perindopril: H = 26.5 + 8.27c; r = 0.9993

SIA/amperometric biosensors system:

S-perindopril: H = 0.32 + 0.008c; r = 0.9963

R-perindopril: H = 9.00 + 0.10c; r = 0.9938

Where H is the peak height in nA and c is the concentration of S- and R-captopril in nmol/L. Linear concentration ranges between 240 pmol/L and 60 nmol/L, and between 6 and 40 nmol/L for S- and R-pdp, respectively, with limits (3 × S.D.) of detection of 120 pmol/L and 4 nmol/L, respectively were obtained when the FIA/amperometric biosensors system was used.

For the SIA/amperometric biosensors system, the linear concentration ranges for the S and R-enantiomers were between 60 and 800 nmol/L and between 60 and 900 nmol/L, respectively, with a limit of detection of 40 nmol/L for both enantiomers. The working concentration ranges as well as the limits of detection demonstrated the suitability of the proposed amperometric biosensors for the on-line monitoring of both enantiomers.

Both biosensors revealed good stability and reproducibility for tests performed over 2 weeks. (The RSD values obtained during this period were < 0.1% for the intercepts and slopes).

8.4.3. Selectivity of the biosensors.

The selectivity of both biosensors was checked using the mixed solutions method, with respect to R(S)-pdp, d-proline, l-proline, and polyvinylpyrolidone (PVP). Table 8.2 gives the results for the selectivity studies Amperometric selectivity coefficients were determined following the method proposed by Wang [19]. The L- and D-proline were selected due to their possible status as by-products. PVP is very often used as a compression compound for tablets [20]. In the evaluation, the concentration of the interferent was selected to be four times that for the enantiomer of interest [21]. As is shown in Table 8.2, the proposed biosensors are enantioselective when used as detectors in a SIA system. The results obtained, revealed that both sensors also have good selectivity over PVP. Inorganic cations such as Na^{+}, K^{+}, and Ca^{2+} do not interfere in the determination.

Table 8.2 Selectivity coefficients pKamp for the amperometric biosensors in the FIA and SIA systems.

Interfering species (J)	S-pdp	R-pdp	L-Proline	D-Proline	PVP
S-pdp					
FIA	–	40 0	1.12	3.40	3.70
SIA	–	3.62	1.10	2.31	2.40
R-pdp					
FIA	4.74	–	3.96	1.96	4.04
SIA	3.92	–	4.00	1.89	3.68

All measurements were made at room temperature; all values are the average of 10 determinations.

8.4.4. Analytical applications.

The flow systems obtained by incorporation of the amperometric biosensors in the FIA and SIA conduits, proved to be useful for the simultaneous assay of S and R-pdp. The recovery tests for each enantiomer in the FIA systems were 99.92 ± 0.34% for S-pdp (n = 10) and 99.86±0.10% for R-pdp (n = 10) as shown in Table 8.3 and in the SIA systems were 99.62 ± 0.05% for S-pdp (n = 10) and 99.93 ± 0.03% for R-pdp (n = 10) as shown in Table 8.4. This demonstrated the suitability of the proposed biosensors/FIA and biosensor/SIA systems for simultaneous assay of the enantiomers.

Simultaneous detection of the enantiomers was done using different ratios between R- and S-pdp. The results obtained (Tables 8.3 and 8.4) demonstrated the suitability of the proposed flow system for the on-line purity tests of S-pdp. No differences were recorded in recovery tests between 1:3 and 1:99.9 (mole ratio, in the favor of each enantiomer).

The recovery test for both S- and R-enantiomers was done only for the raw substance, because the recommendation for the pharmaceutical product is that it must contain only the S-pdp. Therefore, there is no need to perform a uniformity content test with the proposed system for the pharmaceutical formulations.

Table 8.3 The results obtained for the assay of S-pdp in the presence of R-pdp

S:R (mol:mol)	Recovery S-pdp[a] (%)	
	FIA	SIA
2:1	99.87 ± 0.02	99.90 ± 0.01
1:1	99.90 ± 0.01	99.97 ± 0.02
1:2	99.89 ± 0.01	99.94 ± 0.02
1:3	99.90 ± 0.03	99.96 ± 0.01
1.99	99.90 ± 0.02	99.99 ± 0.01

[a] Mean ± S.D. of 10 determinations.

Table 8.4 The results obtained for the assay of R-pdp in the presence of S-pdp

S:R (mol:mol)	Recovery R-pdp[a] (%)	
	FIA	SIA
2:1	99.74 ± 0.02	99.46 ± 0.01
1:1	99.87 ± 0.01	99.42 ± 0.02
1:2	99.86 ± 0.01	99.91 ± 0.01
1:3	99.80 ± 0.03	99.92 ± 0.01
1.99	99.86 ± 0.02	99.93 0.01

[a] Mean ± S.D. of 10 determinations.

Tables 8.3 and 8.4 shows the determination of S-pdp in the presence of R-pdp and R-pdp in the presence of S-pdp.

8.5. Conclusions.

This chapter opens a new and very important field in the use of biosensors/FIA and biosensors/SIA systems for simultaneous assay of enantiomers. This offers an alternative yet convenient and rapid speciation analysis of enantiomers. The exploitation of the advantages inherent within flow systems is applied to its optimum. In view of the fact that generally the

stability of separate enantiomers is limited over a short period of time the flow systems are best suited for this type of analysis.

The main advantages of the proposed systems are: simplicity of construction and operation that involve the introduction for on-line monitoring of enantiomers during the synthesis of enantiomers, high reliability of analytical information, rapidity, and low cost of the analysis. Due to its higher reliability and versatility, as well as due to its lower consumption of reagents, the SIA/biosensors system is preferred to the FIA/biosensors system for the simultaneous assay of enantiomers. The high precision of the flow based systems is due to the fact that all the measurements are done after the same interval of time, (consistent timming). The biosensor itself is a highly selective unit whose differentiation is quite prestine. The combination of the operational procedure of the flow system and the unique character of the biosensor result in one of the most accurate analysis technique for enantiomers.

There are however some procedures to be adhered to for optimal performance. The surface of the biosensors should be continuously washed by the sodium chloride or phosphate buffer carrier streams. The main disadvantage of the utilization of biosensors as detectors in flow system is their short lifetime activity. This then dictates that they can only be used as a once off and not applied for later analysis. Due to the low working concentrations levels the raw material must sometimes be diluted on-line.

Generally, the only possible interferences from the real raw material samples are L- and D-proline. The enantioselectivity versus these compounds was checked, and it was proved that it was better in a flow system, compared with a static method of analysis.

As with most flow systems the reduced amount of reagents and samples required for a single cycle of analysis is highly appreciated. The period required for a single analysis is greately

reduced. Given the sensitivity of enantiomers, the elimination of manual manipulation is an added advantage when flow systems are used for isomer analysis.

The results proved that flow systems are idealy suited for this type of analysis. They are highly automated and these techniques can easily be extended to highly contagious or toxic sample materials by preventing physical handling.

SIA system with its pause and continue has the added advantage of alternating between various samples or more specific reagents that are bias towards particular enantiomers. The ease of manipulation and possibility of accommodating different chemical pathways has proven to be successful for simultaneous enetiomers discrimination.

8.6. References

1. M. Hurst, B. Jarvis: Perindopril: an updated review of its use in hypertension. Drugs. 61(6) [PUBMED] (2001) pp 867.
2. E. Parker, L. Aarons, M. Rowland, G. Resplandy: The pharmacokinetics of perindoprilat in normal volunteers and patients: influence of age and disease state. Eur. J. Pharm. Sci.; 26:1, [PUBMED] (2005 Sep) pp 104.
3. M. Jastrzebskal, K. Widecka, M. Naruszewicz, A. Ciechanowicz, A. Janczak-Bazan, A. Foltynska, I. Goracy, K. Chetstowski, T. Wesotowska: Effects of perindopril treatment on hemostatic function in patients with essential hypertension in relation to angiotensin converting enzyme (ACE) and plasminogen activator inhibitor-1 (PAI-1) gene polymorphisms. Nutr. Metab. Cardiovasc. Dis.; 14:5 Oct. (2004) pp 259.
4. K. Alfakih, A.S. Hall: Perindopril. Expert Opin Pharmacother. ; 7:1, Jan. (2006) pp 63.
5. C.A. Challener, In: Chiral drugs. 1st. Aldershot (England): Ashgate Publisher; Overview of chirality (2001) pp 3.
6. K.M. Rentsch, The importance of stereoselective determination of drugs in the clinical laboratory. Journal of Biochemical and Biophysical Methods, 54(1-3) (2002) pp 1.
7. H. Yoshiji, S. Kuriyama, M. Kawata, J. Yoshii, Y. Ikenaka, R. Noguchi, T. Nakatani, H. Tsujinoue, H. Fukui, The angiotensin-I-converting enzyme inhibitor perindopril suppresses tumor growth and angiogenesis: possible role of the vascular endothelial growth factor. Clin Cancer Res., 7(4) Pubmed, Apr. (2001) pp 1073.
8. T. Toyo'oka, Resolution of chiral drugs by liquid chromatography based upon diastereomerr formation with chiral derivatization reagents. J. of Biochemical and Biophysical Methods, 54(1-3) (2002) pp 25.

9. N. Chikhi-Chorfi, C. Pham-Huy, H. Galons, N. Manuel, Rapid determination of methadone and its major metabolite in biological fluids by gas-liquid chromatography with thermoionic detection for maintenance treatment of opiate addicts. J. of Chrom B, 718 (1998) pp 278.
10. P.A. Got, J.M. Scherrmann, Stereoselectivity of antibodies for the bioanalysis of chiral drugs (review) Pharmaceutical Research, 4(11) (1997) pp 1516.
11. C.E. Cook, Enantiomer analysis by competitive binding methods. In: I.W. Wainer, editor. Drug stereochemistry. Analytical methods and pharmacology. 2nd. New York: Marcel Dekker Publisher, (1993) pp 35.
12. C. Pham-Huy, A. Sahui-Gnassi, V. Saada, J.P. Gramond, Microassay of propranolol enantiomers and conjugagate in human plasma urine by HPLC after chiral derivization for pharmacokinetic study.J. Pharm. and Biomed. Anal., 12(9) (1994) pp 1189.
13. R.I. Stefan, J.F. van Staden, H.Y. Aboul-Enein, Talanta 51 (2000) pp 1969.
14. C. Pham-Huy, B. Radenen, A. Sahui-Gnassi, J.R. Claude. High performance liquid chromatography determination of (S) - and (R) - propranolol in human plasma and urine with a chiral β-cyclodextrin bonded phase. J. Chrom. B 665 (1995) pp 125.
15. C. Pham-Huy, N. ChickhiChorfi, H.H. Galons, N. Sadeg. Enantioselective HPLC determination of methadone enantiomers and its major metabolite in human biologi fluids using a new derivatized cyclodextrin-bonded phase. J. Chrom. B 700 (1995) pp 155.
16. R.I. Stefan, J.F. van Staden, H.Y. Aboul-Enein, Biosens. Bioelectron. 15 (2000) pp 1.
17. R.I. Stefan, J.F. van Staden, H.Y. Aboul-Enein, Electroanalysis 11 (1999) pp 1233.
18. R.I. Stefan, J.F. van Staden, H.Y. Aboul-Enein, Electrochemical Sensors in Bioanalysis, Marcel Dekker, New York (2001).
19. J. Wang, Talanta 41 (1994) pp 857.
20. H.E. Abdellatef, M.M. Ayad, E.A. Taha, J. Pharm. Biomed. Anal. 18 (1999) pp 1021.

21. R.I. Stefan, J.F. van Staden, H.Y. Aboul-Enein, Electrochemical Sensors in Bioanalysis, Marcel Dekker, New York, (2001).

Chapter 9

Conclusions

While all flow techniques are more or less suitable for online analysis systems, the sequential injection analysis (SIA) is especially qualified for online applications. Unlike all other flow techniques, the SIA integrates the ability to perform quality assured analysis within an automated system without any supplementary devices (e.g., valves or autosamplers). This leads to analytical systems that are more portable than comparable systems which make these systems especially suitable for monitoring applications in remote locations or in transit.

Established flow-injection techniques allow advanced solution handling for laboratory purposes, but chemical sensing and continuous monitoring of chemical processes require dramatically simplified flow schemes and instrumentation with the potential for miniaturization and an inherent ruggedness. Considerations based on the random walk model have led to the concept of sensor injection and sequential injection analysis. This new approach to automated analysis is designed to fill a gap in present flow-injection methodology.

In SIA sample handling is automated enhancing wet chemistry procedures to be rapid, precise, and efficient. Minute solution zones are manipulated under controlled dispersion conditions in narrow bore tubing.

- Reagent use is drastically reduced. Typical FIA experiments make use of at least 1mL of reagent per measurement. SIA typically makes use of 50 μl. This means that in a 24-hour period assuming one measurement per minute, the FIA analyzer would consume 1440 ml of reagent. The SIA analyzer would consume 72 ml. It has been

noted that the most frequent reason for process analyzer failure is running out of reagents.

- Flow manifolds are simple and robust typically comprising a pump, selection valve, and detector connected by tubing. The same manifold can be used for widely different chemistries simply by changing the flow program rather than the plumbing. Analyzer maintenance is therefore simplified.

- The selection valve replaces the injection valve and provides a means for selecting different sample streams and calibrants. This enables convenient automated calibration.

- Components used in a SIA manifolds are amenable to laboratory, field, and plant operation. In addition to these, SIA enjoys all of the benefits of FIA.

SIA makes use of a single flow-channel even with multicomponent chemical systems. In FIA, additional flow-channels are required if more than one reagent is to be used.

• With SIA the sample and reagent consumptions are drastically reduced.

• The single-channel operation of SIA enables the use of the same manifold for the implementation of wide range of determinations.

• In SIA, the selection valve provides a means for performing convenient automated calibration.

• In SIA, accurate measurements of sample and reagent zones necessitate computer control and, therefore, automation becomes essential.

The application of SIA for speciation ranging from inorganic species, biological systems and synthetic medicinal compounds has been demonstrated with results that were on average

acceptable and accurate in all instances. The versatility of this technique has been exploited with appreciable results and very low quantities of reagents. In all the actual chemical speciatition analysis from chater 3 to chapter 8 the results showed a low % RSD as compared to the standard methods as this gave an excellent precision. Furthermore, the results in all cases were in close agreement with the standard methods.

The application of SIA and FIA to both real and synthetic samples showed a great correlation and consitent results. With the possibility of incorporating tubing with varying chemical properties and strength opens up a wide spectrum of application as ranging from organic and inorganic reagents.

Since both SIA and FIA have automatic control and use fairly low concentrations of samples and reagents it therefore means that it is very possible to minitiarize these processes and extend it to portable systems. In conclusion these developed methods proved that they can be adapted as alternative methods for chemical speciation at a fraction of the time as required for conventional methods.

Recommendations and future work.

Although this work was completed in 2003, there is a great potential to extend the technique to different types of samples more specially to gas analysis. Chemical speciation through sequential injection analysis is still relevant to the modern world and with complex chemical species being introduced into the environment through anthropogenic and natural factors there will always be a need for a technique that is economical in terms of reagents and the finances thereof. Coupling of Sequential Injection Analysis with different methods of sample manipulation in order to accommodate different types of physical state of chemical species. This would greatly enhance the scope of analysis that can be carried out. The possibility of sample derivatisation will be ideal for sequential injection analysis.

The ease with which the conduits of sequential injection techniques can be adapted makes it ideal that two or more sequential injection methods can be hyphenated to extend the quality of analysis up till the fingerprinting level, considering the cost of setting up a Sequential Injection Analysis technique in comparison to competing techniques will be ideal to extend the scope of analysis to high magnitude levels.

The introduction of several detectors either in parallel of in series would further increase the scope of analysis that could be performed per sample. At any stage of the analysis the sample can be manipulated to feed into a different detector to isolate a specific parameter or chemical character of a single sample. Miniaturise and adaptation of the Sequential Injection Analysis

technique to nano scale technology would be a novel scientific revelation with a whole new host of possibility